

**NISTIR 4591**

**NASA CR-187115**

# **Material Flammability Test Assessment for Space Station Freedom**

**T. J. Ohlemiller  
K. M. Villa**

**U.S. DEPARTMENT OF COMMERCE  
National Institute of Standards  
and Technology  
Building and Fire Research Laboratory  
Gaithersburg, MD 20899**

**Sponsored by:  
NASA Lewis Research Center  
Cleveland, Ohio 44135**

**U.S. DEPARTMENT OF COMMERCE  
Robert A. Mosbacher, Secretary  
NATIONAL INSTITUTE OF STANDARDS  
AND TECHNOLOGY  
John W. Lyons, Director**

**NIST**

## LIST OF FIGURES

	<b>Page</b>
Figure 1. Typical Sample Holder for Test 1 .....	32
Figure 2. LIFT Apparatus in Horizontal Orientation .....	33
Figure 3. Pre-Heated NASA Test .....	34
Figure 4. LIFT data and fitted model lines; cotton toweling with Kaoboard backing .....	35
Figure 5. LIFT data and fitted model lines; 12.7 mm Pyrell foam in vertical orientation; Kaoboard backing .....	36
Figure 6. LIFT data and fitted model lines; 25.4 mm Pyrell foam; Kaoboard backing .....	37
Figure 7. LIFT data and fitted model lines; Kydex with Kaoboard backing .....	38
Figure 8. LIFT data and fitted model lines; Lexan 9034 with Kaoboard backing .....	39
Figure 9. LIFT data and fitted model lines; Lexan 9600 with Kaoboard backing .....	40
Figure 10. Cone Calorimeter data for rate of heat release; Lexan 9034; Kaowool backing .	41
Figure 11. Cone Calorimeter data for rate of heat release; cotton toweling; Kaowool backing .....	42
Figure 12. Cone Calorimeter data for rate of heat release; 12.7 mm Pyrell foam; Kaowool backing .....	43
Figure 13. Peak rate of heat release variation with incident heat flux .....	44
Figure 14. Data and model prediction for maximum char length versus absorbed radiant flux; cotton toweling .....	45
Figure 15. Data and model prediction for maximum char length versus absorbed radiant flux; Nomex .....	46

## LIST OF FIGURES (continued)

		Page
Figure 16.	Data and model prediction for maximum char length versus absorbed radiant flux; flame-retardant cotton .....	47
Figure 17.	Data and model prediction for maximum char length versus absorbed radiant flux; epoxy/glass circuit board .....	48
Figure 18.	Data and model prediction for maximum char length versus absorbed radiant flux; Kydex .....	49
Figure 19.	Data and model prediction for maximum char length versus absorbed radiant flux; Lexan 9034 .....	50
Figure 20.	Cone Calorimeter data for rate of heat release; Lexane 9034 with air gap below sample .....	51
Figure 21.	Cone Calorimeter data for rate of heat release; cotton toweling with air gap below sample .....	52
Figure 22.	Cone Calorimeter data for rate of heat release; epoxy/glass circuit board with air gap below sample .....	53
Figure 23.	Cone Calorimeter data for rate of heat release; Nomex with air gap below sample .....	54
Figure 24.	Cone Calorimeter data for rate of heat release; flame-retardant cotton with air gap below sample .....	55
Figure 25.	LIFT data and fitted model lines; cotton toweling with air gap below sample .....	56
Figure 26.	LIFT data and fitted model lines; epoxy/glass circuit board with air gap below sample .....	57
Figure 27.	LIFT data and fitted model lines; Kydex with air gap below sample .....	58
Figure 28.	LIFT data and fitted model lines; Lexan 9034 with air gap below sample .....	59
Figure 29.	LIFT data and fitted model lines; flame-retardant cotton with air gap below sample .....	60

## LIST OF FIGURES (continued)

	Page
Figure 30.	LIFT data and fitted model lines; Nomex with air gap below sample ..... 61
Figure 31.	Simple upward spread model ..... 62
Figure 32.	Flame height versus time for single NASA igniter striking both sides of a thin, inert sample (ceramic paper); actual flame height is 6 mm greater than values shown ..... 63
Figure 33.	Rate of heat release data used as inputs to flame spread model; for a given material and flux, the above lines specify the value of Q ..... 64
Figure 34.	Burn time, $t_b$ , as determined from rate of heat release data ..... 65
Figure 35.	Burn time, $t_b$ , as determined from rate of heat release data ..... 66
Figure 36.	Example of model prediction of pyrolysis front height as a function of time for three pre-heat flux levels ..... 67

## Material Flammability-Test Assessment for Space Station Freedom

### Abstract

The NASA Upward Flame Propagation test, which measures response to a well-defined laminar flame at the bottom of a test sample, is currently used to screen for flammability all materials intended for use in the interior of manned spacecraft. The response of a series of materials was compared in this test and in the standard NIST flammability tests (Cone Calorimeter for rate of heat release and LIFT tests for ignitability and lateral flame spread). The goal was to see if these differing flammability assessment approaches provide comparable information on the potential hazards of a material. In the first phase of this study only one of the samples exhibited appreciable flame spread in the NASA test, yielding very limited data for comparisons with the NIST test results. The NIST tests, which employ a variable external radiant flux as an additional test parameter, revealed a widely varying response to this flux. The flux simulates radiation that could come from another burning object or from the same object if it is so shaped as to feed radiation back to itself. In the second phase of the study, the NASA test was modified to include radiative pre-heating of the samples before they were exposed to the standard NASA igniter in the standard manner, except that the incident flux continued throughout the test. The response of the materials, as measured by the minimum pre-heat flux (or temperature) to yield upward spread, varied widely; for example, Nomex required very little pre-heating to yield full-length spread whereas Lexan 9034 was resistant. Rate of heat release behavior or lateral flame spread behavior alone did not appear to be predictive of behavior in the modified NASA test. A simplified upward flame spread model, which utilizes inputs derived from the NIST test, was employed in an attempt to predict the behavior in the modified NASA tests. The model greatly under-predicted the necessary pre-heat flux for some materials while doing the opposite for other materials. Thus, at the present, a firm relation between the behavior in the NASA test and in the NIST tests has not been established. It is recommended that NASA consider use of a test similar to the modified NASA test employed here, as a supplementary test for materials that may be used in appreciable quantities. It is also recommended that NASA pursue the comparative behavior in normal gravity and micro-gravity of a series of materials in such a test framework to more firmly establish a footing for earth-based testing of spacecraft materials.

#### 1) Introduction

The advent of longterm space missions made possible by Space Station Freedom, now in the design stage, brings with it a renewed concern about fire safety in manned space vehicles. The projected occupancy time of the order of decades makes unplanned fire ignition events virtually inevitable. This has prompted NASA to re-examine fire prevention and control procedures including a re-assessment of their principal material flammability screening test that is the

subject of this report<sup>1</sup>. This test is but one element of a rigorously applied set of measures designed to minimize the threat of fire in manned spacecraft; these measures have been outstandingly successful in the Space Shuttle program. This test is crucial, however, because it determines, in large measure, the types of controls imposed on a material as a potential fire threat.

In the present study, the behavior of a series of materials has been examined using this NASA test and also a series of flammability tests developed at the National Institute of Standards and Technology. The goal is to ascertain whether the two types of tests give comparable information regarding the potential flammability hazard of a material. Since this is a ground-based study, the comparisons are inevitably valid only for normal gravity. A definitive assessment of the applicability of any of these test methods to a micro-gravity environment awaits a quantitative interpretation of the role of gravity in flammability.

## 2) NASA Upward Propagation Test

The principal screening test for spacecraft interior materials currently used by NASA examines the potential for upward flamespread on a material as a result of exposure to a small flaming ignition source. Upward flame spread has been interpreted as being a worst-case configuration on the basis of limited, stagnant atmosphere micro-gravity flame propagation studies done onboard Skylab [1]. In this view the flammability behavior that a material exhibits in the upward spread mode is inherently more severe than it would exhibit in a micro-gravity environment. This has recently been brought into question for at least one condition. Opposed flow flame spread on thin sheets of paper extends to lower ambient oxygen levels in the presence of flow velocities characteristic of spacecraft ventilation (0(10) cm/sec) than it does at other (higher or lower) flow velocities [2]. At lesser or greater flow velocities, opposed flow spread on this material requires a greater ambient oxygen level. The generality of this result cannot be assessed at present but it provides an incentive to clarify further the relation between normal and micro-gravity flammability.

Figure 1 taken from Ref.3 shows a diagram of the sample holder used in the NASA screening test. There one sees that a 5 cm by 30 cm exposed portion of the sample is subjected on its bottom edge to an electrically-initiated flaming chemical igniter (hexamethylenetetramine). The characteristics of this igniter are narrowly defined as to flame temperature (1100 C), peak flame height (6.4 cm), duration (25 sec) and total energy release (750 cal. or 3140 joules). The rationale for this ignition source appears to be that it is intended to represent a localized, finite duration source such as a severe electrical short; it has been judged to be more severe than any likely electrical short onboard a manned spacecraft.

---

<sup>1</sup>NASA utilizes several other tests for more specialized applications such as for electrical wire insulation; these were not examined in this study.

The material being screened must be at its "worst case thickness" and in its "worst case environment". The former specification presumably requires the potential user to test all contemplated thicknesses; the latter requirement usually translates into a 30% oxygen environment. Failure of the test occurs when the burn length reaches 15 cm in any of six repeats. Transfer of burning debris from the sample also constitutes failure.

### 3) NIST Flammability Tests

Rationale. The test sequence that has evolved at NIST has been driven by the need to obtain a quantitative description of the flammability of a material which can be utilized in the context of full scale fire models. The tests and the models have largely been directed at interior finish fires in terrestrial structures. This approach to flammability assessment is still under development, but has shown a great deal of promise [4].

In this approach three elements of flammability are recognized: ignitability, rate of heat release and flame spread characteristics. Ignitability is measured by the time necessary for a given flux to yield flaming combustion of the sample in the presence of a pilot ignition source that resides in the gases evolved from the heated sample surface. This ignition delay time increases as the incident heat flux (radiative in nature) decreases and it becomes infinite when the incident flux is insufficient to generate a flammable mixture of gases from the sample. Rate of heat release subsequent to sample ignition is measured by the Cone Calorimeter device (ASTM E 1354) now under consideration by NASA in the draft revision of Reference 3. Rate of heat release is measured in terms of the kW/m<sup>2</sup> evolved from a sample as it burns. This is usually a rather complex time-dependent function which is increased in magnitude but shortened in duration by increasing incident heat flux on the burning sample. The heat release process helps drive flame spread either with (concurrent spread) or against (opposed flow spread) any flow over the sample.

Opposed flow spread is measured in the LIFT device (lateral ignition and flame spread test, ASTM E 1321) which yields the complete dependence of the spread rate on external radiant flux level in a single test; this includes the minimum flux for opposed flow spread. Concurrent spread is examined in tests which have yet to be standardized; no NIST concurrent flame spread tests were utilized in this study.

It should be noted that this NIST approach in all cases includes a variable not found in the NASA test, an external radiant heat flux. This has been prompted by the observation that most building materials (residential and commercial construction) do not burn appreciably in the absence of such a flux. This is due in part to the fact that most such materials are thermally thick in typical fire scenarios.<sup>2</sup>

---

<sup>2</sup>The term thermally thick, as applied here, means that the temperature wave in the sample, due to whatever form of surface heating applied, does not reach the rear surface of the material. Thermally thin behavior is the opposite extreme in which the thermal wave permeates the solid to such an

The external radiation applied in the NIST tests simulates that seen in real fire scenarios from two potential sources. First, there may be another burning object nearby which irradiates its surroundings. Second, there may be only one object burning but it may be shaped in such a way that there is a finite radiative view factor between elements of the burning surface. This means that part of the radiation emitted from the burning surface is intercepted by other elements of the surface and conversely. This radiative self-feedback may be sufficient to sustain combustion. This is the rationale behind the use of interior corner ignition in tests of interior room finish materials.

Tests and Procedures. The apparatus and underlying rationale of the LIFT test are described, along with the general NIST approach to flammability assessment, in Ref. 5. The LIFT, which was used in this study, will thus be only briefly described here.

A schematic of the essential elements of the device is shown in Fig. 2. This device can be used to obtain both ignitability and opposed flow flame spread behavior. For ignition, a 15 cm square area of the sample surface is nearly uniformly irradiated with radiation from a gas-fired panel. The panel temperature is typically low enough ( $\leq 1000$  C) that virtually all of the radiation is in the infrared where the sample absorptivity can be expected to be high. A strong pilot flame, using pre-mixed acetylene and air, is positioned to intercept the plume of gases that will be evolved from the sample surface as it is heated. As soon as ignition occurs the delay time is noted, using a stopwatch. A sequence of samples at several flux levels, typically from 10 to 50 kW/m<sup>2</sup>, provides the desired measure of sample ignitability. These data can be manipulated to infer an effective ignition temperature and an effective value of the thermal inertia of the sample; these parameters can in turn be used in the context of a simple algebraic model of ignition to predict ignitability at other heat fluxes.<sup>3</sup>

For opposed flow flame spread studies in the LIFT device, the sample size is increased to 15 by 79 cm. The long direction of the sample is exposed to a spatially varying incident radiant flux from the gas-fired panel. The well-defined length-wise variation is due to the fact that the sample is at an angle with respect to the panel. The spatial variation of heat flux is pre-calibrated. The sample is pre-heated in this flux field, typically until it is essentially at equilibrium. This imposes a spatially-varying temperature distribution along the length of the sample. When the pre-heat is completed, a pilot ignition source is introduced causing ignition at the high flux end; flame spread then occurs along the length of the sample. The local spread rate is a consequence of the local incident heat flux history. Spread continues until the front reaches a region of the sample where the incident flux (coupled with the flame heat flux) is insufficient to overcome heat

---

extent that there is no temperature gradient between the front and rear of the sample.

<sup>3</sup>Appendix A discusses the data reduction procedure.

losses and spread stops. The data on spread velocity versus incident flux can be used again to infer a model parameter and obtain a simple algebraic description of opposed flow spread behavior (Appendix A). Sample orientation is usually vertical since the test was originally focused on wall materials. In this study, some of the materials were thermoplastic, which means they would melt out of a vertical holder. Because of this, virtually all of the LIFT tests in this study were run with the sample laying horizontal with the exposed face upward.

The Cone Calorimeter used here was essentially the same as that being considered by NASA for adoption. The sample holding conditions were varied somewhat; they will be described below.

It should be noted that all tests in this study were run in open air. Higher oxygen levels could be expected to enhance the flammability of the samples used here but the qualitative conclusions are not expected to depend on oxygen level.

#### 4) Modified NASA Test

Rationale. In the second phase of this study, as described below, the NASA screening test was modified to permit pre-heating of the sample. The initial intent was to use pre-heat temperature as an additional parameter, analogous to the radiant flux in the NIST tests. (A possible alternative to pre-heat temperature might be ambient oxygen level but the peak oxygen level in a spacecraft is well-controlled whereas pre-heating or radiation self-feedback may not be.) One would seek the minimum pre-heat temperature which would yield full length spread up the sample. Pre-heat temperature and external flux are quite comparable in their impact on flammability. The goal was to obtain more quantitative information on the flammability of a sample beyond the simple fact that it might pass the standard (room temperature) NASA test. Minimum conditions for upward spread would provide a quantitative measure of whether a material provides a small or large margin of safety relative to passage of the original NASA acceptance criterion.<sup>4</sup>

Preliminary tests with a box heater enclosure as a pre-heat device led quickly to the conclusion that some of the samples utilized here would cool very rapidly after removal of the box furnace (in seconds) unless some supplemental heat source counteracted the cooling process. An available electrically-powered radiant panel was employed for this purpose initially. It became evident, however, that the radiant panel would function most simply if it replaced the box heater entirely. It was only necessary to provide supplemental electrical cartridge heaters in contact with the two metal sides

---

<sup>4</sup>While this information by itself sheds light on potential material hazards, it is not readily translatable into a clearcut measure of the flaming potential of a material in a given usage. It is still necessary to find a relation between the minimum conditions for upward spread on the sample and realistic conditions (particularly of radiative feedback) that the sample is likely to encounter in practice. That is the subject of a current study.

of the NASA sample holder since an external radiation flux tends to heat the sample much more rapidly than it heats the relatively massive holder.

Test and Procedure. Figure 3 is a diagram of the modified NASA test. The radiant panel is a Research Inc. Model 4083 Pyropanel which contains up to twelve 500 watt linear quartz halogen lamps.<sup>5</sup> Throughout nearly all the tests here only eight lamps were used because of power supply limitations; the peak incident heat flux on the sample surface was about 18 kW/m<sup>2</sup>. The flux was varied by varying the power to the lamps. In a few tests at the end of the study, the number of lamps was increased to twelve yielding a peak heat flux of 32 kW/m<sup>2</sup>.

The panel is not large enough relative to the 30 cm sample length to provide a completely uniform heat flux along the sample length. The non-uniformity present translated into about a 25 C lower steady-state sample surface temperature near the top of the sample when the mid-height temperature was about 110 C; the temperature deficit at the bottom of the sample was only 10 C under these conditions. This non-uniformity can be expected to have some retarding effect on upward spread near the top of a sample in the tests discussed below, but no real qualitative impact.

Because the quartz halogen lamps operate at much higher temperatures than a gas fired radiant panel, they emit much more radiation in the visible and near-infrared where the sample's visual color can affect its absorptivity. Thus a given incident flux can yield differing steady-state temperatures for samples which differ in their absorption of this flux (see Section 5.2.1 below). This effect was compensated for here by measuring the steady-state surface temperature of each type of sample as a function of incident heat flux prior to flammability testing. (Thermocouples made from 0.0076 cm dia. wire were sewn or melted into the sample surface.) This information was used to infer the effective reflectivity of each sample, as discussed below.

In performing the tests, allowance had to be made for the differing rates of temperature rise of sample (fast) and sample holder (slow). The sample holder was allowed to heat for ten minutes prior to ignition of the sample. During the last three minutes of this interval the radiant panel was on, bringing the sample up to its steady-state temperature. Note that the NASA igniter was also in this radiation field; this had no apparent detrimental effects. The behavior of the sample subsequent to exposure to the radiation plus the igniter was videotaped for subsequent analysis.

## 5) Discussion of Results

### 5.1) Phase 1 Sample Behavior

In the first phase of this study a series of samples, obtained from or

---

<sup>5</sup>Mention of specific manufacturers is done for clarity only; it does not imply any endorsement by the National Institute of Standards and Technology.

recommended by NASA, was subjected to both the standard NASA test and to the NIST Cone and LIFT tests described above.

#### 5.1.1) NASA Tests

The samples used in this phase of the study are described in Table 1. They were tested in the conventional manner in the standard NASA test configuration in air. The results are shown in Table 2; they are the average from six repetitions with each material. The reporting of results is somewhat different than usual. In the second column, rather than report char length, we report the maximum height, relative to the bottom of the sample, reached by the attached flame front. This was discernible from the video tapes of the tests mainly because these materials bubble as they burn; this measure of the flame front position can be more difficult to implement with other, non-bubbling materials. This height is expected to be somewhat less than the char length normally reported but it is a quantity more in keeping with the NIST approach to analyzing flame spread behavior.

In the second column we report a computed average flame spread rate but it should be apparent from the comments that only the cotton toweling exhibited a spread process that was not totally dominated by the igniter flame. That being the case, there is not very much meaningful information in the spread velocities. This lack of much in the way of flammability behavior makes it difficult to make comparisons with the NIST test results on the same materials, as will be seen below.

#### 5.1.2) NIST Tests

In this first phase of the study all of the materials were tested with their rear surfaces insulated either with Kaoboard (LIFT) or Kaowool (Cone Calorimeter). This has been standard practice in the past, even with thermally thin materials; this was changed in the second phase of the study, as will be seen below.

The LIFT results for a material can be conveniently plotted on a single graph which displays both ignitability and opposed flow flame spread behavior as a function of incident heat flux on the sample surface. Figures 4 - 9 are such plots. In each of these Figures are displayed both the data points and the prediction of the fitted models for ignition and flame spread behavior. Consider, for example, the results in Fig. 4 for the cotton toweling material. The time to ignite this material is a strong function of the incident heat flux. Below a flux of about  $10 \text{ kW/m}^2$  the incident radiation is insufficient to raise the surface temperature to the point where a flammable mixture of gases is evolved from the surface. On the other hand, if a flame is produced locally on some portion of this material (by a local heat flux that exceeds the minimum), it will spread at a finite rate (here about  $2\frac{1}{2} \text{ mm/sec}$ ) even in the absence of any assistance from external radiation. If such external radiation is present, the flame will spread faster, with the spread rate approaching infinity as the flux approaches the minimum flux for ignition. (In this latter limit the whole surface ignites at once, hence the infinite spread rate.)

Decreasing flammability on such a plot implies several things. First, the minimum flux for opposed flow flame spread should increase; so also should the minimum flux for ignition. The spread rate should be as low as possible at any given flux and the ignition delay should be as large as possible. Simplified model equations for ignition and flame spread indicate which material properties must change to achieve such changes in flammability. For ignition delay time (thermally thick solid in the absence of heat losses) one has<sup>6</sup>

$$t_{ign} = (\pi/4) (k\rho C) \left( (T_{ign} - T_o) / q_f \right)^2 \quad (1)$$

where the product  $k\rho C$  (thermal conductivity, density and heat capacity) is the thermal inertia of the sample;  $T_{ign}$  is the ignition temperature;  $T_o$  is the initial temperature of the sample;  $q_f$  is the incident heat flux. The minimum flux for ignition can be shown to be directly proportional to the ignition temperature,  $T_{ign}$ .

For opposed flow flame spread rate one has (again for a thermally thick material)<sup>6</sup>

$$V_s = \Phi / (k\rho C)(T_{ign} - T_s)^2 \quad (2)$$

where  $\Phi$  is a measure of the heat feedback from the flame to the surface and  $T_s$  is the temperature of the surface ahead of the flame (recall that an incident radiant flux may have preheated the sample).

With these expressions in mind one sees that increasing thermal inertia both increases the ignition delay time at any given heat flux and slows the flame spread rate subsequent to ignition. Increased ignition temperature has a similar effect; it also will increase the minimum incident flux necessary to produce ignition since it raises the heat loss rate from the surface. An alternative way to slow flame spread is to weaken the heat feedback from the flame to the surface (decrease the value of  $\Phi$ ); this can be achieved, for example, by the addition of flame retardants.

The materials in Figures 4 to 9 are arranged in the order of increasing value of the minimum flux for opposed flow flame spread; this ordering also appears to coincide with that of the minimum flux for ignition. Table 3 lists the actual values for these two quantities. In view of the data scatter, the minimum ignition fluxes for Kydex and for Pyrell foam cannot be said to be different. As noted above, the minimum flux for ignition reflects mainly the

---

<sup>6</sup>Thermally thick equations were employed in the analysis of the Phase 1 sample behavior since the samples had thermally thick insulative backings; analogous equations for thermally thin samples are developed in Appendix A. The pertinent properties are nearly the same though the dependencies are different.

ignition temperature of the material. That, in turn, reflects the thermal stability of the polymer(s) in the solid. The aromatic nature of the polycarbonate in Lexan makes it substantially more stable than the cellulose in the cotton toweling. It is interesting to note that adding the flame retardant (a halogen) to Lexan has no really appreciable effect on its behavior in these tests.

The effective values of thermal inertia, inferred from the ignition data, vary by nearly two orders of magnitude for these materials. The data here have been reduced on the assumption that the sample is thermally thick; actually the sample plus its insulating backing form a thermally thick unit and this influences the apparent thermal inertia. The effective values of thermal inertia, when utilized in the above models (actually, an analog to Eq. 1 is used; see Ref. 4) produce the predicted results shown as the solid lines in the Figures 4-9. It is apparent that the fit is rather rough for some of these materials. Some of these materials undergo drastic changes in physical dimensions and form as they are heated. Pyrell foam, for example, shrinks considerably during heating while Lexan, and to a lesser extent, Kydex, foam up. These sorts of alterations, which can have a strong effect on the thermal properties of the condensed phase, are not explicitly accounted for in the simplified models underlying Eqns. 1 and 2. The changes are thus lumped into the effective thermal inertia and treated as a constant for all incident flux levels. The behavior of the Lexans, for example, suggests that this is only roughly true.

It was noted above that incident radiation and sample preheating are quite analogous in their effects. The last two columns of Table 3 quantify this point for the materials studied in the first phase. The minimum spread temperature is the steady state temperature that a black material would achieve at the incident flux where flame spread ceased in the LIFT apparatus. Thus it would appear that while the cotton toweling can sustain opposed flow flame spread at room temperature, the Lexans require preheating to temperatures well in excess of 300 C. Viewed in this way, one might conclude that a material such as Lexan is inherently safe in applications where operating temperatures are well below this level. However, one must bear in mind that real applications may include material configurations that enable radiative feedback between elements of the material surface; this could possibly provide the requisite preheating effects if a sustained ignition source was present. This issue is addressed in a current study.

The rate of heat release measurements for certain of these materials are shown in Figures 10 - 12. Heat release rate is the product of heat of combustion of the evolved gases (kJ/kg) and the rate of generation of these gases per unit area of the burning surface (kg/m<sup>2</sup>sec). The heat of combustion generally stays fairly constant regardless of extent of degradation (time) or the incident heat flux but the rate of gasification can vary strongly with both of these parameters. Thus one sees that as the external flux from the Cone

heater is increased, the ignition delay time shortens<sup>7</sup>, the burning duration tends to get shorter and the peak value of rate of heat release gets higher. (Note that the vertical scale for Lexan is two times greater than for the other two materials.) The peak rate of heat release is generally the quantity which is most utilized in flammability studies (though, strictly speaking, the whole curve is relevant). The area under the curve -- the total heat released-- is proportional to the sample thickness, which is not an intrinsic flammability parameter. Figure 13 shows that the peak increases monotonically with increasing incident flux for all of the materials but the rate of increase can vary. This rate of response to increasing flux is dependent on the chemical and physical properties of the fuel; thus one can have crossovers in relative behavior, as seen in Fig. 13.

Note that peak heat release rate is not a predictor of performance in the NASA or in the NIST tests. Lexan, the most flame resistant material in both the NASA and NIST tests, has the highest peak heat release rate. The cotton toweling and Pyrell foam, which differed appreciably in the NASA and NIST tests do not differ appreciably in Fig. 13. Note also that rate of heat release is not included in either Eq. 1 for ignition delay time or Eq. 2 for opposed flow flame spread rate. Rate of heat release is probably implicit to some extent in the factor  $\Phi$  in Eq. 2. It is much more explicit in models of concurrent flame spread, as will be seen below. However, it must be combined with other aspects of the behavior of a material in order to be used for a flammability prediction. This does not mean that heat release rate should be downplayed; total heat release rate is probably the best measure of fire size and, in many normal gravity room fire situations, it is the principal measure of the hazard which the fire poses [6]. This total heat release rate is the product of the release rate per unit area and the area burning, implicating both flame spread behavior and local heat release rate per unit area.

### 5.1.3 Comparison of NASA and NIST Test Behavior

Table 4 is an attempt to discern a correlation between the results of the NASA and NIST LIFT tests. The first column gives the mean upward spread velocity in the NASA test but it should be recalled that only the cotton toweling exhibited full upward spread. The mean upward spread velocities, as crude as they are in view of the very limited spread, do appear to correlate (inversely) with the minimum flux for opposed flow spread and the minimum flux for ignition as listed in the next two columns. This suggests that the same underlying properties of the materials are determining the responses in these differing tests. The last column is more ambiguous. From Eq. 2 (or its analog for a thermally thin material) one expects the computed quantity there

---

<sup>7</sup>The Pyrell foam appears to be an exception, probably because, even though the ignition time decreases, the instruments from which the rate of heat release is calculated cannot respond any faster.

to increase directly with the magnitude of the spread velocity<sup>8</sup>. Again there is some indication that this may be the case but the issue is obscured by the effective thermal thickness of the samples during spread, especially for Pyrell foam (see footnote to Table 4). In any event it is probably stretching things too far to seek this correlation when the behavior in the NASA test was so minimal.

## 5.2) Phase 2 Sample Behavior

The standard NASA test provided very little quantifiable information on most of the materials tested in Phase 1 other than their failure to yield upward flame spread. (That is, of course, the only intended output of the test.) It appears to be desirable to elicit more information from such a test, if possible. In particular, it would be informative regarding material usage, to know what conditions a material does require in order to sustain upward flame spread<sup>9</sup>. Recall, as noted previously, the most legitimate concern is not with raising the oxygen level until one sees spread but with quantifying the potential effects of external radiation (or self-feedback) on upward flame spread. In particular, we have extended the test in an attempt to determine the minimum incident radiant flux level necessary to yield full upward spread.

In the second phase of the study we also made some changes in the test materials. In particular, the Pyrell foam was dropped because the extreme dimensional changes it undergoes make interpretation of its behavior more difficult. Kydex was also de-emphasized. Three other materials were obtained from NASA; these are described in the lower portion of Table 1.

### 5.2.1) Behavior in Modified NASA Test

Since one goal here is to compare behavior in the NASA and NIST tests, there is an issue regarding the best manner to expose the samples in the two types of test methods. At least two of the samples required physical support in the NIST tests because of their thermoplastic behavior (Lexan and Kydex). The minimum support is a thin sheet of aluminum foil under the sample which must be oriented horizontally. On the other hand, preliminary tests showed that aluminum foil on the back (non-irradiated) face of a thermally thin sample in a NASA test appreciably lowers its flammability. Aluminum foil was thus used

---

<sup>8</sup>Eq. 2 is for opposed flow spread while the NASA results are for concurrent (upward) spread but the same quantity has a similar effect on both modes of spread.

<sup>9</sup>This implicitly assumes that such conditions carry over to, or are correlated with, the necessary conditions for concurrent flame spread in microgravity. Testing of this assumption awaits a capability for forced flow flamespread studies in a facility with a longer test time than that in a drop tower.

only in the NIST tests of Lexan and Kydex and not at all in the NASA tests. All of the NIST tests were run with horizontal samples, however, for consistency with the thermoplastic samples. This led to some ambiguities in efforts to use the NIST results to predict the NASA results, as discussed below. The NASA tests were performed in the normal vertical mode with no aluminum foil. The igniter in the NASA test was placed so as to play equally on the front and back of the sample, making spread up both surfaces equally likely.

The samples were preheated to an essentially steady temperature at the selected incident radiation level. Recall that the steady temperature versus incident heat flux was pre-calibrated for each sample type. Because of the allowance of a longer preheat time for the NASA holder, as described above, the sample and holder were very nearly at the same temperature when the NASA igniter was triggered. The subsequent behavior of the sample was determined from a video tape taken from the irradiated side.

Recall that the radiation from the quartz/halogen lamps used here peaks in the near-infrared so that sample reflectivity is a real concern. The effective value of this reflectivity was inferred from the following steady-state energy balance.

$$(1-r)F_0 = (h_f + h_b)(T_{s,s} - T_a) + (\epsilon_f + \epsilon_b)\sigma(T_{s,s}^4 - T_a^4) \quad (3)$$

Here  $r$  is the desired value of sample reflectivity for the halogen lamp radiation,  $F_0$  is the known value of incident heat flux,  $h_f$  and  $h_b$  are the convective heat transfer coefficients for the front and back surfaces of the sample (these are assumed to be equal and calculated from a standard heat transfer correlation, Ref. 7),  $T_{s,s}$  is the measured steady-state sample temperature at the given incident flux,  $T_a$  is the ambient temperature,  $\epsilon_f$  and  $\epsilon_b$  are the emissivities of the front and back surfaces of the sample (assumed equal and taken as 0.90 due to the low sample temperatures which imply far infrared radiation),  $\sigma$  is the Stefan-Boltzmann constant.

Table 5 lists the calculated values of reflectivity for the Phase 2 materials. The calculations were mainly carried out at the high end of the measured steady-state sample temperatures; calculations at two different temperatures for Nomex show that this makes little difference. Similarly, reasonable variations in the parameter values in the above equation had only a weak effect on the calculated reflectivities. This is not an entirely satisfactory way in which to obtain the reflectivity values but it should be adequate for the present purpose. Note that the values are substantially greater than zero for nearly every material. Thus the actual absorbed flux for most materials was rather limited.

Figures 14 to 19 show the results of the pre-heated NASA tests, arranged in order of increasing resistance to upward spread. Plotted there (open circles) is the maximum upward extent of the char zone as a function of the absorbed heat flux. (The incident flux has been multiplied by one minus the reflectivity for a given material from Table 5.) The dashed line across the graph at 30.4 cm indicates the top of the sample; the solid curved lines are model predictions which will be discussed later. At the top of each plot is

shown the steady-state temperature that corresponds to the heat flux directly below it on the abscissa. The char length here is believed to be essentially equal to the maximum height of the attached flame front. Thermocouple measurements in Nomex samples indicated that the two appear to coincide.

Note that full length spread as a result of radiative pre-heating was obtained only on the Nomex fabric (Fig. 15). (Full length spread was, of course, achieved also on the cotton toweling with no preheating; see Fig. 14.) This Nomex required a surprisingly small degree of preheating in order to yield full length spread. An FTIR spectrum run on the sample confirmed that it was indeed Nomex, though it cannot be asserted that the behavior seen here is necessarily typical of other samples of Nomex. In most, but not all, of the NASA tests of this material, a portion of the sample edge became exposed after shrinkage caused it to pull out of the sample holder. While this might easily contribute to the material's apparent flammability, the fact that full length spread occurred even in the absence of such edge exposure indicates that this was not the source of the relatively poor performance of this material.

The flame-retarded cotton cloth (Fig. 16) also exhibited a unique behavior. It tended to show very fast but very brief spread of the char front in response to exposure to the NASA igniter flame. This was the only material exposed to higher fluxes with the 12 lamp radiant panel. The maximum char length continued to increase with increases in the incident flux but never quite reached the top of the sample at the peak incident flux ( $32 \text{ kW/m}^2$ ) from this enhanced radiant source. This means that, in spite of the fact that a flame spread process appeared to extend well beyond the immediate influence of the NASA igniter flame, it did not become self-sustaining. This material exhibited unusual behavior in the NIST tests also, which made its data interpretation more difficult.

The epoxy/glass circuit board material (Fig. 17) was less flammable than expected. Although it was labelled as a NEMA grade G-10 material (not explicitly flame-retarded), it behaved as if it was flame-retarded; it gave a positive qualitative analysis test for halogen content implying that it was indeed retarded. All but one of the tests of this material were done using three NASA igniters bundled into the igniter wire (to assure that failure to ignite was not limiting the observed behavior); this gives a somewhat higher flame which lasts about 50 seconds. Flaming on the sample persisted only as long as the igniter flame persisted. This suggests that this material might continue to burn in the presence of a pilot flame; such a situation could conceivably occur in a real application and it raises the question as to the best way to test such a retarded material.

The preheating tests with Kydex (Fig. 18) were stopped by its thermoplastic nature. At fluxes higher than that for which the last data point is shown, the material slowly ran out of the NASA holder during the preheat interval.

One test with Lexan 9034 (Fig. 19) is shown as achieving full length spread but this thermoplastic material actually melted downward at about the same rate at which the flames spread upward. This particular result was not reproducible; it appeared to stem from a build-up of dripping, flaming material on the wire which supports the NASA igniter. Note that the other

Lexan tests yielded virtually no flame spread. Testing of this material was impeded by its thermoplastic character and probably could not be carried out at higher degrees of preheating.

If time had permitted, others of the sample materials could have been exposed to higher incident heat fluxes with the enhanced radiant panel. However, only the epoxy/glass circuit board might have yielded more useful information.

The peculiar mix of sample behaviors seen here somewhat frustrated the goal of finding the full effects of preheating on upward flame spread tendency. However, it is clear that there is a wide variation in response of materials to preheating. That varied response potential is not necessarily revealed by the behavior in normal NASA tests at room temperature.

#### 5.2.2) Behavior in the NIST Tests

Recall that the sample backing conditions were changed somewhat for the NIST tests in the second phase of this study. Instead of an insulating ceramic fiber board being in contact with the back of the samples, as in the first phase, the samples had an air gap of at least 1.3 cm. Only Lexan and Kydex had thin aluminum foil in contact with the sample back side; other materials had nothing in contact with their back surface. In the LIFT tests a blackened cooled metal plate beyond the air gap simulated a cold ambient. In the Cone Calorimeter tests the gap was backed by a layer of ceramic wool. In both types of tests these backing conditions largely suppressed flaming on the back of the sample due to poor air supply. These changes were made so that the sample could behave in a thermally thin manner thereby more closely resembling the behavior in the NASA tests. It would have been desirable to have the samples burn equally on their front and back surfaces, as in the NASA tests, but the existing sample holder configurations for the NIST tests preclude this.

The Cone Calorimeter results for rate of heat release as a function of incident heat flux are shown in Figures 20 to 24; they are arranged in order of decreasing peak heat release rate. For the two materials that are nominally the same in the two phases of the study, i. e., Lexan 9034 and the cotton toweling, there appear to be some differences in behavior; the differing heat flux levels make this a little difficult to quantify, however. Lexan does not burn in a very reproducible manner as a result of its tendency to intumesce. The cotton toweling used in the second phase of the study was actually from another manufacturer's batch; this, as well as the differing sample backing conditions could be the source of the differences between the results in Fig. 11 and Fig. 21.

Inspection of Figures 20 to 24 reveals that there is a considerable diversity of heat release rates among the phase 2 materials. Lexan 9034 is by far the highest. The heat release behavior from the flame-retarded cotton cloth, at the opposite extreme, is so short-lived that the shape of the curves is probably being distorted by the response time of the oxygen analyzer at the

heart of the Cone Calorimeter. Note that for incident heat fluxes for which no heat release rate curve is given, ignition was not obtained in these tests.

The ignition and lateral flame spread behavior of these materials is shown in Figures 25 to 30; they are arranged in order of increasing minimum flux for ignition. (Cotton toweling and epoxy/glass appear comparable here but cotton toweling is placed first on the basis of its clearly lower minimum ignition flux in Phase 1.) An ordering based on minimum flux for lateral spread appears similar, although the vague behavior of the flame retarded cotton may or may not fit this scheme.

The solid lines through the LIFT data are the predictions of the ignition and lateral spread models, obtained as discussed in Appendix A. There is clearly a varying degree of success in this fitting process. The biggest discrepancies occur with the flame retarded cotton. This material was problematical in its behavior in that it exhibited a vague transition from true ignition, with a flame attached to the solid surface, to a condition where, as the incident flux decreased, a brief flash would be the only sign of combustion. Its flame spread behavior was equally difficult to pin down.

### 5.2.3) Comparisons Between Modified NASA and NIST Test Results

The first type of comparison one might wish to make is between the modified NASA test behavior and one or more of the direct measures of flammability properties seen in the NIST tests. For example, the peak rate of heat release has been correlated with some success with room fire hazards [8]. Here, however, if one compares the behavior in the modified NASA tests (Figs. 14-19) with the Cone Calorimeter results for the same materials (Figs. 20-24) there clearly is not the expected result. Lexan 9034, with its very high rate of heat release, was found to be the most resistant material in the modified NASA test. Nomex, with its low rate of heat release, was found to be weakly resistant to upward spread when pre-heated in the NASA test.

Recall that in discussing the results of the LIFT ignition and lateral flame spread tests it was noted that a shift to the right (toward higher flux) in the minimum fluxes for ignition and lateral flame spread indicates lower flammability in these tests. By that measure Nomex is the least flammable in the LIFT tests which does not accord with its behavior in the modified NASA tests.

This issue is examined more closely in Table 6 which compares the minimum flux for lateral spread with that for upward spread, as found here in the modified NASA tests. These limiting conditions for spread might be thought of as being influenced by comparable considerations of heat transfer and heat loss so that one could expect them to correlate. That is, one might expect the minimum flux for upward spread to be some approximately fixed fraction of the minimum flux for lateral spread. One expects the fraction to be less than one in keeping with the notion that upward spread is more easily achieved due to its more effective transfer of heat from the flame to the unburned material. (Hence the idea that an upward spread test is more severe than a lateral or

downward spread test.) The data in Table 6 do not contradict any of these notions directly but they also cannot fully confirm them. The possibility of a correlation between the two types of spread limits is obscured by the failure to reach the upward spread limits for most of the materials. The behavior of Nomex is certainly consistent with the idea that upward spread occurs more readily but the behavior of the epoxy/glass circuit board material appears to be on the verge of contradicting this notion. More data are needed before one abandons the idea that upward spread is always more likely than opposed flow spread.

#### 5.2.4) Comparisons Between a Simplified Upward Spread Model and Results of Modified NASA Tests

The following is a more extended attempt to find a relation between some of the NIST test results and the modified NASA test results. This attempt was ultimately unsuccessful, probably for a variety of reasons, as discussed below. It is instructive, however, about what aspects of flammability are implicit in the ability of flames to spread upward on a surface.

Simplified Upward Flame Spread Model. The model that was applied here was chosen because it is simple enough to have analytical solutions thereby showing the explicit parameter dependencies of the spread behavior. The model is due to Cleary and Quintiere [9]; it has been shown to be quite successful in predicting fire growth on interior wall surfaces in full-scale room fire tests. In such applications the flames are turbulent, the burning materials are thermally thick and they are burning on one side only. Here the flames are laminar, most of the materials are thermally thin and they are burning on both surfaces. The implications of these differences will be discussed below.

The model describes the upward movement of the tip of the flames, the top of the pyrolysis front (attached flame front) and the bottom end of the flaming zone (burnout front); see Fig.31. In so doing it utilizes results from some of the NIST tests. Calculation of the time-dependent changes in these three measures of overall flame zone movement requires the solution of the following three equations:

$$dy_p/dt = (y_f - y_p)/\tau_{ig} \quad (4)$$

$$dy_b/dt = (y_p - y_b)/\tau_b \quad (5)$$

$$(y_f - y_b) = k_f [Q_{ign} + Q(y_p - y_b)] \quad (6)$$

Here  $y_p$  is the locus of the pyrolysis front (attached flame front, corresponding to the char front measured in the experiments),  $t$  is time (starting from the beginning of the ignition interval),  $y_f$  is the locus of the flame tip,  $\tau_{ig}$  is the time that it takes the flames playing on the material surface above the flame front to ignite that material (implicitly the flame

heat flux is a constant from the tip of the flames down to the pyrolysis front),  $y_b$  is the locus of the burn-out front (bottom edge of the flame zone),  $t_b$  is the total burning time of the material at any given location (not the total burning time of the sample),  $k_f$  is a proportionality constant,  $Q_{ign}$  is the rate of heat release from the igniter per unit width (transverse to the spread direction),  $Q$  is the average rate of heat release per unit area of the sample material.

Equations 4 and 5 make simple statements; the flame front moves up at the rate at which the material ignites due to heating by the flames and the burn-out front follows at the rate at which the material burns through. Equation 6 is less obvious. It is a linearized version of a relationship seen experimentally for turbulent flames. For turbulent flames the flame height is found to be proportional to the total heat release rate per unit width raised to the 2/3 power; for laminar flames the power appears to be weaker (see below). Thus Eq. 6 implies that the model, in this aspect at least, will overestimate the ability of flames to spread upward. This is because Eq. 6 overestimates the response of the flame length to the heat release process and Eq. 4 implies a greater flame length will increase flame speed. The assumption of a first power dependence in Eq. 6 is necessary to facilitate an analytical solution to the model equations.

In applying the above model, it is assumed that the starting condition is that the material is ignited up to the tip of the igniter flame. The model equations then predict whether the flames will grow or not and at what speed. The outcome depends, of course, on the model input parameters. The particular combination of parameters of most importance and the origin of the parameter values used will be seen below.

The above three equations have to be solved for three possible time domains in the present application. The first domain is for the time interval during which the NASA igniter is still burning and the initially-ignited material has yet to burn out. The second domain is a possible interval during which the NASA igniter has ceased but the initially-ignited material is still burning. The third domain is the principal one of interest here: the time after both NASA igniter cessation and burn-out of the initially-ignited material. This is the long time behavior which determines whether the flame is indeed progressing upward or not. The long time behavior of the pyrolysis front position, which is what is measured experimentally, is of the form below.

$$y_p(t) = y_{p0} [1 + A + B \exp(\alpha(t - t_b))] \quad (7)$$

Here  $y_{p0}$  is the initial height of the pyrolysis zone as dictated by the igniter flame height,  $A$  and  $B$  are combinations of model parameters which can be thought of as constants here. The factor which determines whether the flame front progresses or (non-physically) regresses is the sign of  $\alpha$  in the above exponential term. This translates into the following condition for upward spread; the rate of heat release per unit area of the material must exceed a critical value given by

$$Q^* = (1/k_f)[(t_{ig}/t_b) + 1] \quad (8)$$

In the experiments one does not look for exponential upward spread but rather for the flame front to reach the top of the sample. Because of the finite value of the constant A in Eq. 7 this occurs in the model calculations before Eq. 8 is satisfied; typically one finds that the top of the sample is reached when the rate of heat release from the sample reaches approximately 80% of the critical value in Eq. 8.

Equation 8 indicates that the critical flammability properties controlling the possibility of upward flame spread are the rate of heat release, the proportionality factor between heat release rate per unit width and flame height, the material's ignition delay time at the flame heat flux and the material's burn time. To apply the model here it was necessary to obtain values for these parameters pertinent to the conditions of the modified NASA tests; recall that all of these parameters, except the factor  $k_f$ , depend on the extent, if any, to which the sample has been pre-heated.

Consider first the ignition time at the flame heat flux. Laminar flame heat fluxes tend to be higher than those from turbulent flames. The NASA igniter flame, whose temperature is comparable to the flames expected on the burning samples, has a cold wall heat flux measured at about 50 kW/m<sup>2</sup> in this study. As the wall warms up the net flux decreases to a value of about 30 kW/m<sup>2</sup> [Ref. 10]; this is for a laminar diffusion flame on PMMA and is assumed to apply here as well. Here the experimental value of ignition delay time at 40 kW/m<sup>2</sup> was used. This was corrected approximately for pre-heating using the measured value of pre-heat temperature at a given incident flux, the ignition temperature inferred from the LIFT ignition data and a thermally thin version of Eq. 1, which is proportional to the first power of the temperature increase above the initial value. This correction consists of reducing the experimental ignition delay time by a factor

$$(T_{ign} - T_s)/(T_{ign} - T_a)$$

where  $T_{ign}$  is the sample's ignition temperature,  $T_s$  is the pre-heat temperature of the sample prior to the application of the NASA igniter, and  $T_a$  is the ambient temperature. For a thermally thick material (such as the cotton toweling) this factor is squared, in accord with Eq. 1.

The value of the proportionality factor  $k_f$  has been well-established for turbulent flames but no data were found for the laminar flames pertinent here. Thus a value for  $k_f$  was inferred from measurements of the NASA igniter since its behavior was readily measured and its total heat content was known. Measurements of igniter flame height versus time were made with the flames playing on both sides of an inert material. This was done for both a single igniter and for three igniters bundled together (a configuration used for the epoxy/glass samples). Fig. 32 shows a typical result for a single igniter; the shorter flame height compared to the 6.4 cm specification is a consequence of splitting the flame to the front and back of the sample. To obtain a value

of  $k_f$ , one first fits a simple polynomial dependence (a parabola was used here) to the observed flame height versus time variation. If the heat release rate is then assumed to be linearly proportional to flame height (as in Eq. 6 above), one can obtain the proportionality constant ( $k_f$ ) from the requirement that the time integral of the heat release equal the known energy content of the NASA igniter. The value one gets for a single igniter (.0077 m<sup>2</sup>/kW) is different than the value for three igniters (.00115 m<sup>2</sup>/kW). This immediately implies that the first power dependence between heat release rate and flame height assumed in Eq. 6 is incorrect. In fact the results imply that the power is close to  $\frac{1}{2}$ , lower than for turbulent flames. Again, this implies that in this aspect the model overestimates the ability of the flame to move upward on a material.

The average rate of heat release and the burn time for a material are both obtained from Cone Calorimeter data. However, there are some difficulties. Figures 10 to 12 and 20 to 24 show that the rate of heat release varies with incident heat flux on the sample and, at a given flux, it varies with time. The model demands a temporally constant heat release rate (there are models which can handle the time-varying behavior but they require numerical solution). An average value for  $Q$  and a value for the burn time  $t_b$  are computed by approximating the heat release process as a square wave equal in height to the peak heat release rate seen experimentally. Energy conservation then allows calculation of  $t_b$ .

Figures 33 to 35 show the flux dependence of these approximate measures of the heat release rate behavior. The first thing to note is that the Cone Calorimeter data must be extrapolated to the lower heat flux levels that were used to pre-heat the samples in the modified NASA tests. For reasons which are not completely clear, the samples would not burn in the Cone Calorimeter at the heat fluxes where they partly or fully burned in the NASA tests. This is particularly striking for a material such as Nomex which gave no ignition in the Cone Calorimeter at fluxes of 20 and 30 kW/m<sup>2</sup> whereas it burned in the modified NASA test at an incident flux of about 10 kW/m<sup>2</sup>. Possible reasons for such differences include both the sample orientation and the vast differences in igniters. Recall that the samples were horizontal in the Cone Calorimeter. There is mixed evidence from studies of other materials as to how the flame feedback flux differs with sample orientation; some results imply higher feedback with a vertical orientation [11] while others indicate that a horizontal orientation usually gives greater heat feedback from the flame [12]. The heat release rate behavior of only one of the test materials used here (epoxy/glass circuit board) was measured in both orientations; the peak rate of heat release was consistently higher for the vertical orientation. A higher feedback would be expected to help stabilize a flame attempting to spread upward. The igniters differ drastically in strength; the Cone Calorimeter uses a weak spark gap held in the evolved gases from the sample whereas the NASA igniter is a sustained flame. The discrepancy suggests the need to further explore the influence of orientation and ignition conditions on Cone Calorimeter data, particularly at low incident heat fluxes.

There is a further difficulty in using the Cone Calorimeter data for the present model predictions. In the Cone the samples all burned on one side

only due to the design of the system; the samples in the modified NASA test burned on both sides. It thus is necessary to translate the one-sided Cone data to the two-sided NASA test condition. For a thermally thick material this can be done unambiguously by simply cutting the burn time in half, using the same peak heat release rate. Within the assumptions of the above model, the same procedure should be used for thermally thin materials. However, a real thermally thin material can be expected to exhibit a higher two-sided rate of heat release than it does for one-sided burning because the extra heat flux will drive the sample temperature upward and make it gasify faster (cutting the burn time by more than a factor of two, at the same time). This enhancement of the rate of heat release due to two-sided burning is chemistry-dependent so it will differ with the nature of the material. There is no present way to correct for this effect. The data were necessarily treated in the above manner for use in the model (i. e., keeping the same peak heat release rate and dividing the burn time by a factor of two). In this aspect, for the thermally thin samples, i. e., all but the cotton toweling, the model is expected to under-predict the ease of upward flame spread. Thus there are at least two opposing factors of unquantified magnitude which can be expected to make the model depart from experiment.

A typical model prediction of pyrolysis height versus time for several pre-heat fluxes is shown in Fig. 36. The downward movement of the front seen there is, of course, non-physical; it is a consequence of burnout of the initially ignited material and the subsequent weakening of the overall rate of heat release driving the flames. Essentially it indicates that the flames are dying. Experimentally one measures only the maximum height that the flame front reaches.

The model predictions of maximum flame front height (essentially equal to char length) versus absorbed flux are shown in Figures 14 to 19 as the solid lines (except for Kydex in Fig. 18). Inspection of those Figures shows that the model strongly under-predicts the observed flammability for three of the materials (cotton toweling, Nomex, flame-retarded cotton) and strongly over-predicts the flammability of two materials (epoxy/glass and Lexan 9034).

The quantitative failure of the model in this context is disappointing but not particularly surprising in view of the various caveats explained above. As a practical matter, however, it does indicate that we have been unable to reconcile the results of the NIST tests and the modified NASA tests. There is good reason to believe that these two types of results could be reconciled with further efforts. More detailed models of upward flame spread do exist with fewer simplifying assumptions, though at the cost of numerical solution and thus obscured parameter dependencies. Better input data from the Cone Calorimeter data could be obtained though this would call for some development work on how best to ignite and burn on both sides of the sample. A check was made with one of the materials (epoxy/glass) to see if Cone data obtained in a vertical orientation rather than a horizontal orientation would improve the model prediction. This orientation change by itself was not helpful in this regard.

#### 6) Some Practical Implications of This Study

The lack of agreement between the above model and the results of the modified NASA test should not obscure some of the more basic implications of this study. In particular, the NIST tests on the Phase 1 and Phase 2 materials indicate that they are all flammable, even though only one failed the standard NASA test. The viewpoint adopted in the NIST test approach is that virtually all organic materials are flammable but most real materials require some additional heat input, typically from "external" radiation in order to continue to burn and spread flames. Many familiar, common building materials behave this way.

The standard NASA test has functioned as a go/no-go discriminator for the acceptability of materials and it has undoubtedly contributed substantially in reducing potential fire hazards aboard spacecraft. However, the standard NASA test must be seen as too black and white as regards the conclusions that are drawn from it. A material which passes this test, even in "worst case conditions" is not necessarily non-flammable under all plausible conditions aboard a spacecraft. While the test subjects the material to the highest oxygen level it will see in practice and, perhaps (no guarantee) the largest ignition source it will see in practice, it does not include the flame-sustaining effects of "external" radiation. The results of this study show that materials vary widely in their response to this radiative pre-heating effect.

The standard NIST tests also do not at present offer a clear-cut measure of susceptibility to upward spread, as a consequence of radiative pre-heating, in the NASA test configuration. Some measure of the susceptibility of a material to enhanced flame spread as a consequence of "external" radiation is desirable in order for users to more realistically assess its potential hazards. This seems particularly desirable for materials which are present in appreciable amounts in a spacecraft. The LIFT test provides such information for opposed flow flame spread. In accord with the idea that concurrent spread is a more severe test of a material, however, one is led back to upward spread. Then the modified NASA test, as used in this study, becomes a possible candidate for this role. It clearly would require some further development for this purpose. For example, the radiant panel used should be larger in dimensions for improved flux uniformity and lower in temperature so that reflectivity effects are minimized.

If a radiative pre-heating element is added to the testing of spacecraft interior materials, some guideline as to how much pre-heating is realistic needs to be developed. Recall that the most probable source of this is self-feedback of radiation among parts of the same burning object. A program to quantify these effects is planned at NIST as a logical extension of the present study.

#### 7) Some Recommendations Concerning the Problem of Relating Normal Gravity and Micro-Gravity Flammability

It is apparent that the only practical way to assess potential flammability of materials in a micro-gravity environment is by normal gravity testing. This implies a need to pursue both near-term and long-term goals. In the near-term

there is a need to establish the relation between normal gravity and micro-gravity flammability for a set of realistic materials in a test configuration incorporating both pertinent gas flow rates and "external" radiation effects. The objective is to validate an extended flammability test method and demonstrate, at least in a limited manner, that it is conservative (or at least not non-conservative) in worst case conditions.<sup>10</sup> In the long-term there is a need to develop a sufficient understanding of micro-gravity flammability to assure control of any potential fire threat aboard a spacecraft.

Near-term goal. This is an extension of the work of Kimzey [13] to include two additional variables that can be expected to enhance micro-gravity flammability (flowing ambient gas and external radiation). However, it must be decided which aspects of flammability to focus on. If the controlling concern is fire growth, then rate of flame spread and total fire size are the factors to be examined. If the controlling concern is toxicity, rate of toxic gas generation and total amount of toxicants are to be examined. The complication here is that the worst case conditions for fire growth and for toxic gas generation may not be similar.

It is suggested that a configuration analogous to the modified NASA test used here could serve the purpose if the principal concern is fire growth. Its principal attraction is its relative simplicity though the relation between external radiant flux and self-feedback flux must be considered. The flat sample configuration maximizes oxygen access to the flames, enhancing completeness of combustion and flame speed. Concurrent flame spread (spread in the direction of gas flow) at the highest realistic oxygen levels should provide worst case conditions. The validation experiments would consist of characterizing flame spread rate as a function of gas flow velocity and external radiant flux, first in normal gravity and then in micro-gravity. The apparatus would be identical for both. It could consist of a simple blow-down tunnel providing flows up to 25 cm/s for up to 60 seconds. Because there are three parameters (heat flux, flow velocity and material), experiment development and extensive parametric studies would be confined to normal gravity (upward spread). A limited number of micro-gravity tests would be done first in airplane flights, then in sounding rockets for materials thick enough to require the longer experiment time. Ignitability is not the focus of the study since it is likely to be generally comparable between normal and micro-gravity. Thus the igniter should be chosen to be big enough to assure local ignition of all samples.

Because such validation testing must be confined to a relatively small number of materials, there will be numerous other materials where direct assessment of the role of gravity cannot be made. This implies a need to understand the factors that control the flame spread behavior, first in normal gravity, then in micro-gravity. In spite of the rather poor showing for the model versus

---

<sup>10</sup>One seeks assurance that the flammability behavior in micro-gravity will, at least, not be any more severe than in normal gravity. At the same time, the test method should not be so conservative that it excludes materials unnecessarily.

experiment comparisons in this study, efforts along this line should be continued. The semi-empirical modeling approach has the greatest likelihood of being able to deal with real materials in the near future. Because the inputs in this kind of model can only be obtained in normal gravity, the model's predictions of micro-gravity behavior must be tested empirically. More detailed and fundamental models are necessary components of a longer-term approach to micro-gravity flammability analysis.

If toxicity is the principal concern, establishing worst case conditions is more difficult. Factors which limit oxygen access to the flame zone may enhance toxic gas generation through incomplete combustion. Testing at the lowest realistic ambient oxygen level ( $\approx 19\%$ ) is indicated. So also is a sample configuration which inhibits oxygen access to the flames such as two parallel sample sheets with concurrent flame spread in the gap between them. The difficulty here is that this is not known to be the worst case, only more severe than a single sheet. Note that such configurations provide self-feedback of radiation, lessening the need for an external flux but it is not clear if that flux should be eliminated. Because of these types of uncertainties, more ground-based experiment development is indicated. It is not realistic to conduct direct animal exposures to determine toxicity through micro-gravity tests. Thus it would be necessary to utilize a model of toxicity based on the principal known toxicants (the so-called N-Gas Model). Such an approach has had reasonable success in ground-based fire studies [14, 15, 16]. Gas samples from micro-gravity tests could be grabbed for later analysis and quantitation of the principal toxicants.

There are no models which predict toxic gas production from first principles; rather one attempts to predict the rate of spread and total mass burning rate and assigns an empirical yield for a given product. In this sense, this problem is analogous to the fire growth problem above and it could be pursued similarly. Understanding the factors in micro-gravity which might increase the yield of specific toxicants is part of a long-term micro-gravity flammability research program.

Long term goal. Understanding micro-gravity flammability sufficiently to assure control of hazards related to potential fires aboard manned spacecraft is a very broad and ambitious goal. The many facets of this have emerged from the 1986 workshop which NASA conducted and subsequent reports expanding on the details and proposed approaches [17, 18, 19, 20]. Reference 20 is particularly comprehensive in delineating the needed areas of research bearing on spacecraft fire safety. We can only concur with the need to press forward in these many areas. Getting a firmer grasp on the potential fire hazards of spacecraft materials through the near-term study discussed above should help alleviate some of the urgency of these many tasks but it does not obviate them.

#### Acknowledgements

The authors would like to acknowledge the considerable assistance of Robin Breese, Tom Cleary and Randy Shields at several points in the data acquisition and reduction parts of this study.

## References

- 1) Friedman, R. and Olson, S., "Fire Safety Applications for Spacecraft", NASA Technical Memorandum 101463, NASA Lewis Research Center, May, 1989
- 2) Olson, S., Ferkul, P. and T'ien, J., Proceedings of the Twenty-Second Symposium (International) on Combustion, The Combustion Institute, Pittsburgh (1988) p.1213
- 3) NASA, "Flammability, Odor, Offgassing Requirements and Test Procedures for Materials in Environments that Support Combustion", NASA document No. NHB 8060.1B, Washington, DC, 1981
- 4) Quintiere, J., J. Res. Nat'l Bur. Stds., 93, (1988), p.61
- 5) Ohlemiller, T., "Assessing the Flammability of Composite Materials", National Institute of Standards and Technology NISTIR 88-4032, January, 1989
- 6) Babrauskas, V. and Peacock, R., "Heat Release Rate: The Single Most Important Variable in Fire Hazard", presented at Fall 1990 Meeting of the Fire Retardant Chemicals Association.
- 7) Baumeister, T., Avallone, E., and Baumeister III, T. (Editors), Marks' Standard Handbook for Mechanical Engineers (Eighth Edition), McGraw-Hill Book Company, New York (1978), p.4-68
- 8) Babrauskas, V. and Wickstrom, U., "The Rational Development of Bench-Scale Fire Tests for Full-Scale Fire Prediction", Fire Safety Science Proceedings of the Second International Symposium, Hemisphere Publishing Corp., New York, 1989, p. 813
- 9) Cleary, T. and Quintiere, J., "A Framework for Utilizing Fire Property Tests", paper to be presented at the Third International Symposium on Safety Science, Edinburgh, Scotland, July, 1991
- 10) Ito, A. and Kashiwagi, T., "Characterization of Flame Spread Over PMMA Using Holographic Interferometry; Sample Orientation Effects", Combustion and Flame, 71, 1988, p. 189
- 11) Brown, J. E., unpublished work at NIST on composite materials.
- 12) ASTM Task Group E5.21 T.G. 60, "Report to ASTM on Cone Calorimeter Inter-Laboratory Trials", January 3, 1990
- 13) Kimzey, J., "Skylab Experiment M-479, Zero Gravity Flammability", Johnson Space Center Report JSC 22293, August, 1986

- 14) Levin, B, Paabo, M, Gurman, J., and Harris, S., "Effects of Exposure to Single or Multiple Combinations of the Predominant Toxic Gases and Low Oxygen Atmospheres Produced in Fires", Fundamental and Applied Toxicology, 9, 1987, pp. 236-250
- 15) Levin, B., Gurman, J., Paabo, M., Baier, L., and Holt, T., "Toxicological Effects of Different Time Exposures to the Fire Gases: Carbon Monoxide or Hydrogen Cyanide or to Carbon Monoxide Combined with Hydrogen Cyanide or Carbon Dioxide", Polyurethane '88. Proceedings of the Thirty-First Meeting of the Society of the Plastics Industry, Philadelphia, Pennsylvania, 1988, p. 240
- 16) Levin, B., Paabo, M., Gurman, J., Clark, H., and Yoklavich, M., "Further Studies of the Toxicological Effects of Different Time Exposures to the Individual and Combined Fire Gases - Carbon Monoxide, Hydrogen Cyanide, Carbon Dioxide and Reduced Oxygen", ibid, p. 249
- 17) Anon., Spacecraft Fire Safety, NASA Conference Publication 2476, 1987
- 18) Youngblood, W., "Space Station Technology Development Mission Study: Spacecraft Fire Safety", Wyle Laboratories Letter Report to NASA LeRC, June, 1987
- 19) Youngblood, W., "Spacecraft Fire-Safety Experiments for Space Station Technology Development Mission", NASA CR-182114, April, 1988
- 20) Youngblood, W. and Vedha-Nayagam, M., "Advanced Spacecraft Fire Safety: Proposed Projects and Program Plan", NASA CR 185147, October, 1989

Table 1  
Materials Examined in Study<sup>1</sup>

Material	Manufacturer or Designation <sup>2</sup>	Thickness (mm)
Pyrell polyurethane foam	Foamex, Eddystone, Pa.	12.7, 25.4
Cotton toweling	Dundee Mills, Griffin, Ga.	≈ 7
Lexan 9034 polycarbonate sheet (unretarded)	General Electric	1.6
Lexan 9600 polycarbonate sheet (retarded)	General Electric	1.6
Kydex PVC/acrylic sheet	Kleerdex, Mt. Laurel, NJ	1.6
-----		
Epoxy/glass circuit board <sup>3</sup>	WSTF# 87-21537	
Nomex, blue, 6.8 oz./yd <sup>2</sup>	WSTF #88-22485	
Cotton cloth, royal blue flame retarded, 6.0 oz./yd <sup>2</sup>	Rockwell Int'l #P1938	

---

<sup>1</sup>Those listed above the dashed line were used in the first phase of this study; the second phase included those below the dashed line plus certain of those from the first phase, as well.

<sup>2</sup>Mention of specific manufacturers or products is done for clarity only and does not imply any endorsement or approval by the National Institute of Standards and Technology.

<sup>3</sup>This material had a NEMA Grade G-10 designation but contained a halogen compound which probably accounts for its lower than expected flammability.

TABLE 2

PHASE 1 MATERIALS; NASA NHB 8060.1 RESULTS<sup>1</sup>

<u>MATERIAL</u>	<u>MAX. HEIGHT OF ANCHORED FLAME<sup>2</sup> (CM)</u>	<u>MEAN FLAME SPREAD RATE<sup>3</sup> (CM/SEC)</u>	<u>COMMENT</u>
Cotton Toweling	30.5 ± 0	0.62 ± 0.04	Full length spread
Pyrell Foam (12.7 mm)	5.3 ± 0.8	0.32 ± 0.06	Igniter dominated spread
Kydex (1.6 mm)	3.7 ± 0.8	0.21 ± 0.05	" " "
Lexan 9034 (1.6 mm)	0.97 ± 0.3	0.04 ± 0.01	Minimal spread
Lexan 9600 (1.6 mm)	0.75 ± 0.2	0.04 ± 0.01	" "
Kydex (6.4 mm)	0.6 ± 0.1	0.03 ± 0.01	" "
Lexan 9034 (6.4 mm)	0.4 ± 0.1	0.02 ± 0.005	" "

<sup>1</sup>Each value is the average ± standard deviation from six repetitions.

<sup>2</sup>This is the maximum height at which the flame is attached to an active pyrolysis zone. Judged from video tape of test; based on indication of flame attachment to bubbles on sample surface.

<sup>3</sup>Defined as (Max. height of anchored flame)/(Total burn time - Sample ignition time).

TABLE 3

## LIFT DATA ON NASA MATERIALS IN PHASE 1

<u>MATERIAL (THK)/BACKING<sup>1</sup></u>	<u>MIN. IGNITION FLUX (kW/m<sup>2</sup>)</u>	<u>IGNITION TEMP. (°C)</u>	<u>THERMAL INERTIA (mks)</u>	<u>MIN. SPREAD FLUX (kW/m<sup>2</sup>)</u>	<u>MIN. SPREAD TEMP. (°C)</u>
Cotton Terry/Kaoboard	10	302	0.46	≈ 0	≈ 25
Pyrell Foam (25.4 mm)	17	401	0.035	4.2	176
Pyrell Foam (12.7 mm) <sup>2</sup>	17	401	0.057	3.4	122
Kydex (1.6 mm) <sup>3</sup>	15	376	1.40	7.5	257
Lexan 9600 (1.6 mm)	21	445	1.97	13.4	356
Lexan 9034 (1.6 mm)	22	455	2.11	10.7	315
Lexan 9034 (6.4 mm)	24	473	2.70	15.1	380

<sup>1</sup> If type of backing is not indicated explicitly, it is heavy duty aluminum foil plus 2.5 cm Kaoboard. With thermally thin materials the backing can be expected to influence the ignition behavior.

<sup>2</sup> Large mesh wire over exposed face to prevent bowing outward.

<sup>3</sup> Data obtained in the vertically oriented LIFT apparatus.

TABLE 4

NASA / LIFT TEST CORRELATION; PHASE 1 RESULTS

<u>MATERIAL</u>	NASA MEAN UPWARD_ VEL. (cm/sec)	LIFT MIN. FLUX FOR SPREAD (kW/m <sup>2</sup> )	LIFT MIN. FLUX IGN. (kW/m <sup>2</sup> )	LIFT 1/(kρC)ΔT
Cotton Toweling	0.62	≈ 0	10	0.008
Pyrell Foam <sup>1</sup>	0.32	3.6 ± 0.9	17	(0.047) <sup>2</sup>
Kydex	0.21	7.5 ± 0.5	15	0.002
Lexan 9034	0.04	10.7 ± 0.6	22	0.001

-----  
NOTE: Only the cotton toweling spread upward beyond the dominance of the igniter flame.

---

<sup>1</sup>LIFT results are for the average of nine tests with 12.7 and 25.4 mm thick samples, with and without large mesh wire over hottest 20 cm of sample face. However, (kρC) used in last column is that for 12.7 mm samples.

<sup>2</sup>The form of the correlation between flame spread rate and the quantity [1/(kρC)ΔT] depends on whether the sample is thermally thick or thermally thin. Pyrex foam starts out thermally thick but shrinks to thermally thin during igniter exposure and burning. If the sample behaved as thermally thick, this quantity would become 0.0001.

Table 5

Calculated Reflectivity of Phase 2 Samples  
for Radiant Panel Heat Flux<sup>1</sup>

<u>Material</u>	<u>Steady Temperature (C)</u>	<u>Reflectivity</u>
Epoxy/Glass	122	0.53
Flame-retarded Cotton	192	0.52
Nomex	215	0.58
"	137	0.56
Kydex	203	0.16
Lexan 9034 <sup>2</sup>	187	0.67

---

<sup>1</sup>This is the reflectivity for the radiation from the quartz-halogen lamps used in the electrically-powered panel for the modified NASA tests.

<sup>2</sup>A substantial part of the apparently reflected radiation here is actually transmitted without absorption.

Table 6

Comparison of Minimum Absorbed Flux  
for Lateral and Upward Flame Spread

<u>Material</u>	<u>Minimum Flux Laterally (kW/m<sup>2</sup>)</u>	<u>Minimum Flux Upward (kW/m<sup>2</sup>)<sup>1</sup></u>
Cotton Toweling	0	0
Nomex Cloth	33	≈3½
Kydex	12	>5
Lexan 9034	10½	>6
Epoxy/Glass	12	>9
Retarded Cotton	26	≥15½

---

<sup>1</sup>This is the absorbed flux, based on the estimated sample reflectivities for the quartz-halogen lamp radiation, as listed in Table 5. For the LIFT results in the middle column above, the incident and absorbed fluxes are assumed equal because of the middle infrared nature of that radiation.

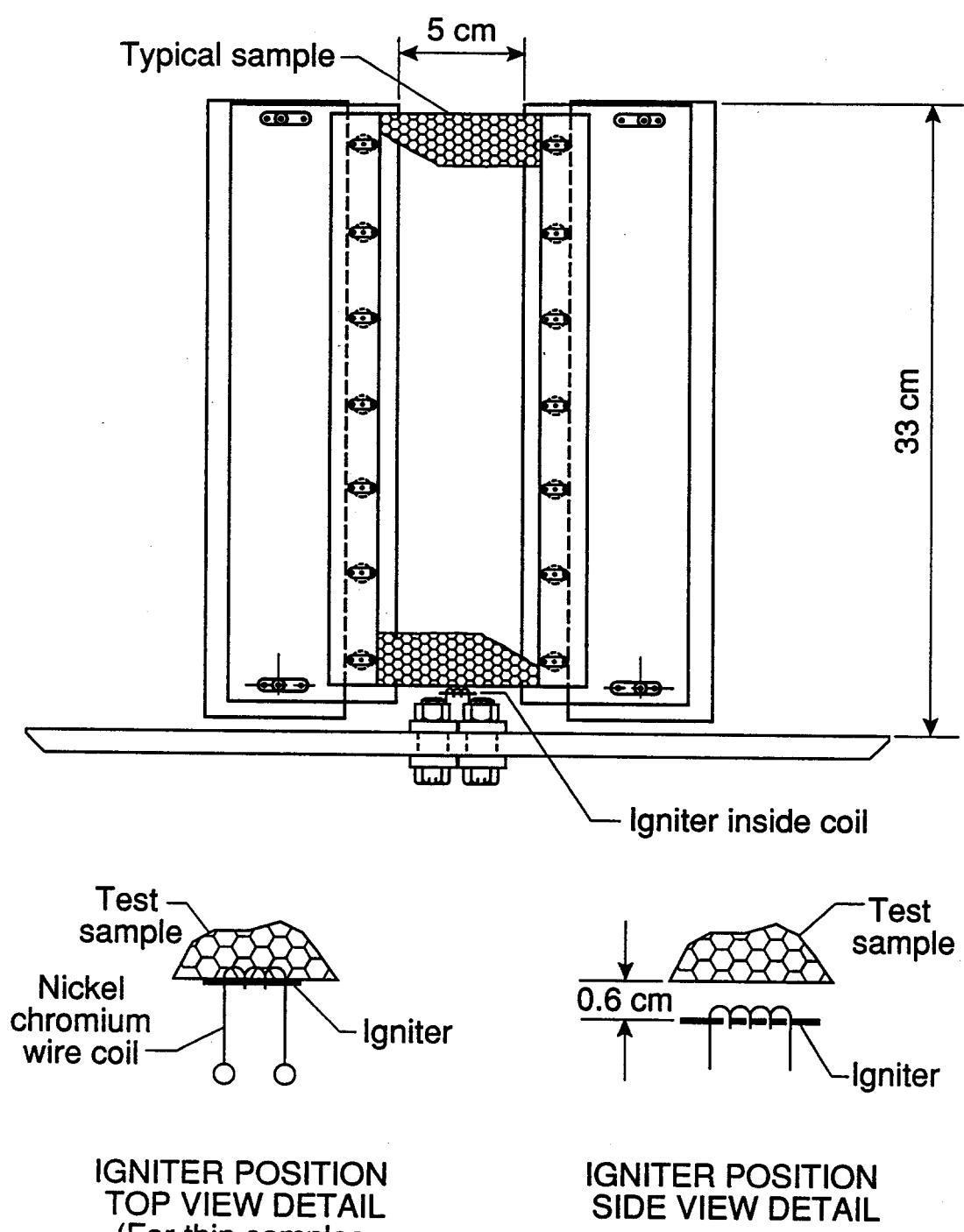


Figure 1. Typical sample holder for NASA 8060.1B upward flame spread test.

# Lift Apparatus in Horizontal Orientation

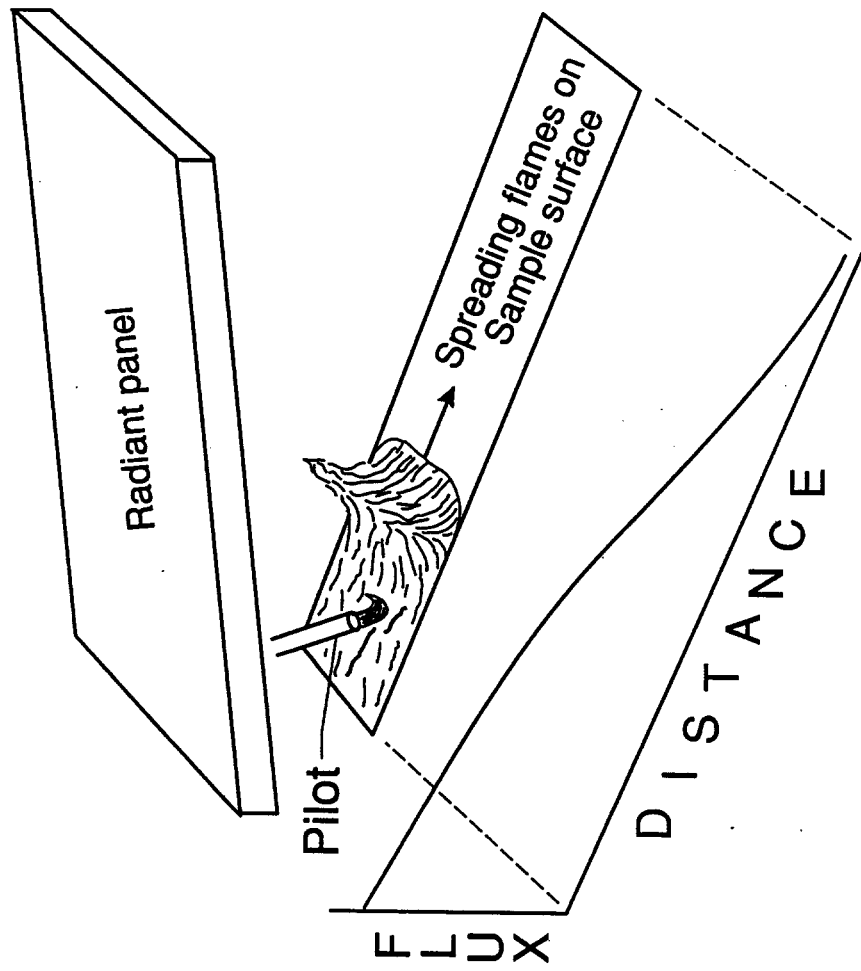


Figure 2. Schematic of Lateral Ignition and Flame Spread (LIFT) test when sample is horizontal.

# Modified NASA Test (1/3 scale)

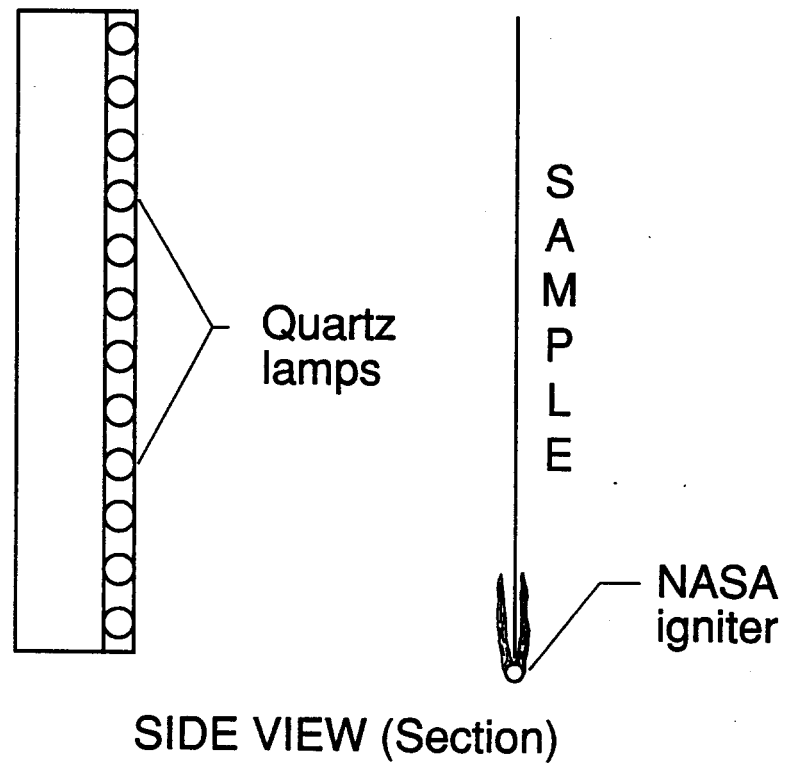
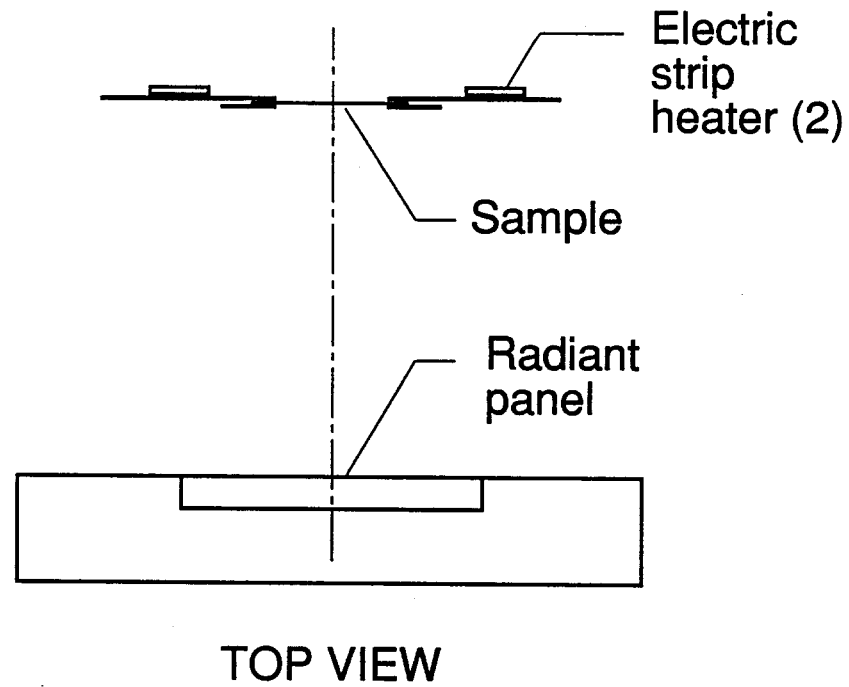


Figure 3. Schematic of NIST modified version of NASA upward flame spread test.

# Cotton Toweling

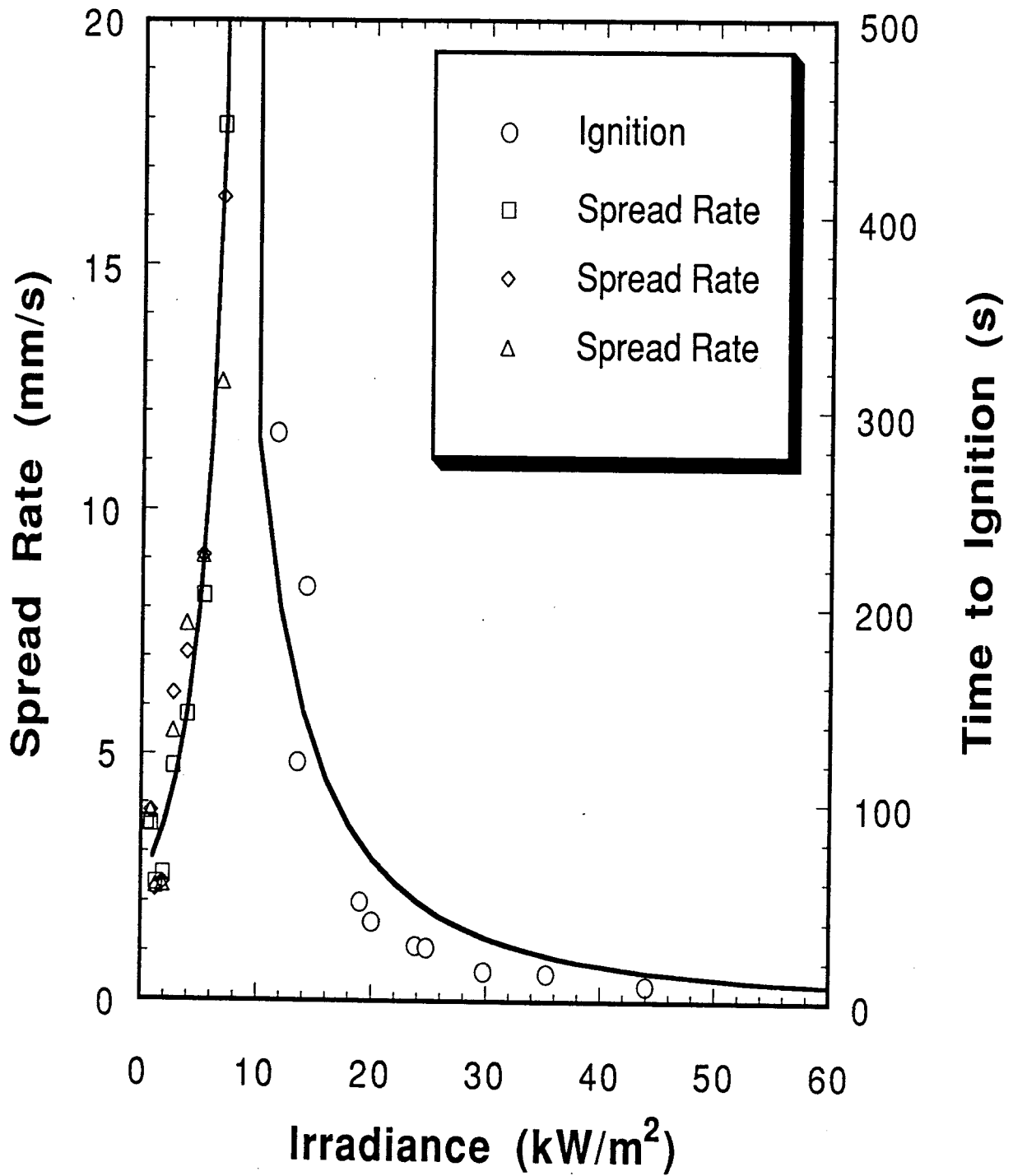


Figure 4. LIFT data and fitted model lines; cotton toweling with Kaoboard backing.

# PYRELL Foam (12.7 mm) (Vertical Orientation)

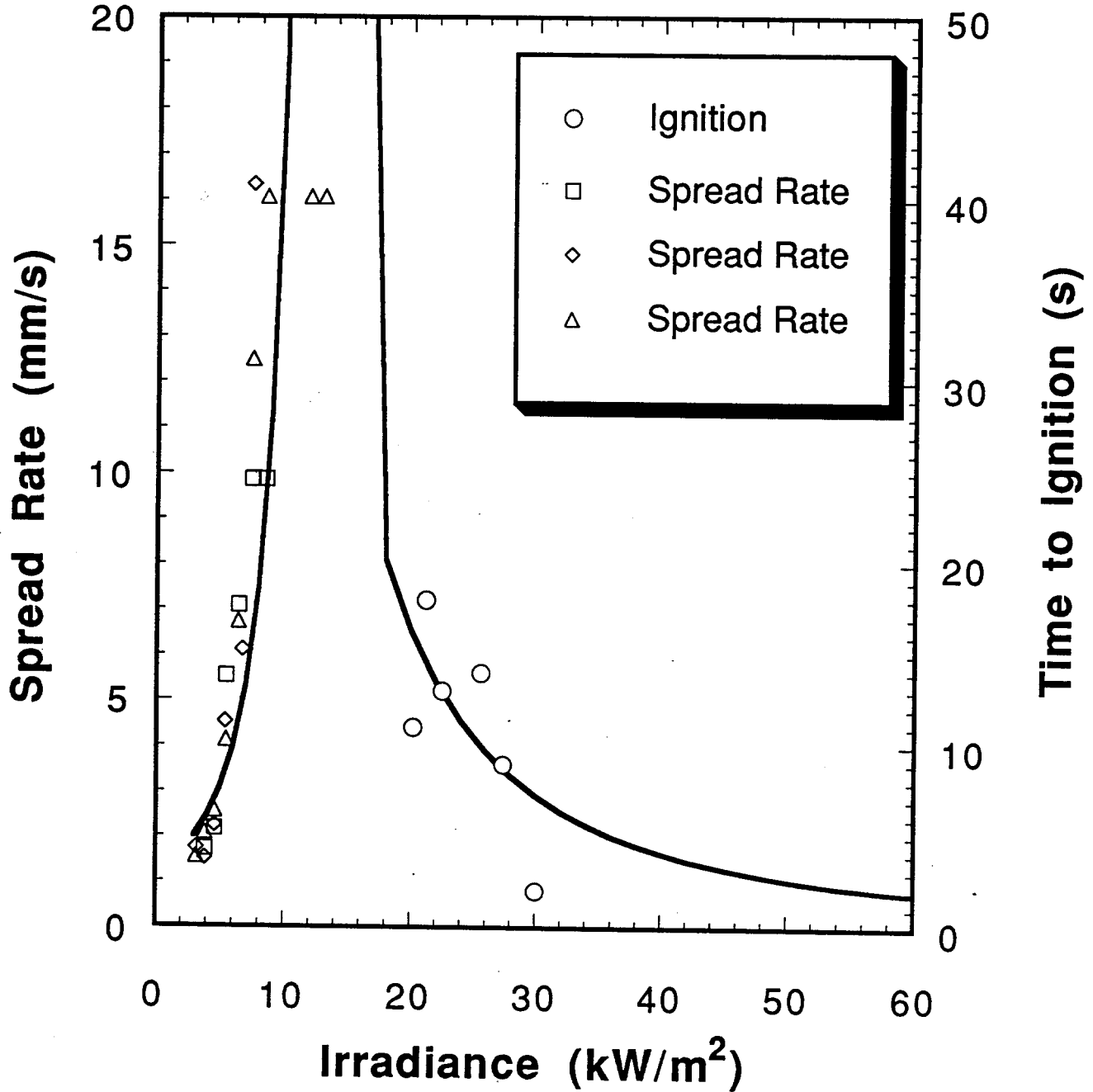


Figure 5. LIFT data and fitted model lines; 12.7 mm Pyrell foam in vertical orientation; Kaoboard backing.

# PYRELL Foam (25.4 mm)

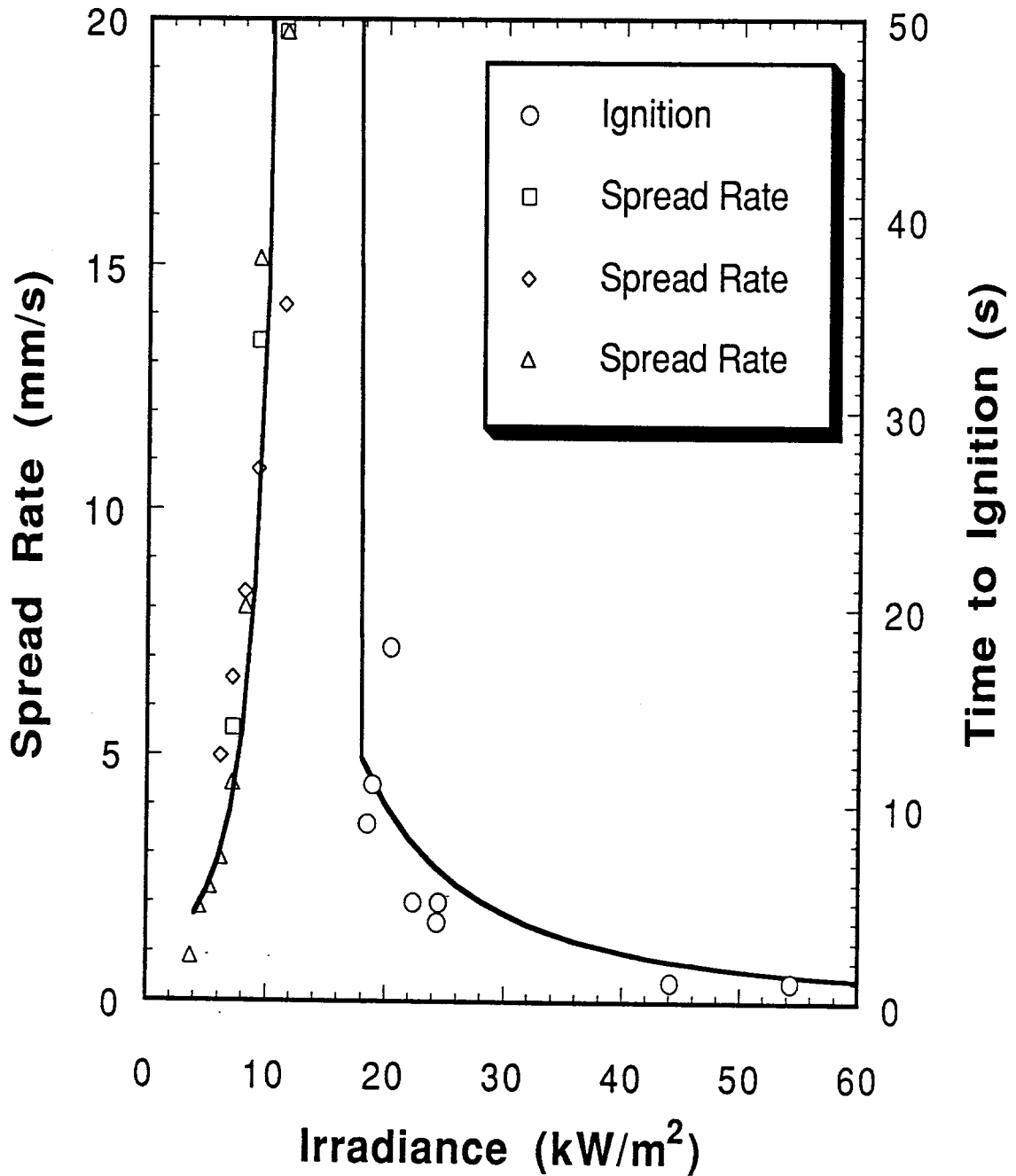


Figure 6. LIFT data and fitted model lines; 25.4 mm Pyrell foam; Kaoboard backing.

Kydex PVC/Acrylic  
(1.6 mm)  
(Vertical Orientation)

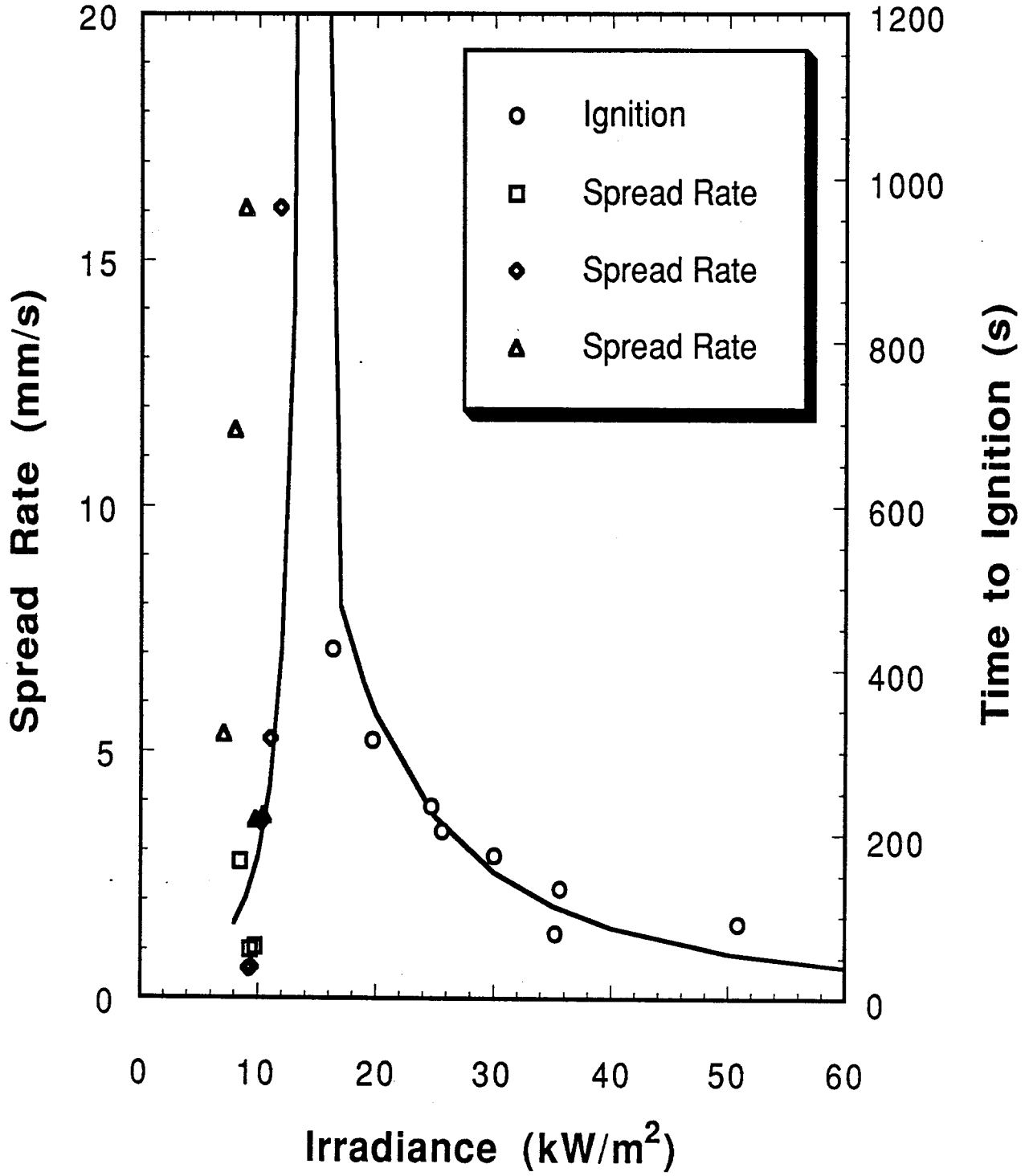


Figure 7. LIFT data and fitted model lines; Kydex with Kaoboard backing.

# LEXAN 9034 (1.6 mm)

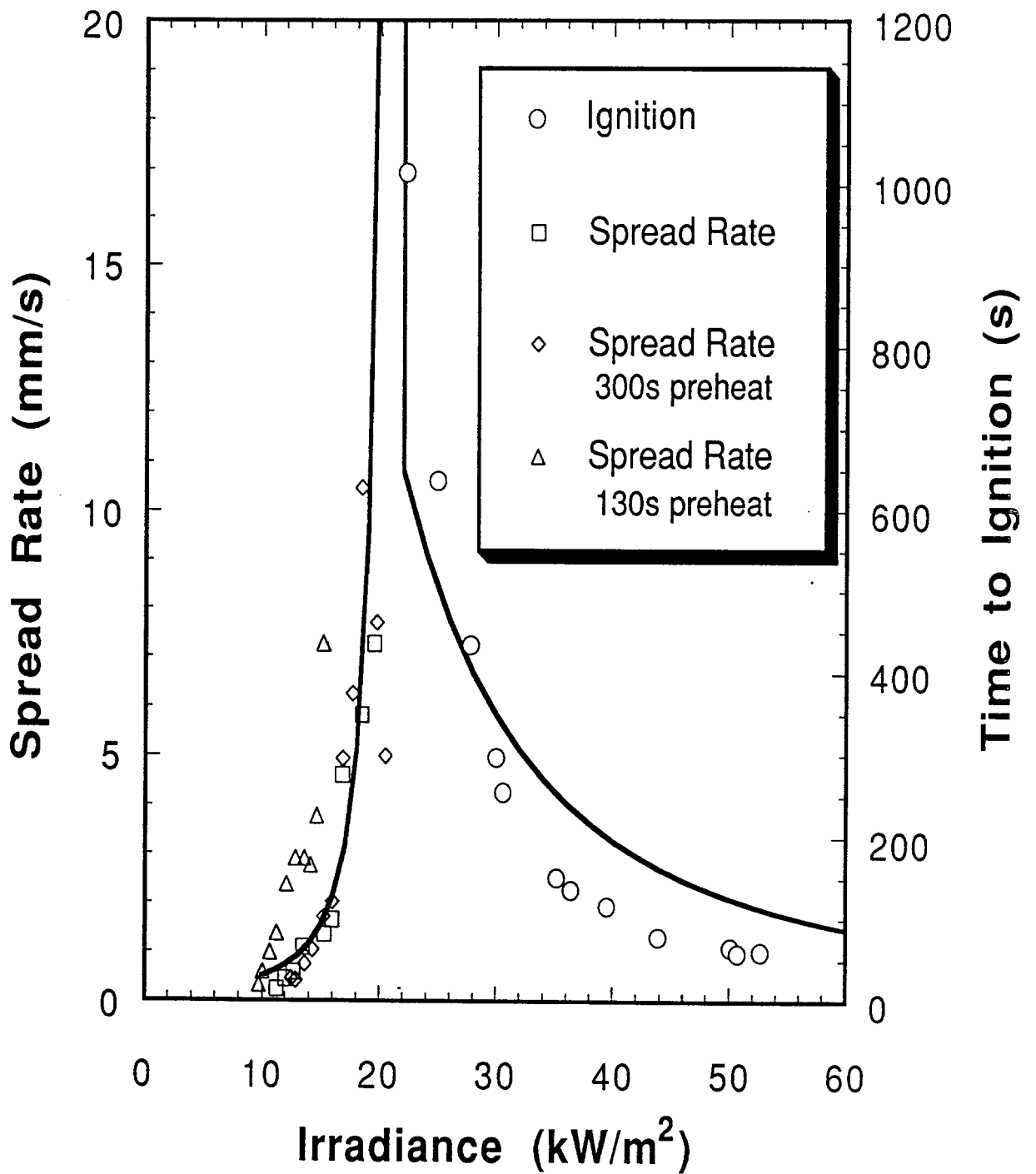


Figure 8. LIFT data and fitted model lines; Lexan 9034 with Kaoboard backing.

# LEXAN 9600 (1.6 mm)

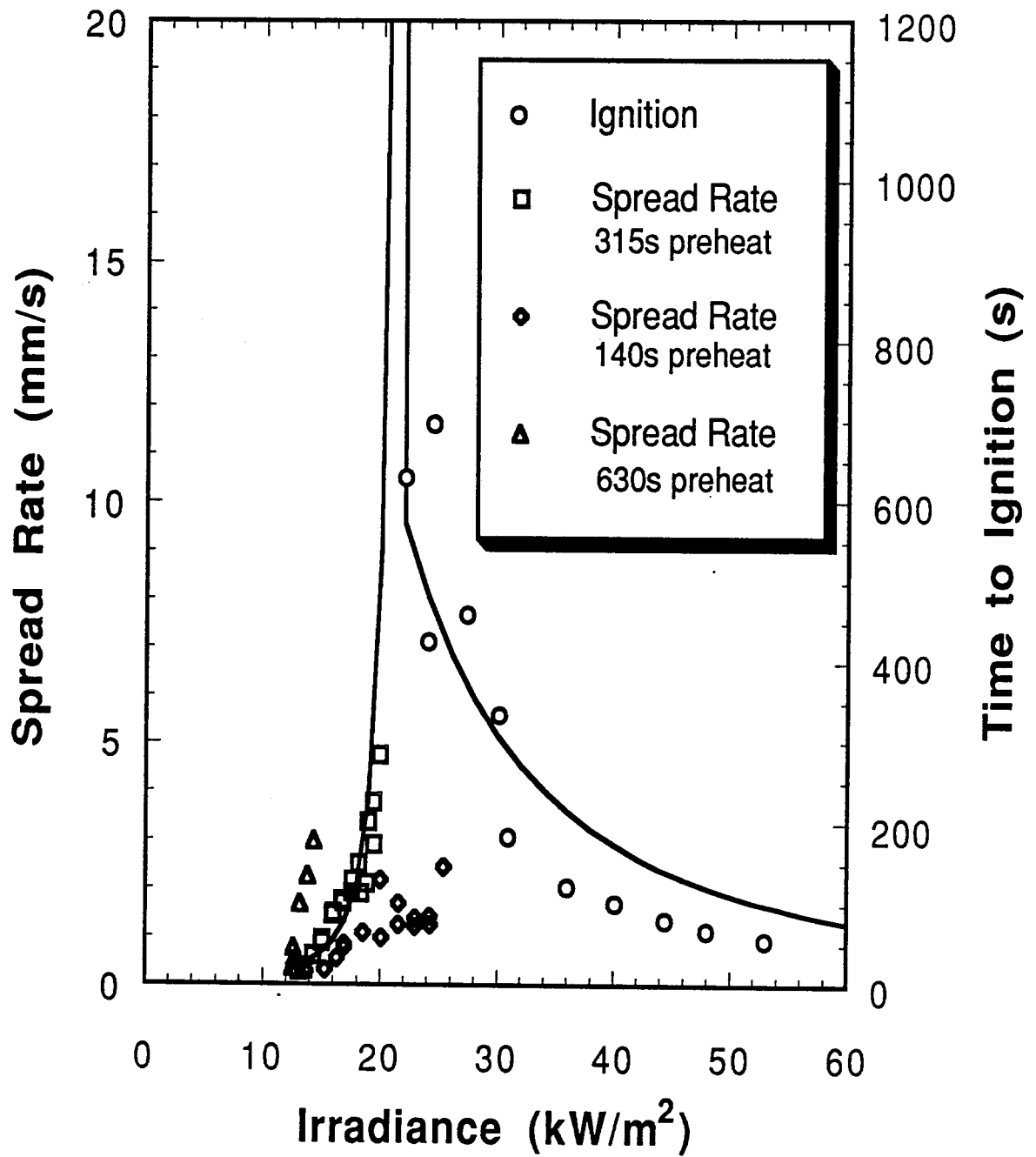


Figure 9. LIFT data and fitted model lines; Lexan 9600 with Kaoboard backing.

# LEXAN 9034

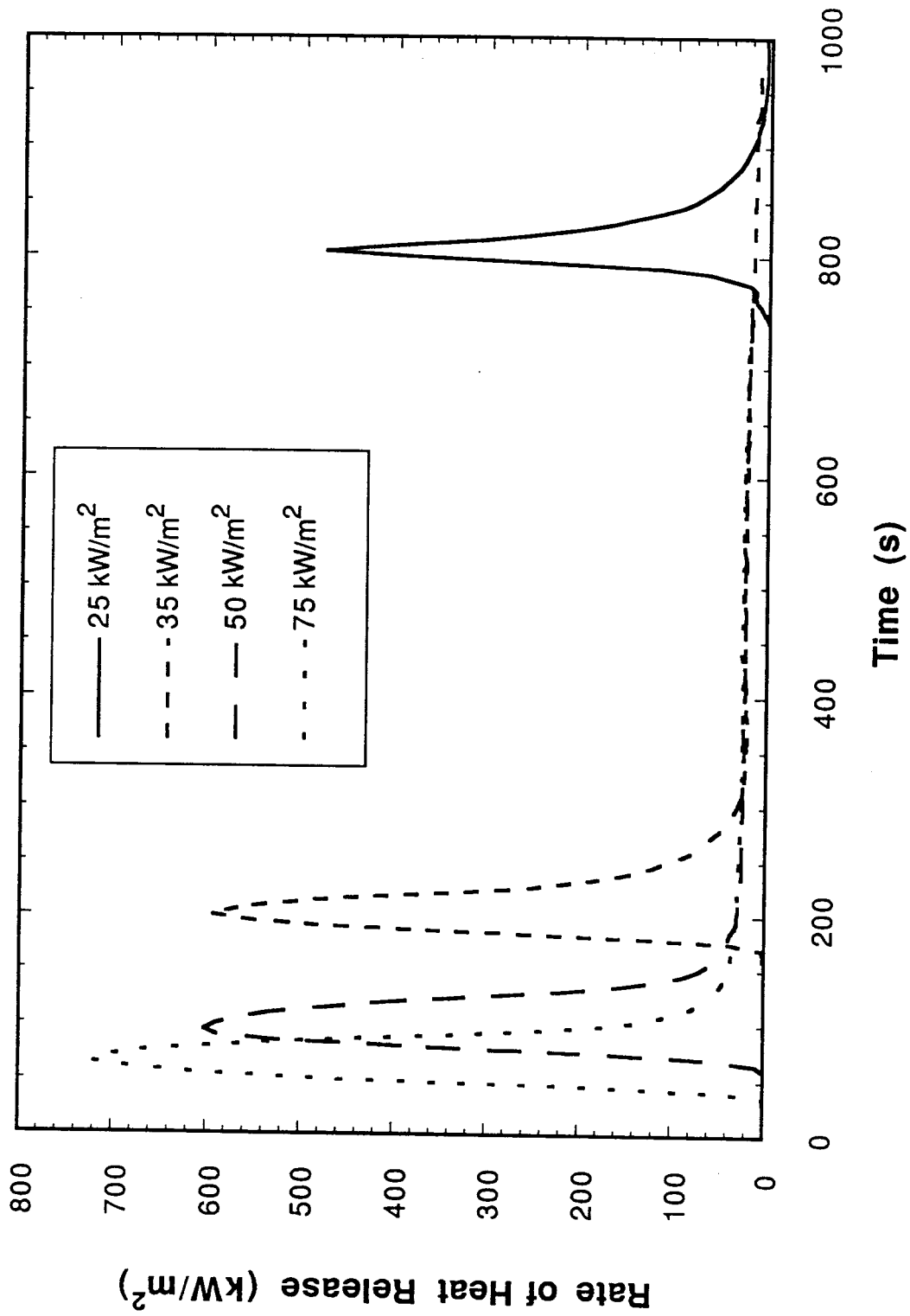


Figure 10. Cone Calorimeter data for rate of heat release; Lexan 9034; Kaowool backing.

# Cotton Toweling

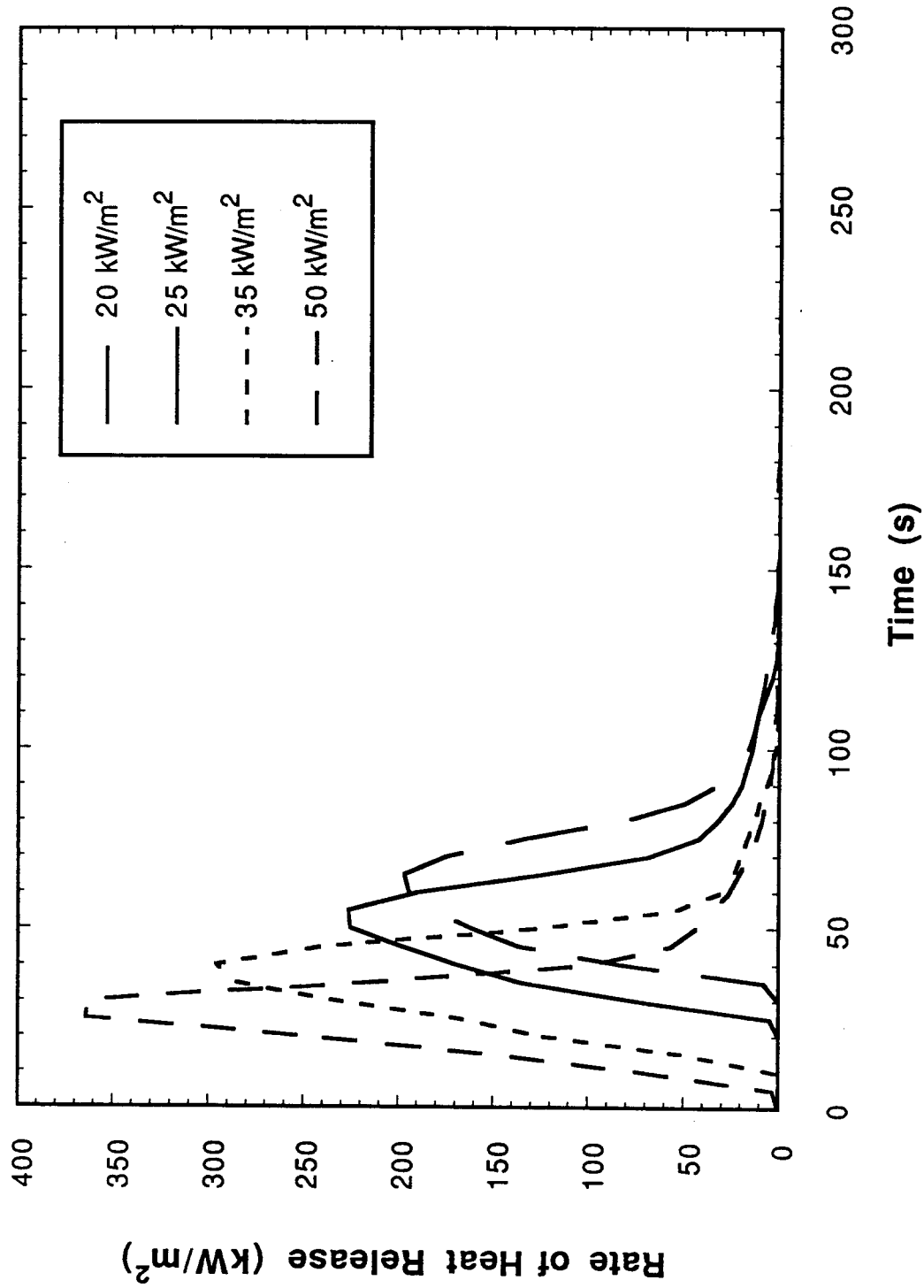


Figure 11. Cone Calorimeter data for rate of heat release; cotton toweling; Kaowool backing.

# PYRELL Foam (12.7 mm)

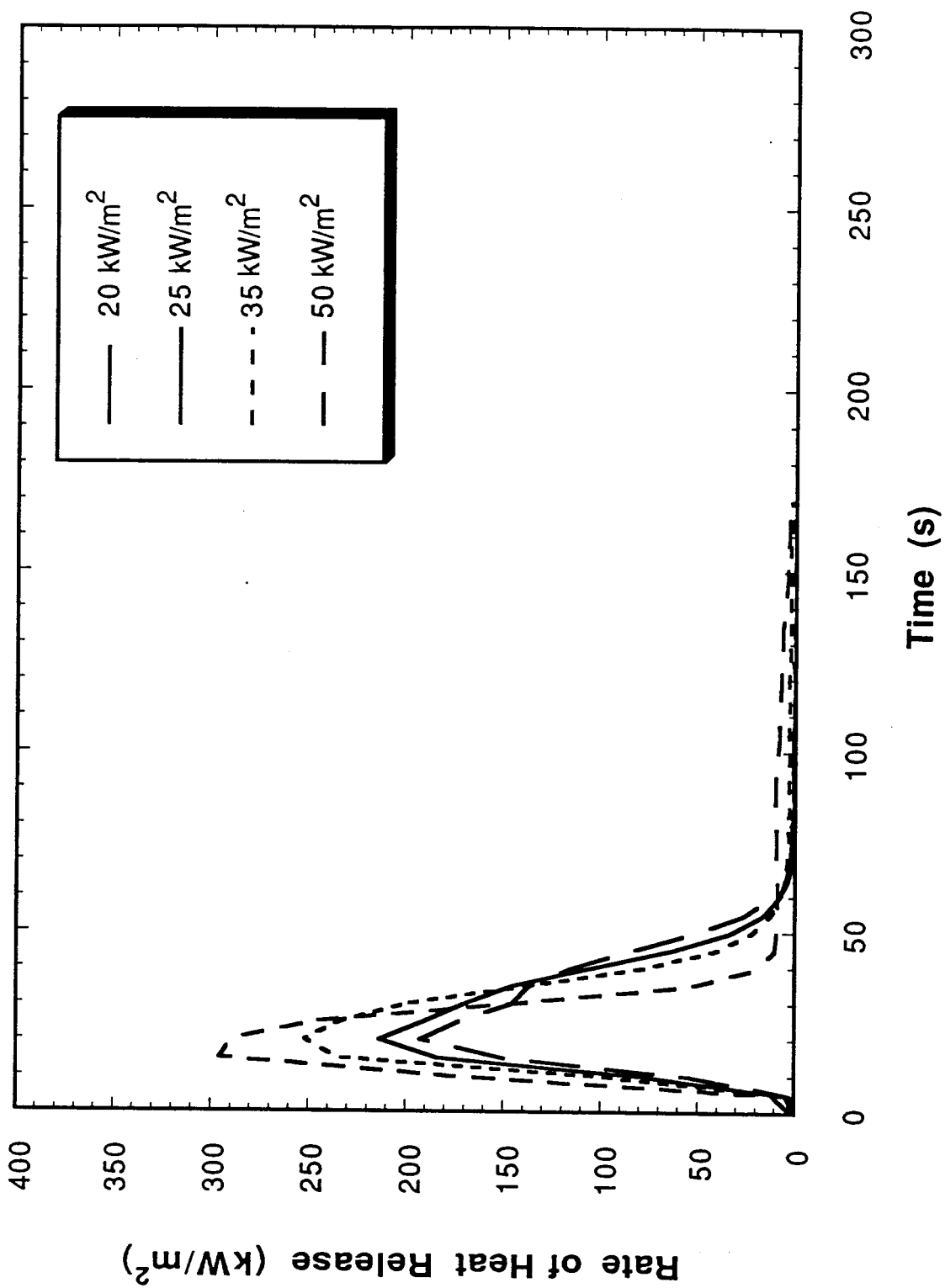


Figure 12. Cone Calorimeter data for rate of heat release; 12.7mm Pyrell foam; Kaowool backing.

# Peak Heat Release Rate vs Irradiance

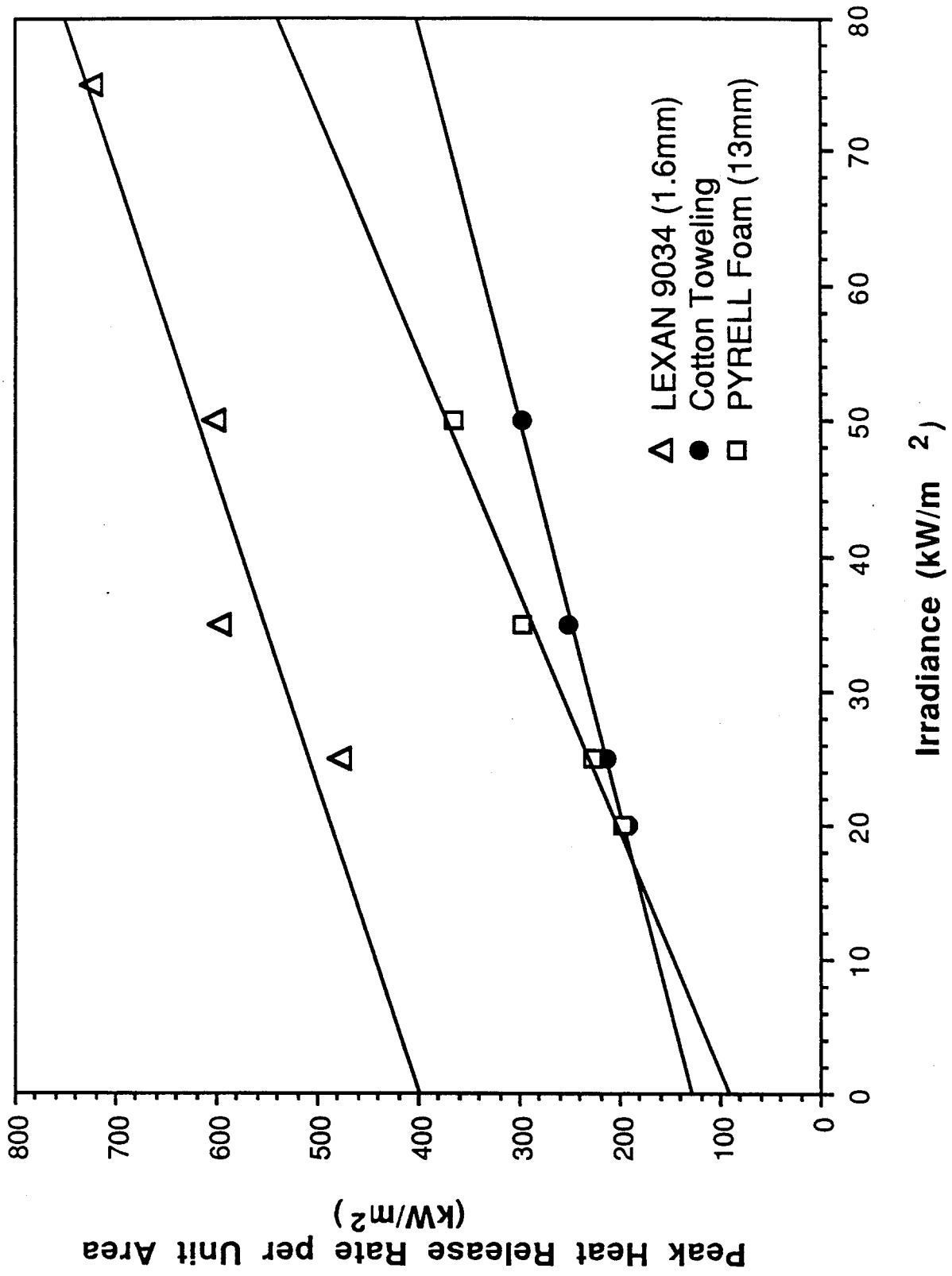


Figure 13. Peak rate of heat release variation with incident heat flux.

# Cotton Toweling

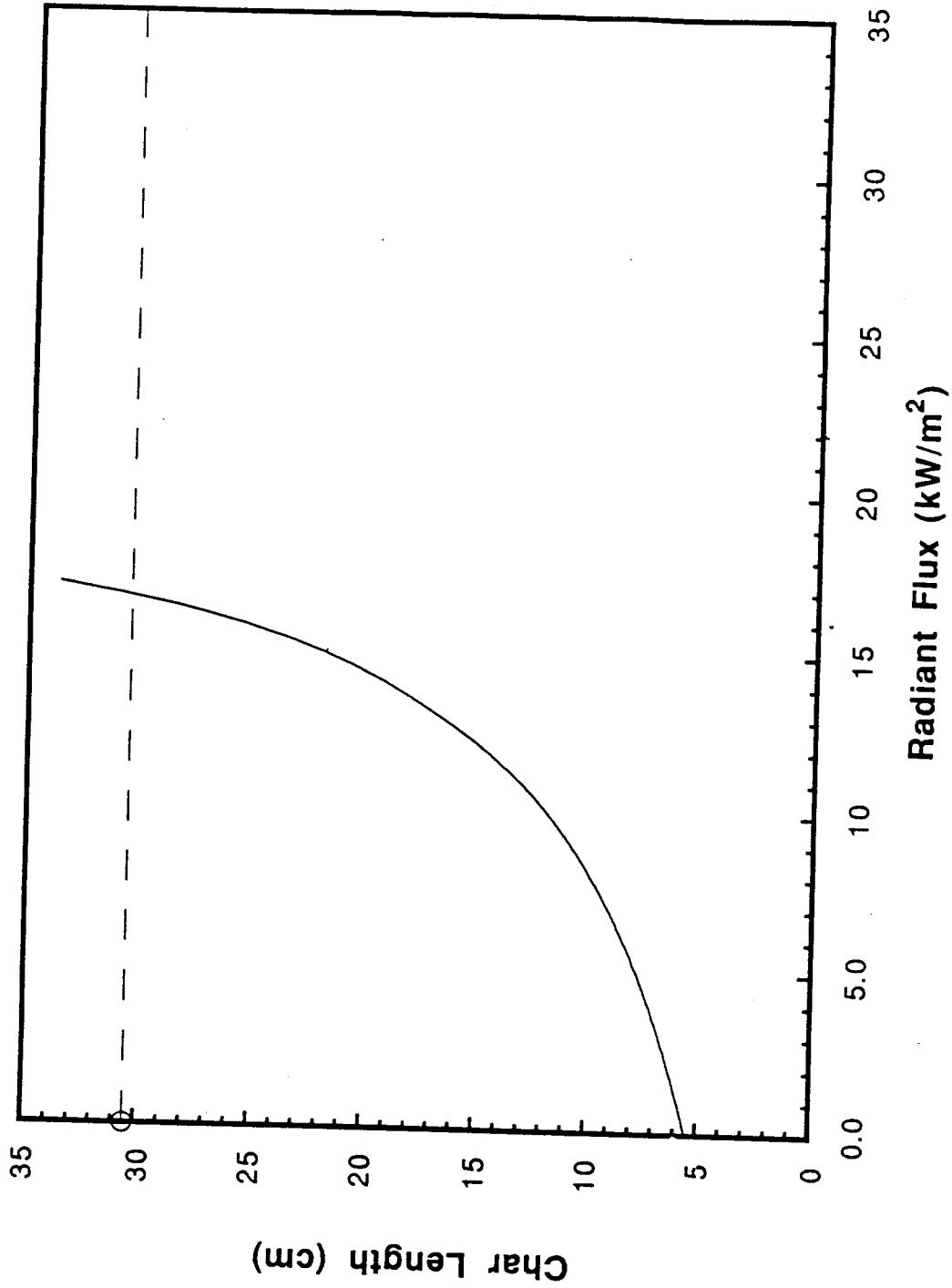


Figure 14. Data and model prediction for maximum char length versus absorbed radiant flux; cotton toweling. Flat dashed line is top of sample.

# NOMEX

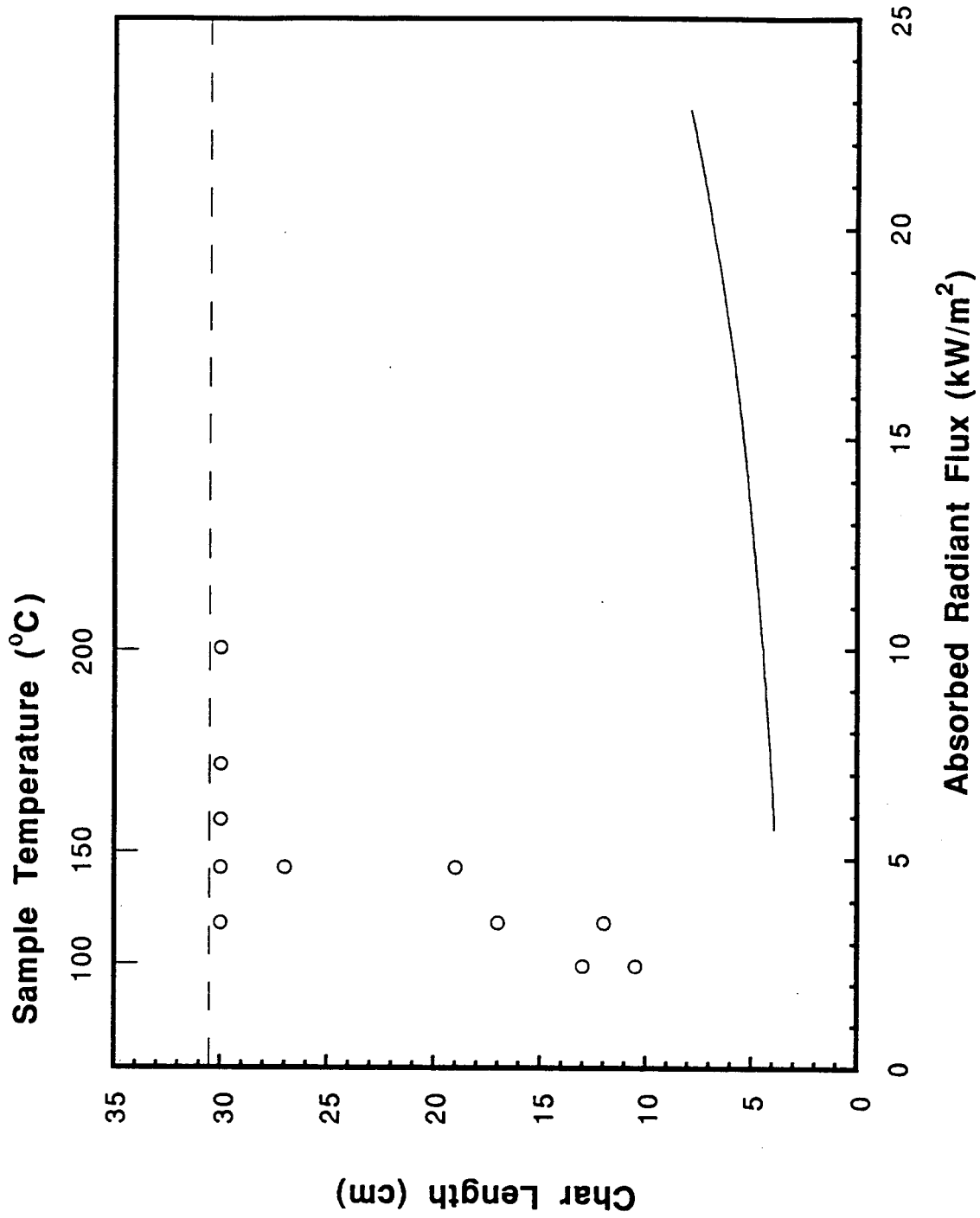


Figure 15. Data and model prediction for maximum char length versus absorbed radiant flux; Nomex. Flat dashed line is top of sample. Sample temperature is steady-state at heat flux on abscissa.

# Flame Retardant Cotton Cloth

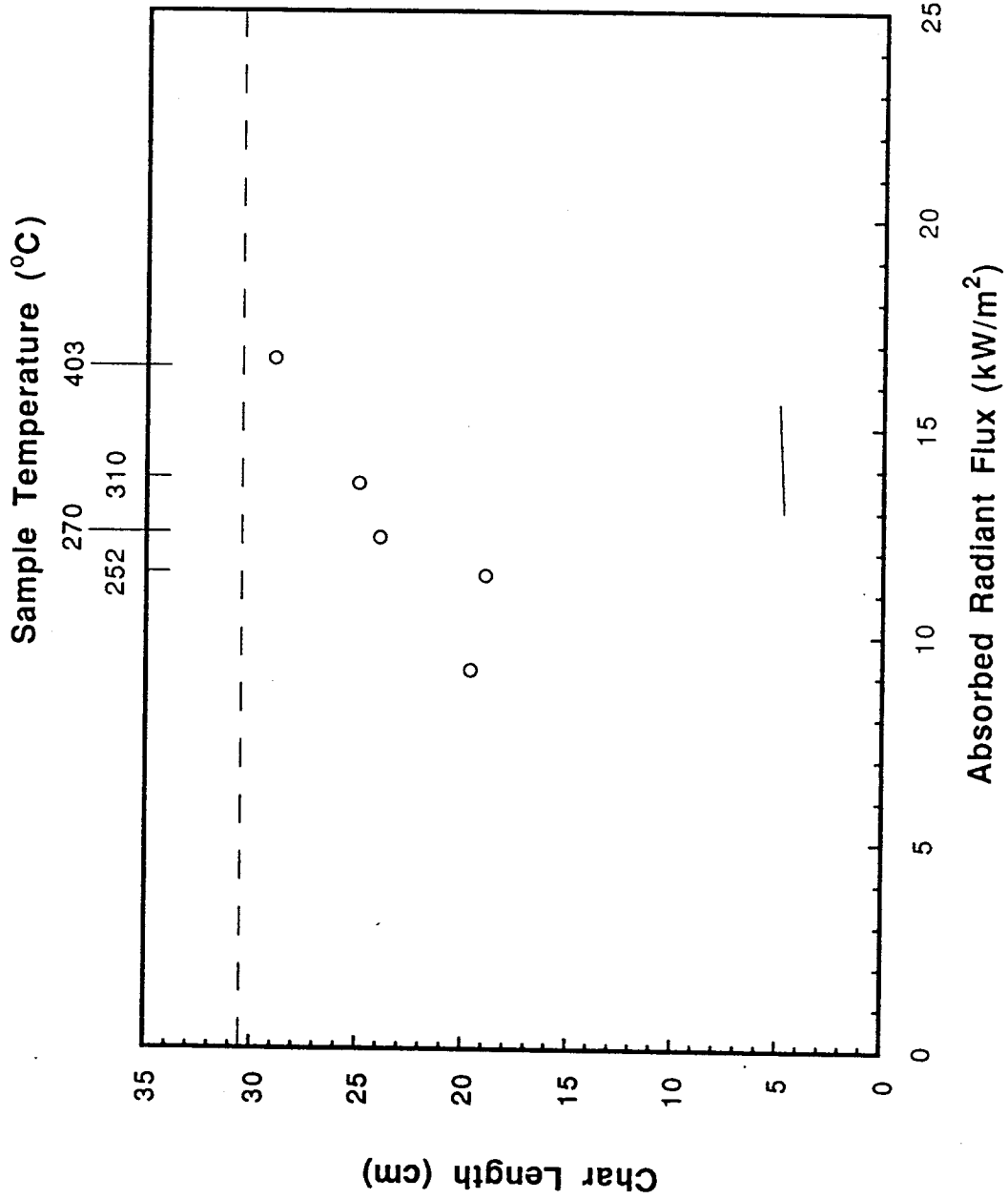


Figure 16. Data and model prediction for maximum char length versus absorbed radiant flux; flame-retarded cotton. Flat dashed line is top of sample. Sample temperature is steady-state value at flux on abscissa.

# Epoxy Circuit Board

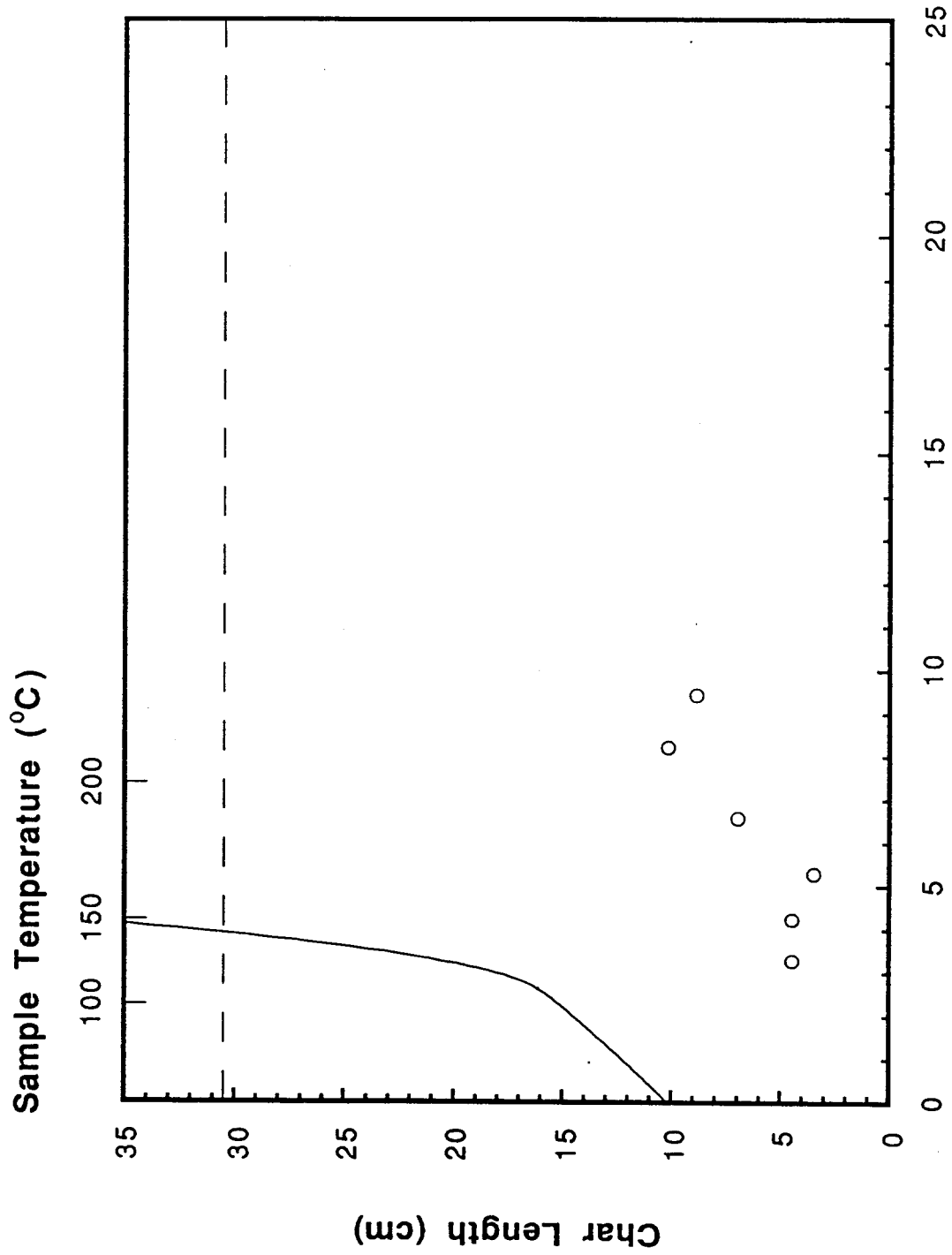


Figure 17. Data and model prediction for maximum char length versus absorbed radiant flux; epoxy/glass circuit board. Flat dashed line is top of sample. Sample temperature is steady-state value at flux on abscissa.

# Kydex PVC/Acrylic

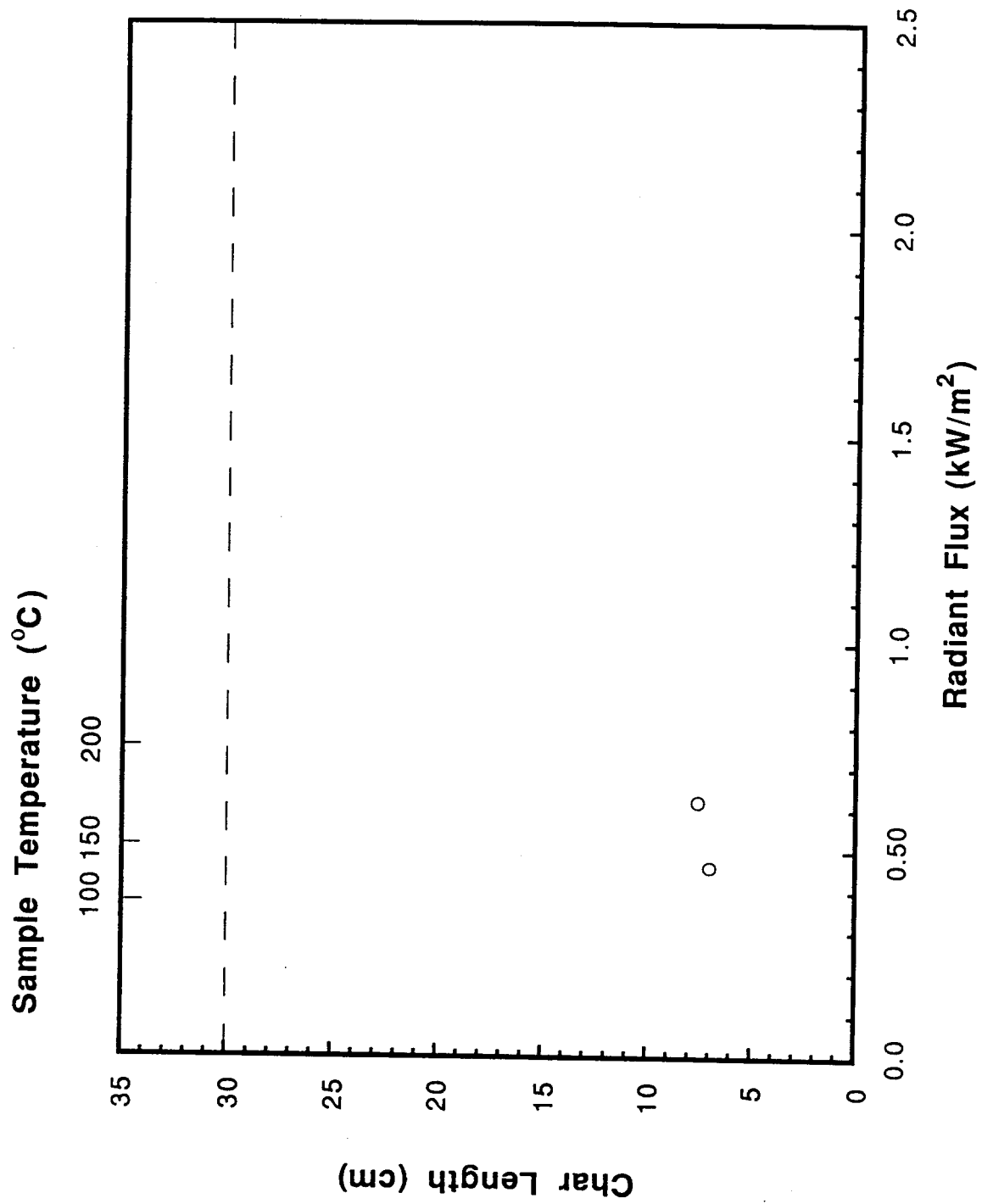


Figure 18. Data and model prediction for maximum char length versus absorbed radiant flux; Kydex. Flat dashed line is top of sample. Sample temperature is steady-state at flux on abscissa.

# LEXAN 9034

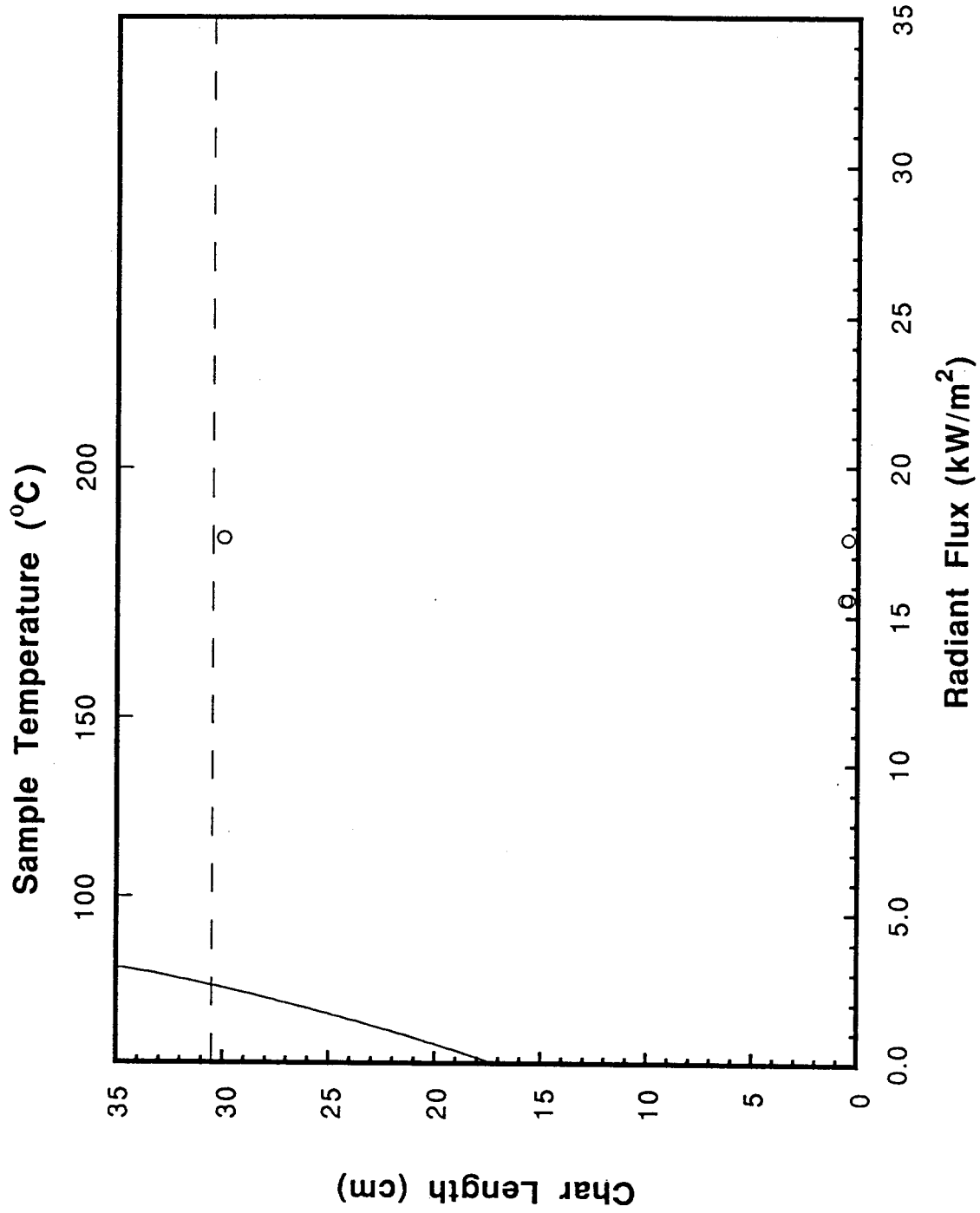


Figure 19. Data and model prediction for maximum char length versus absorbed radiant flux; Lexan 9034. Flat dashed line is top of sample. Sample temperature is steady-state value at flux on abscissa.

# LEXAN 9034

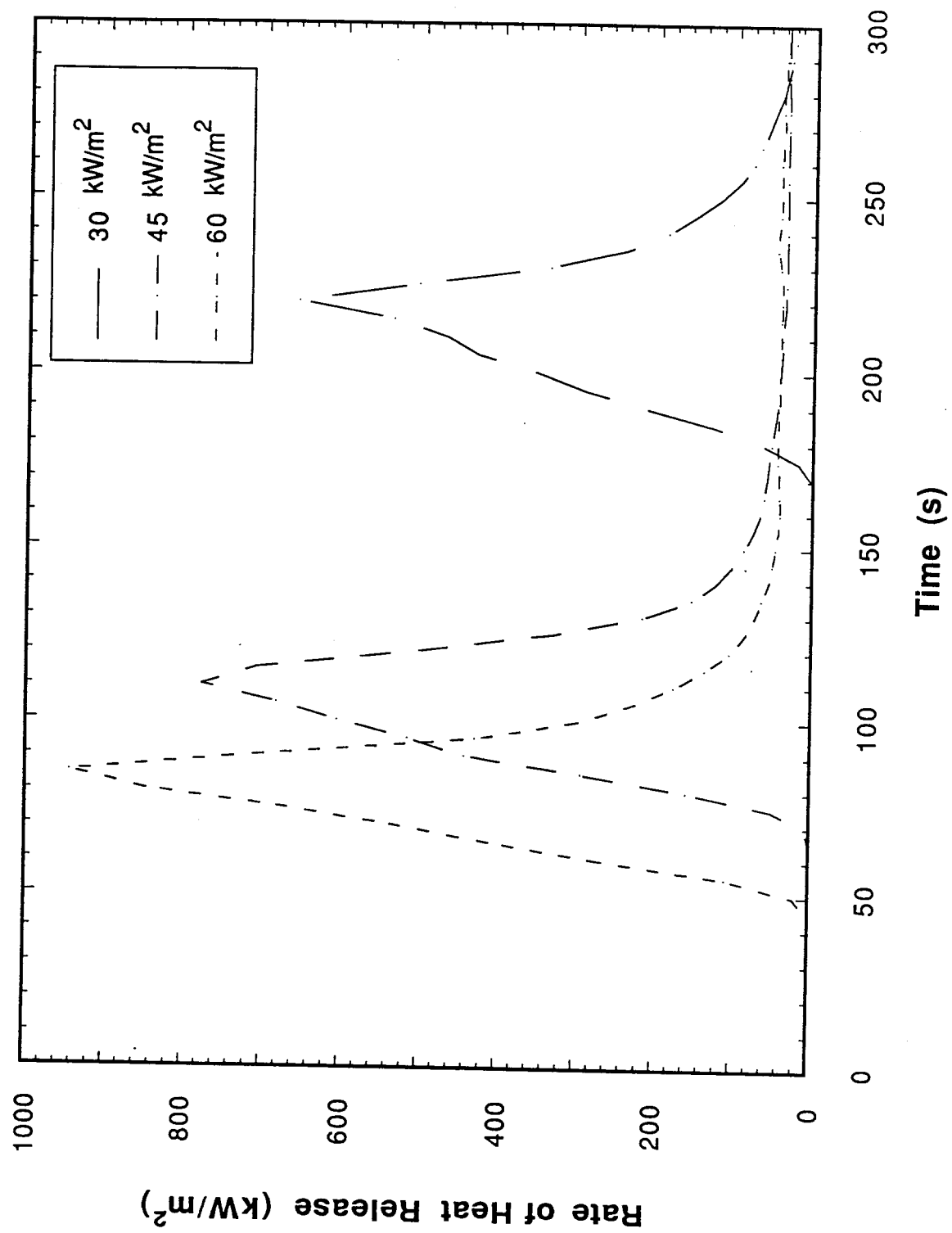


Figure 20. Cone Calorimeter data for rate of heat release; Lexan 9034 with air gap below sample.

# Cotton Toweling

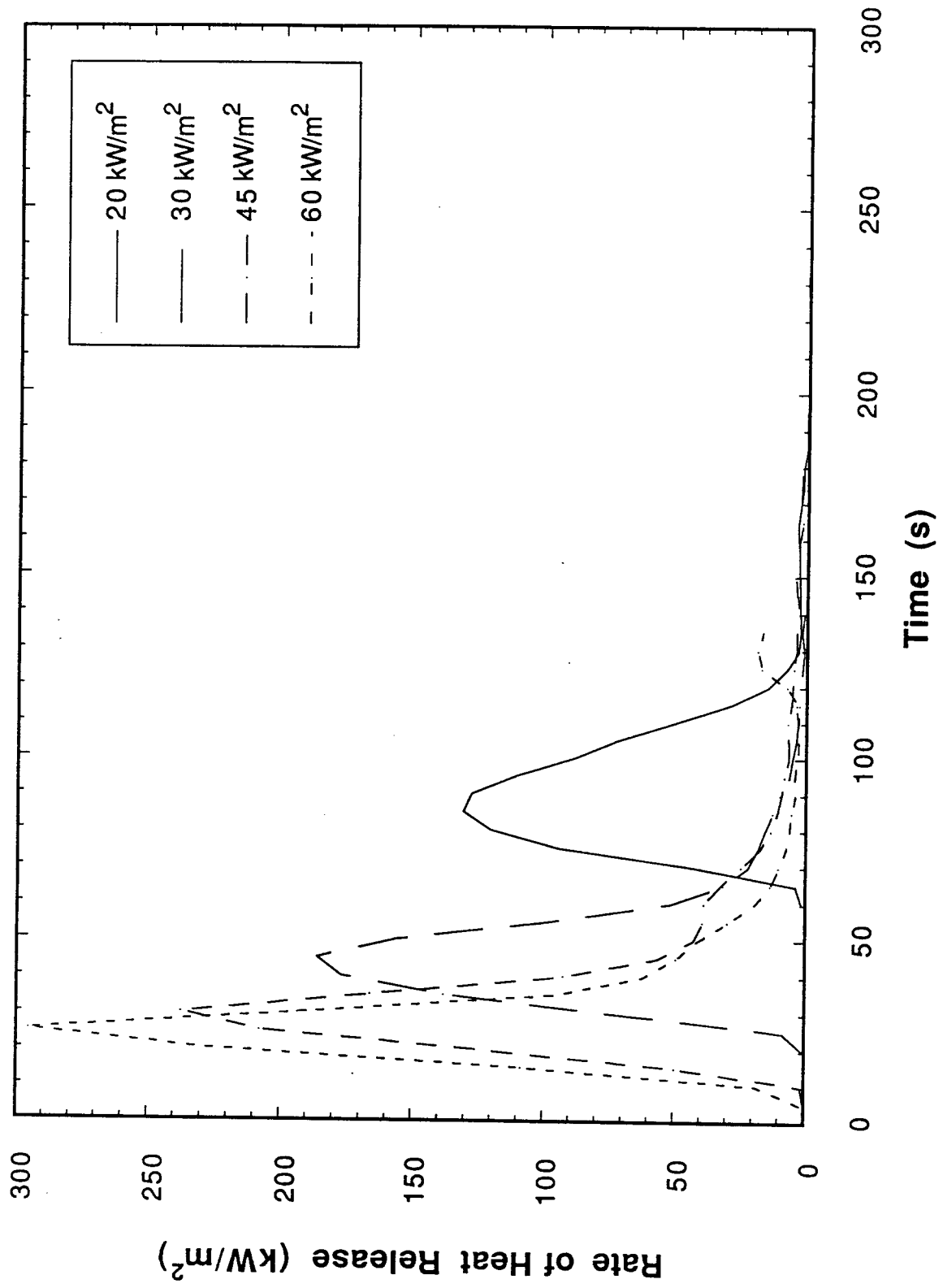


Figure 21. Cone Calorimeter data for rate of heat release; cotton toweling with air gap below sample.

# Epoxy Circuit Board

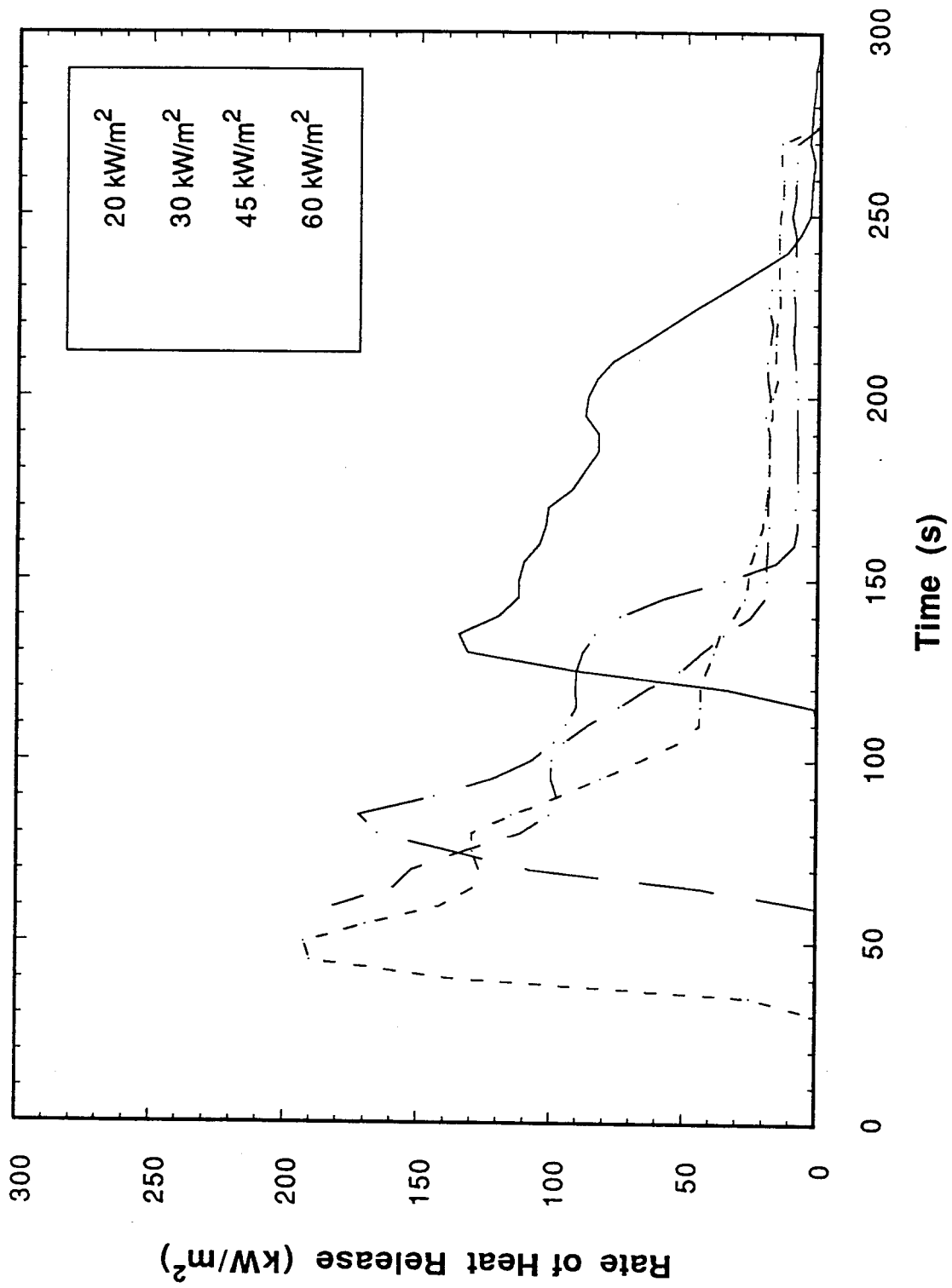


Figure 22. Cone Calorimeter data for rate of heat release; epoxy/glass circuit board with air gap below sample.

# NOMEX

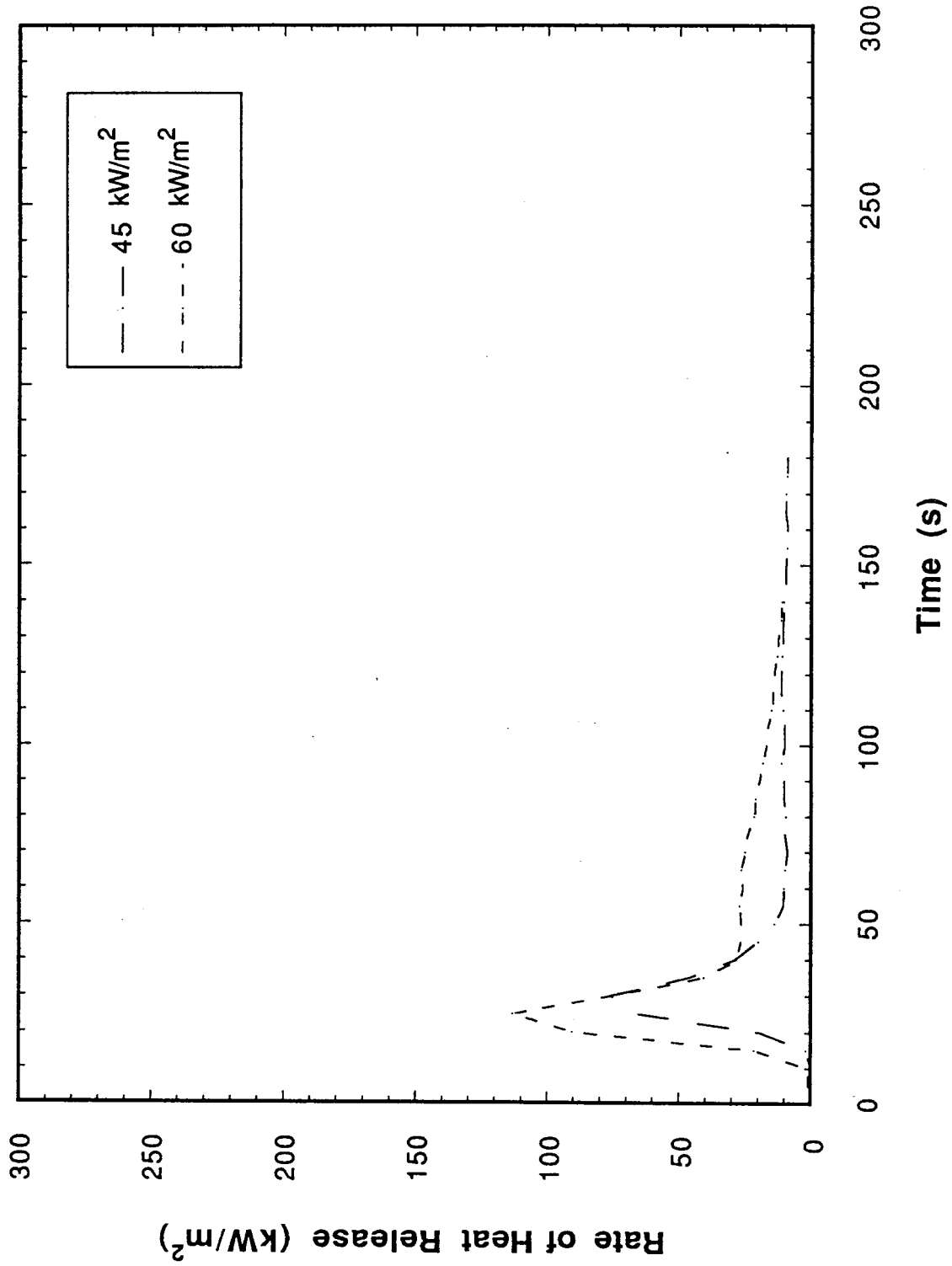


Figure 23. Cone Calorimeter data for rate of heat release; Nomex with air gap below sample.

# Flame Retardant Cotton Cloth

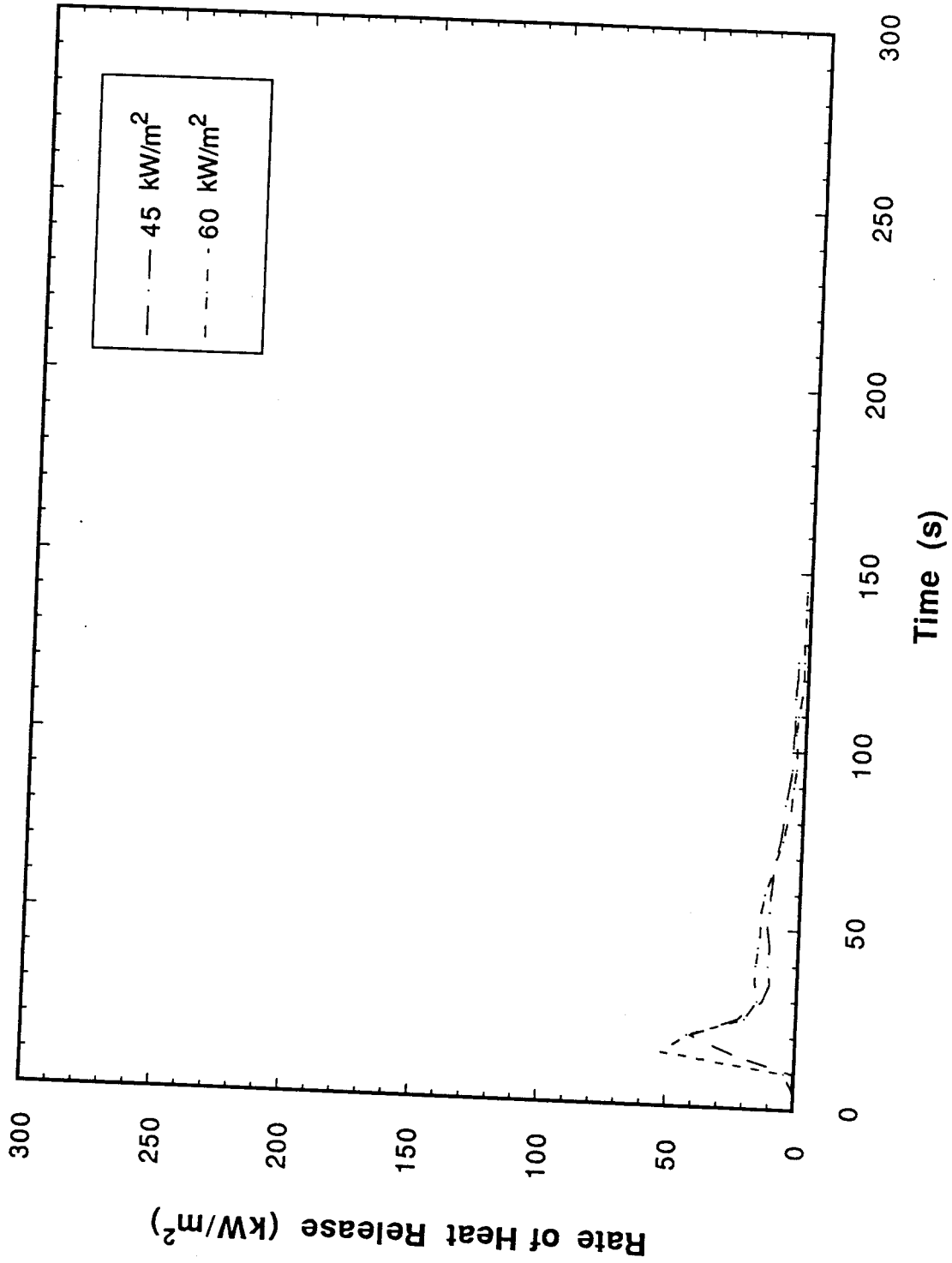


Figure 24. Cone Calorimeter data for rate of heat release; flame-retarded cotton with air gap below sample.

# Cotton Toweling

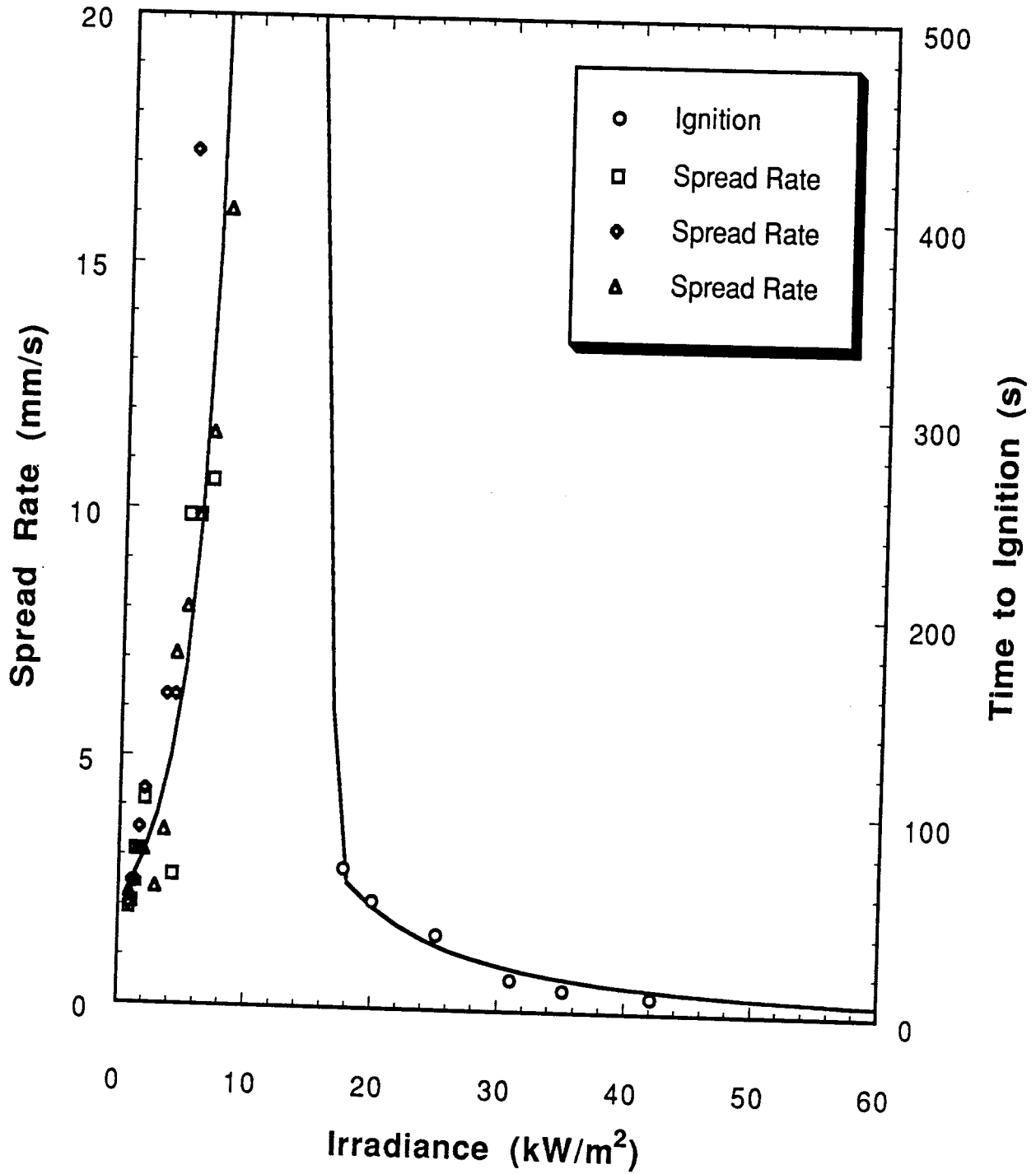


Figure 25. LIFT data and fitted model lines; cotton toweling with air gap below sample.

# EPOXY/GLASS

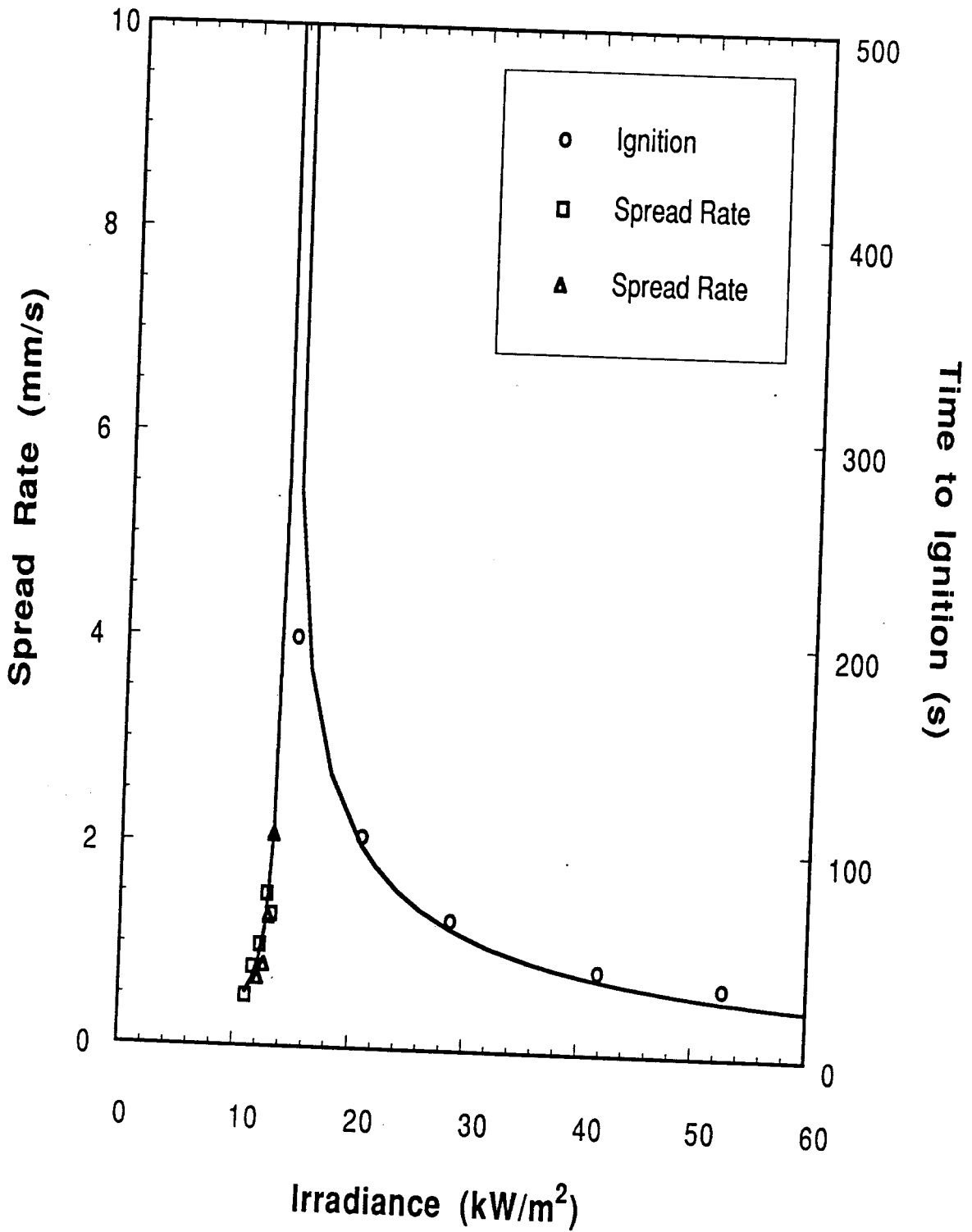


Figure 26. LIFT data and fitted model lines; epoxy/glass circuit board with air gap below sample.

# Kydex PVC/Acrylic

$\alpha = 0.013$

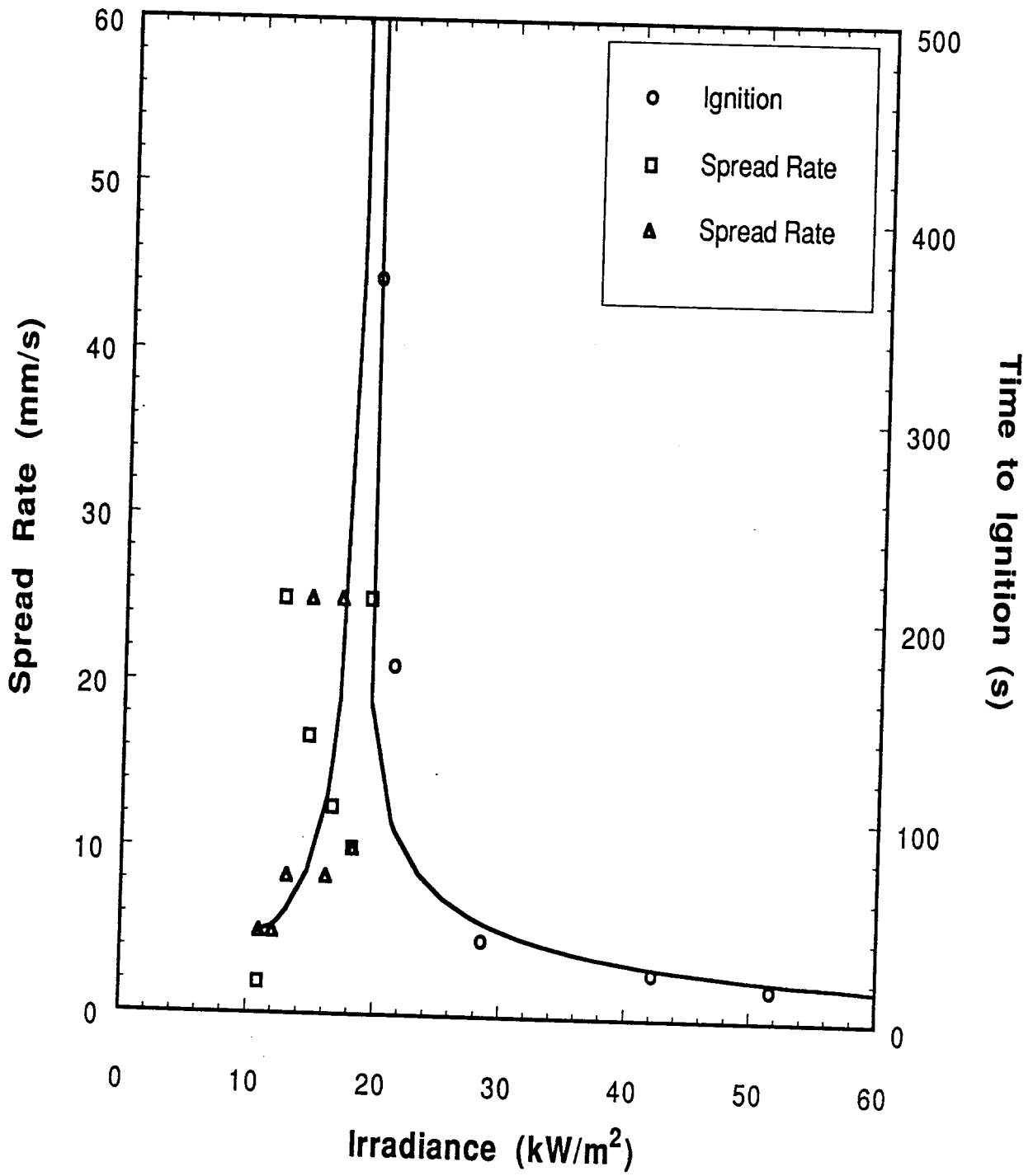


Figure 27. LIFT data and fitted model lines; Kydex with air gap below sample.

# LEXAN 9034

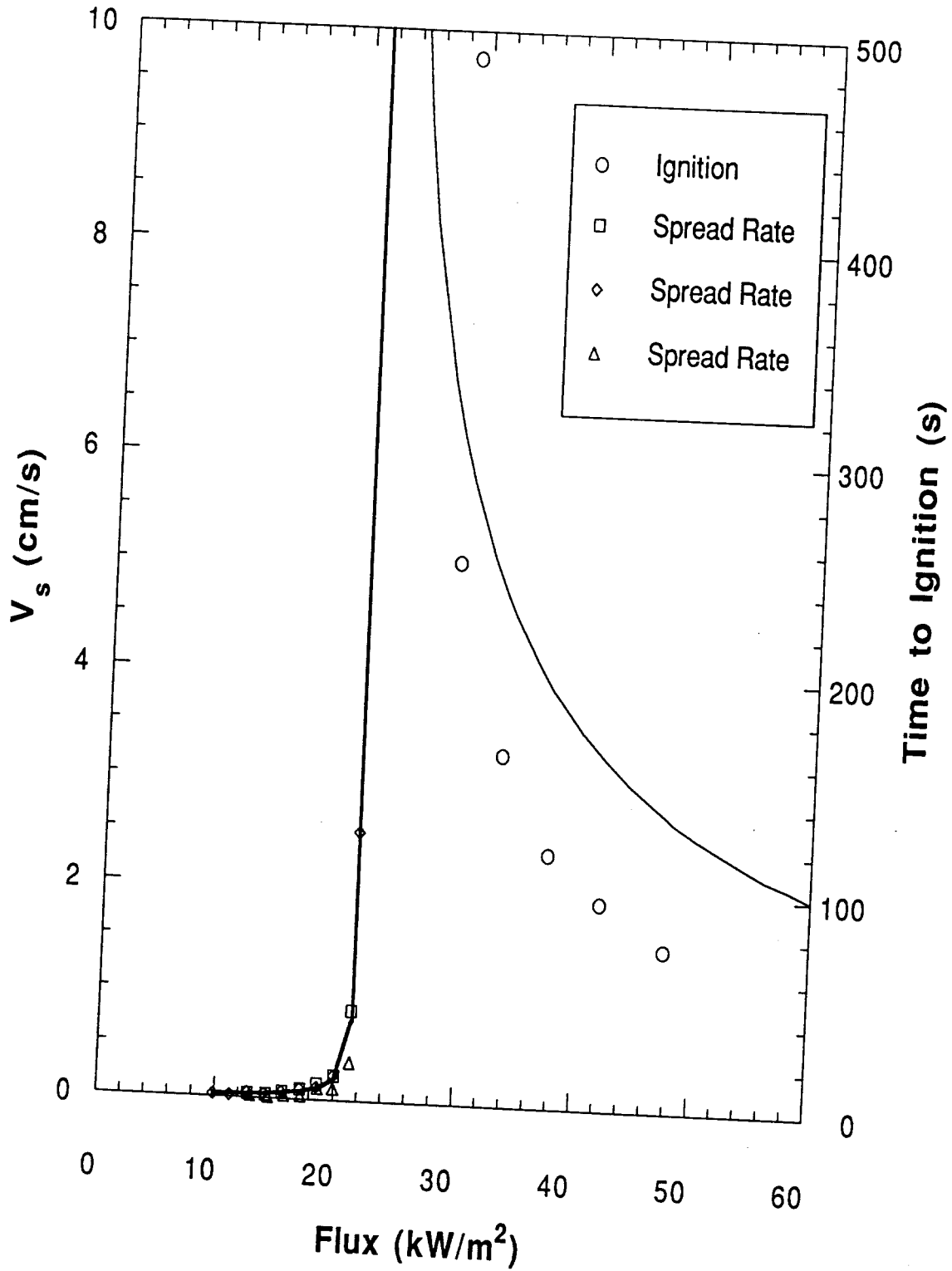


Figure 28. LIFT data and fitted model lines; Lexan 9034 with air gap below sample.

# FR Cotton

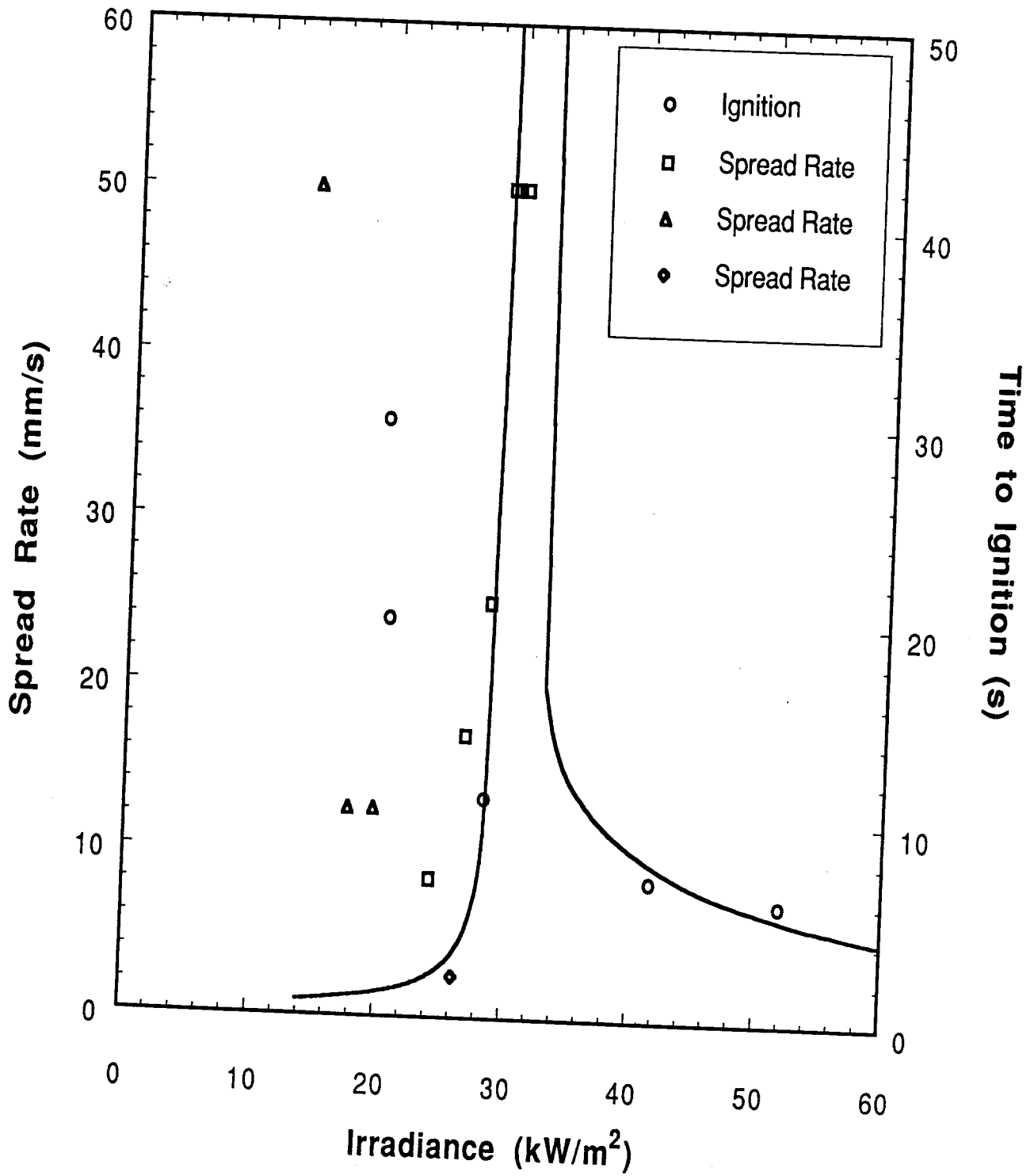


Figure 29. LIFT data and fitted model lines; flame-retarded cotton with air gap below sample.

# NOMEX

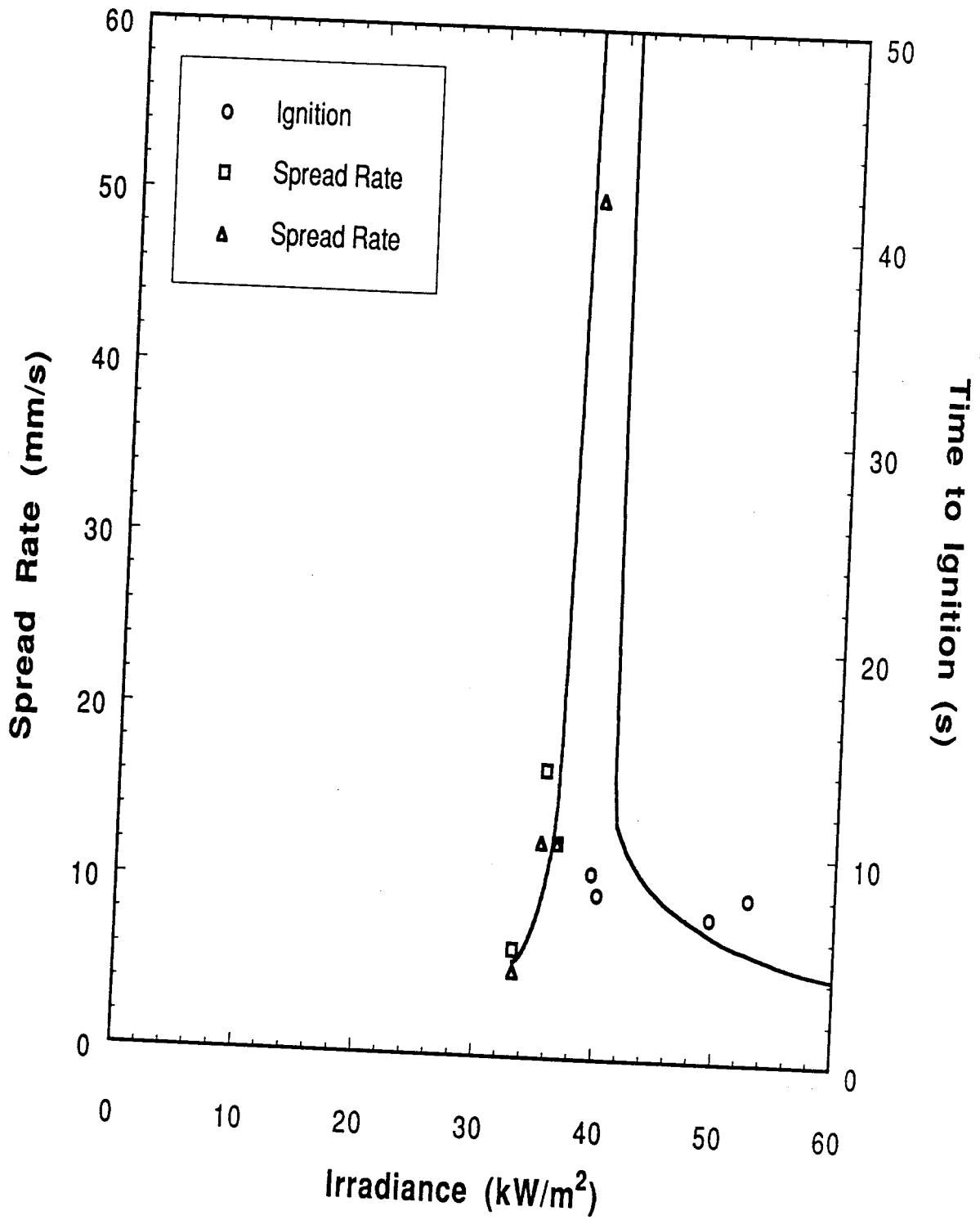


Figure 30. LIFT data and fitted model lines; Nomex with air gap below sample.

## Definitions of Terms in Flame Spread Model

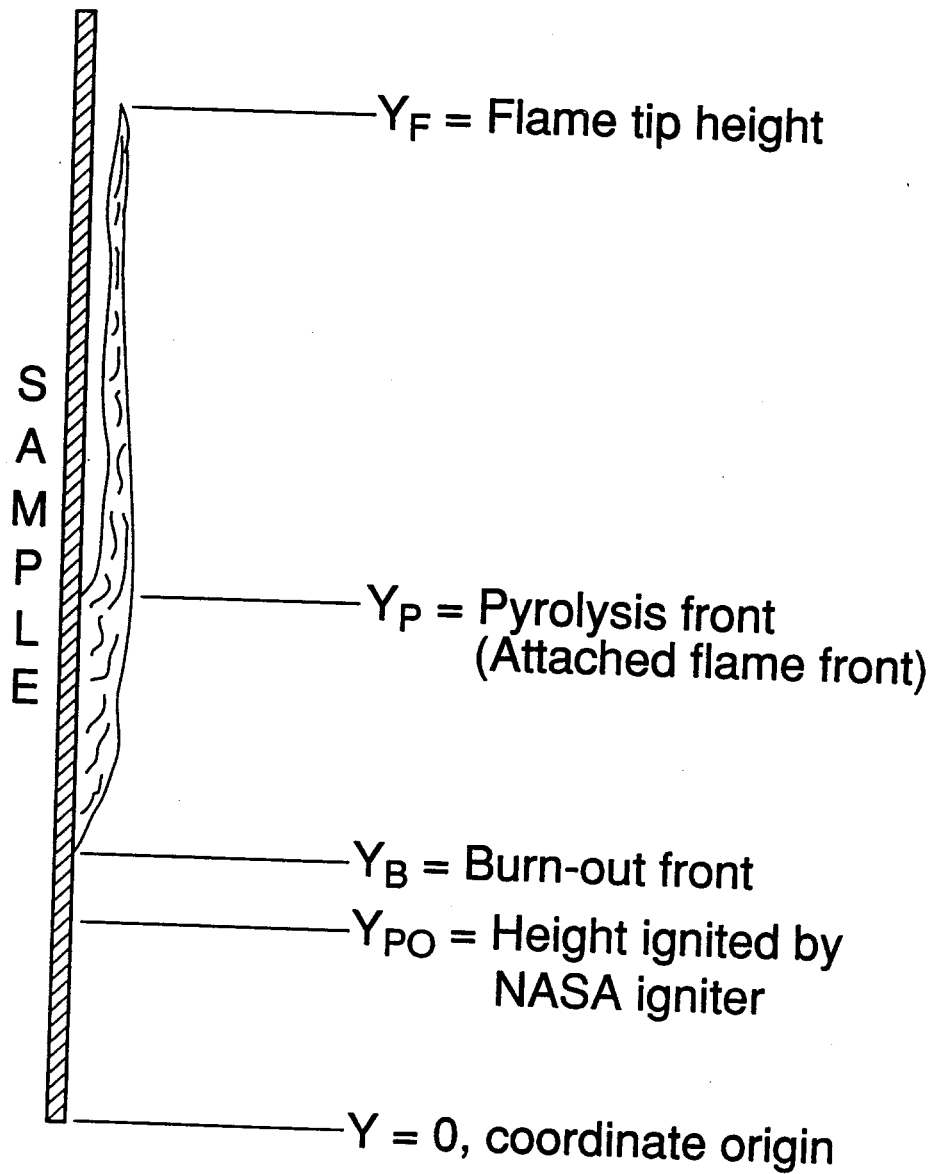


Figure 31. Illustration of various terms in simplified flame spread model.

NAP  
Test 2  
1 Igniter  
Under sample

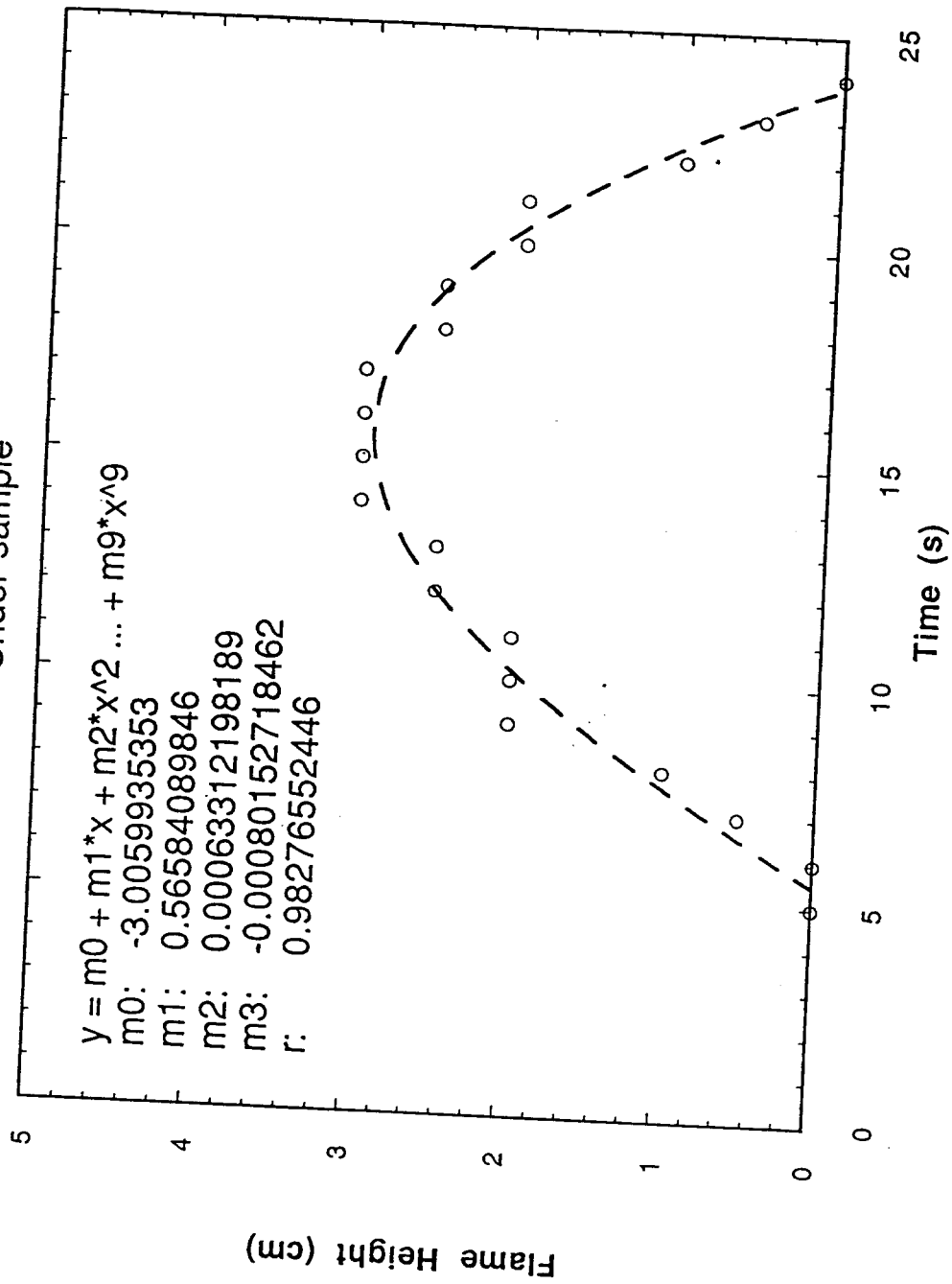


Figure 32. Flame height versus time for single NASA igniter striking both sides of a thin, inert sample (ceramic paper); actual flame height is 6 mm greater than values shown. Dashed line is least squares polynomial fit.

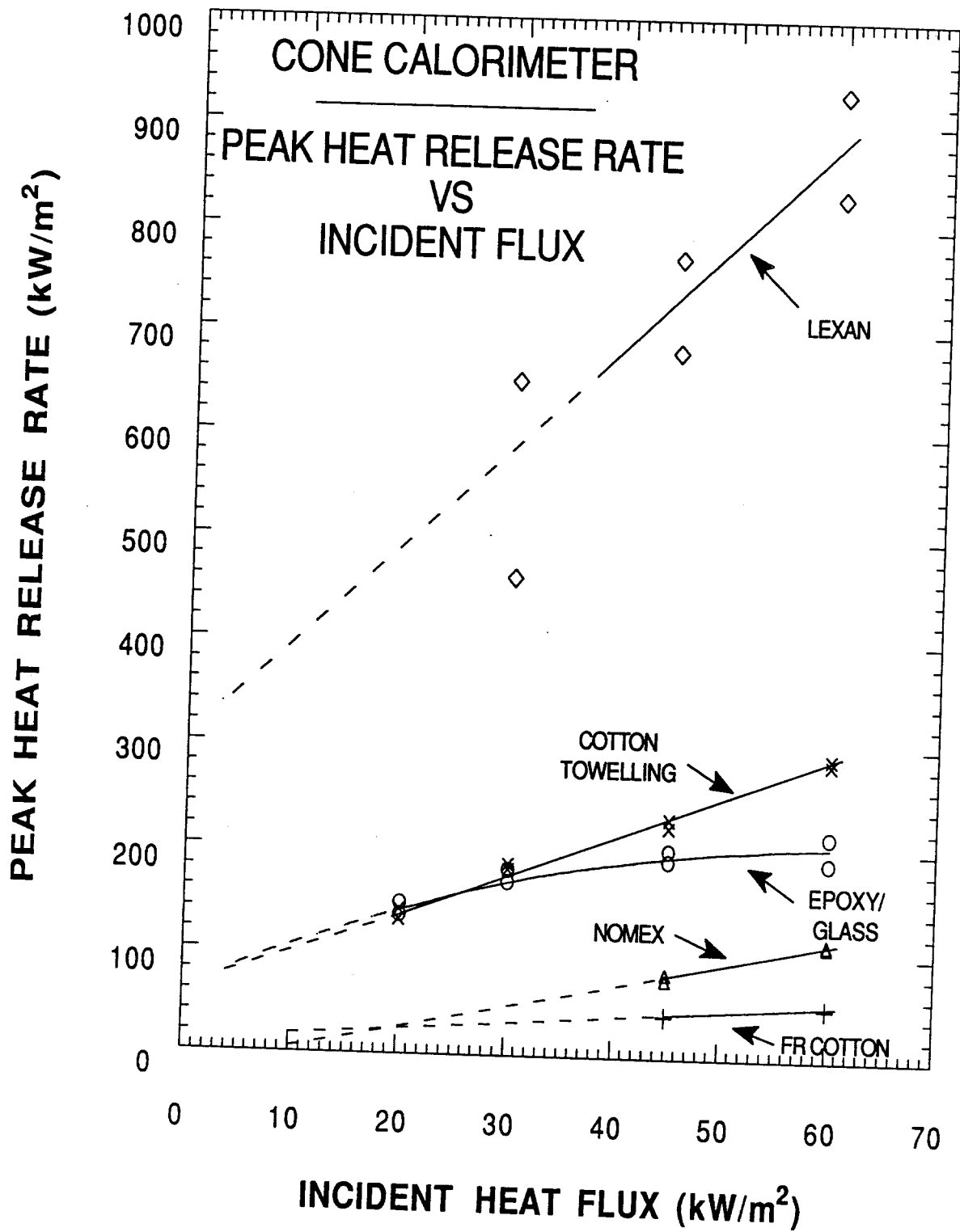


Figure 33. Rate of heat release data used as inputs to flame spread model; for a given material and flux, the above lines specify the value of Q.

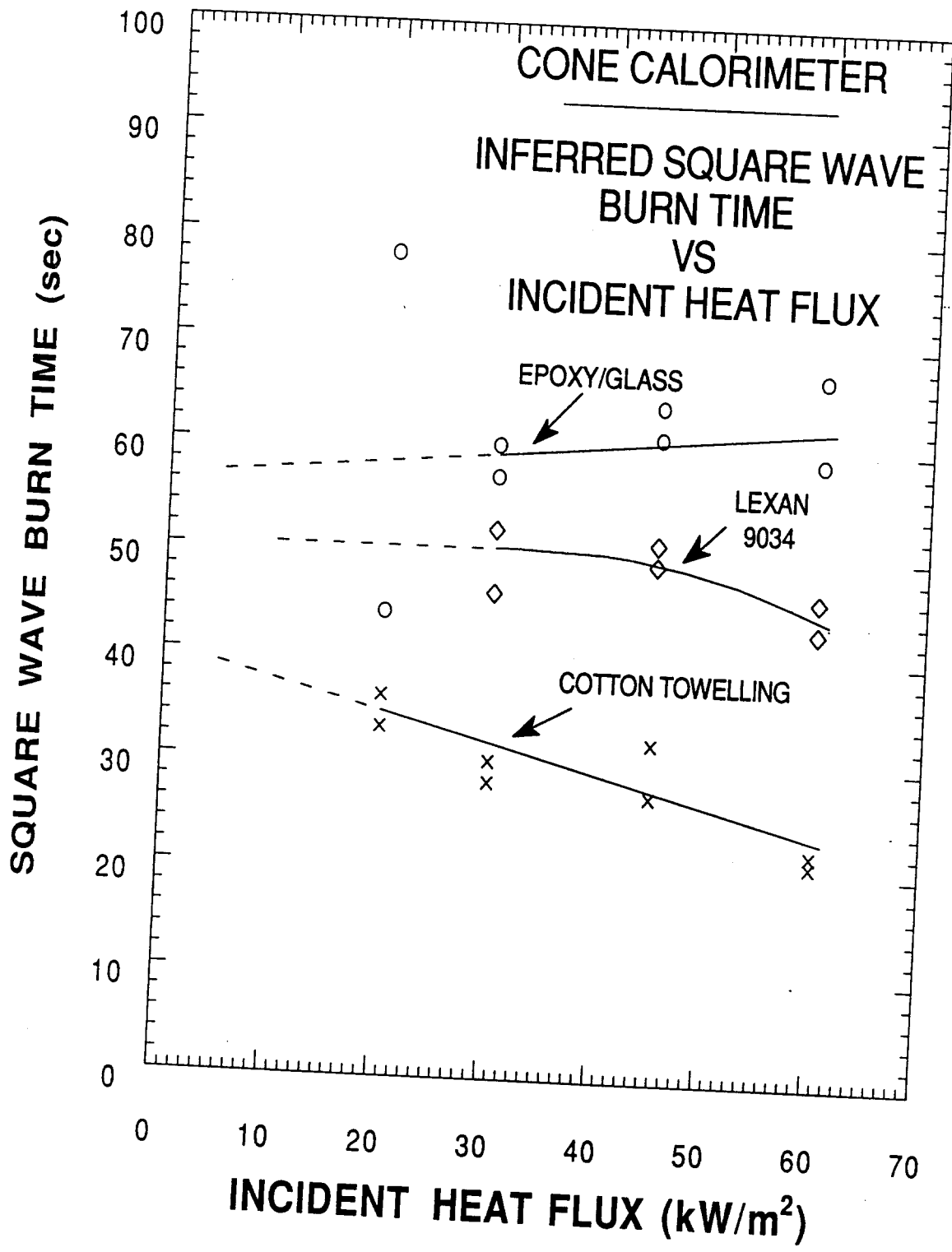


Figure 34. Burn time,  $t_b$ , as determined from rate of heat release data.

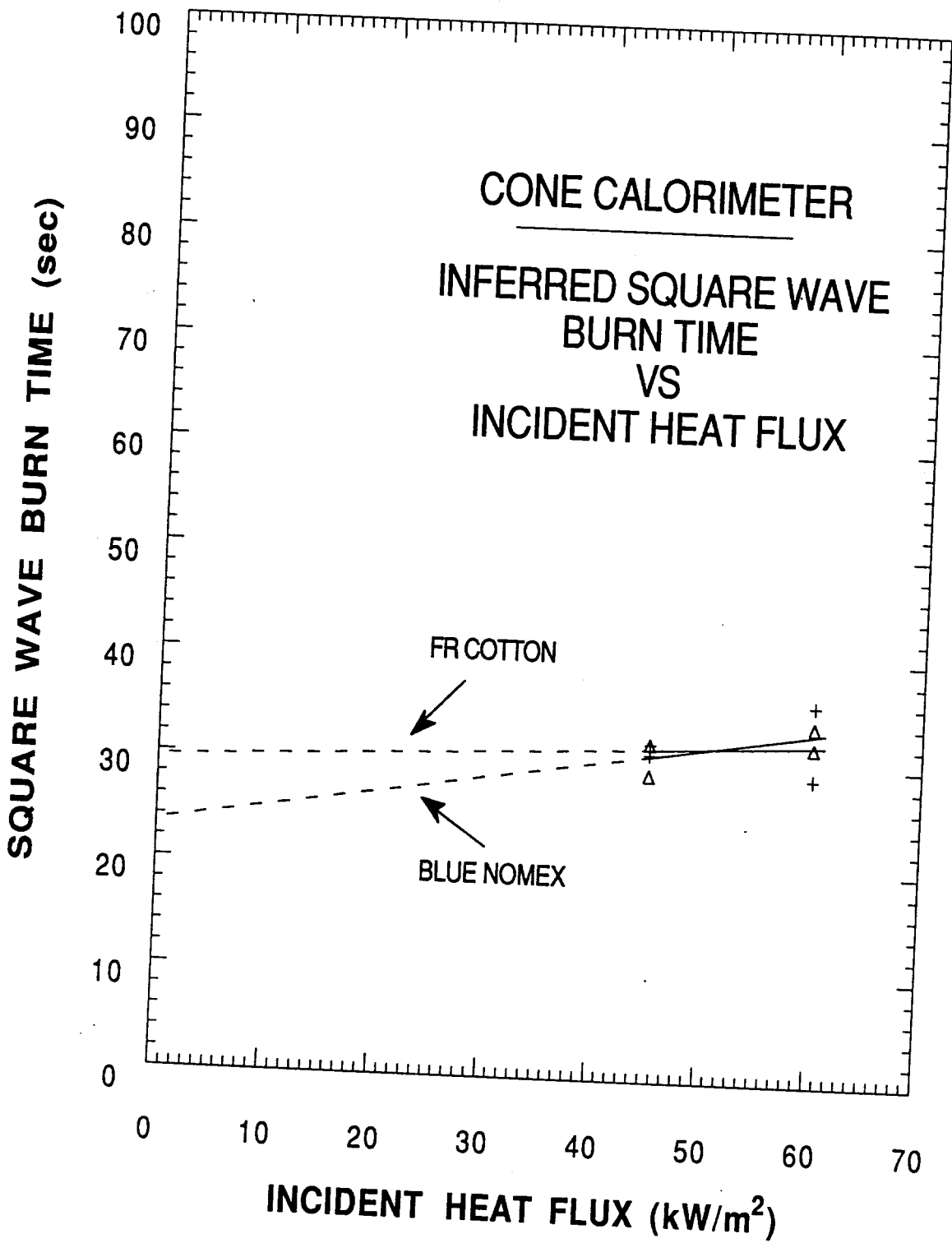


Figure 35. Burn time,  $t_b$ , as determined from rate of heat release data.

# Epoxy/Glass Circuit Board

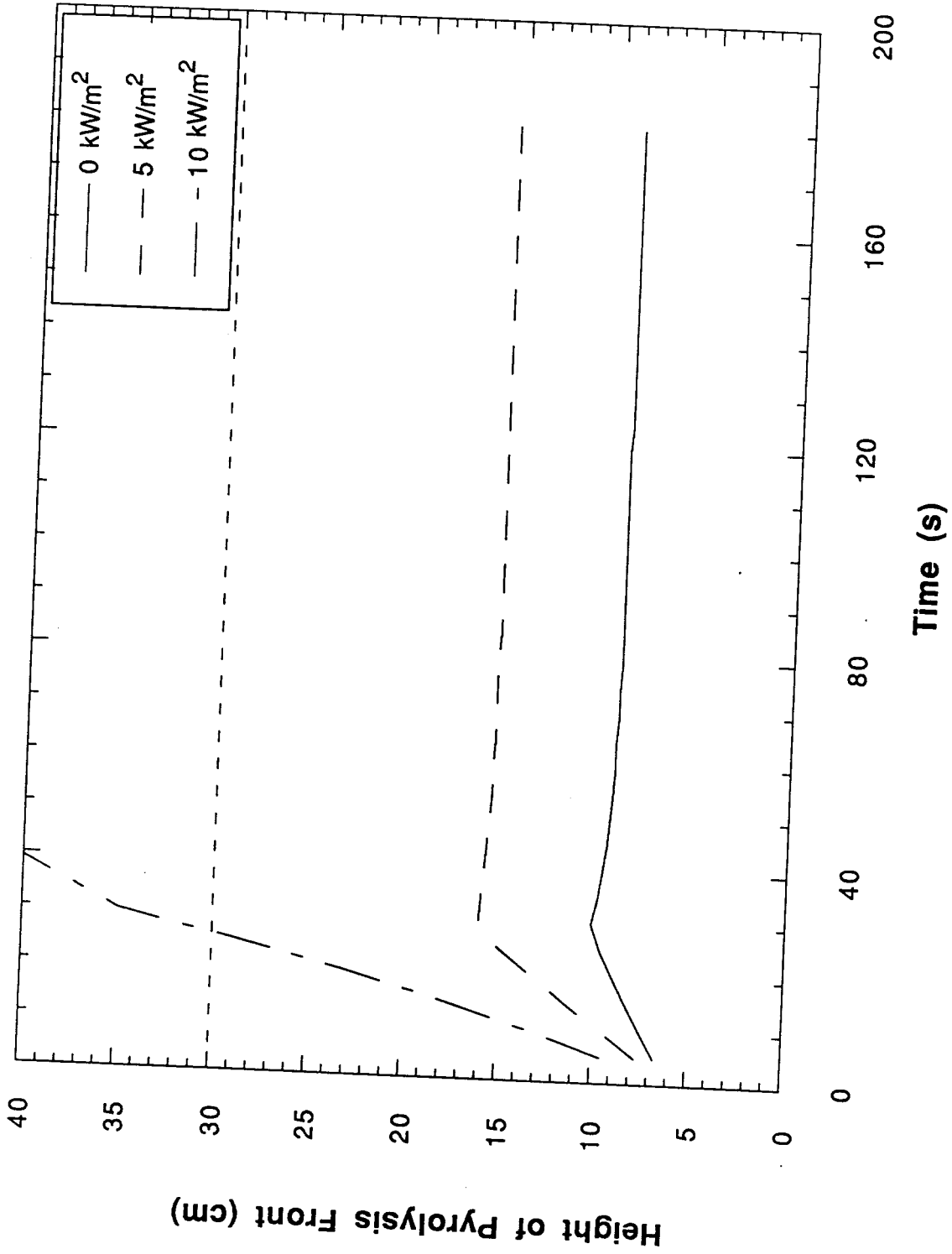


Figure 36. Example of model prediction of pyrolysis front height as a function of time for three pre-heat flux levels. Full length spread first occurs between 5 and 10 kW/m<sup>2</sup>.

## Appendix A

### Data Reduction Procedures in the LIFT Tests

The data reduction procedures for thermally thick materials have been described elsewhere [A-1]; the procedures for thermally thin materials, which are similar, but not identical, are summarized here.

Ignition. Consider a thermally thin material irradiated by a constant flux on one surface and subject to identical convective and radiative losses on its front and back surfaces. Assume that an effective heat transfer coefficient, combining front and back surface convective and radiative losses can be found from the following relation.

$$h_{eq}(T - T_a) = (h_f + h_b)(T - T_a) + (\epsilon_f + \epsilon_b)\sigma(T^4 - T_a^4) \quad (A1)$$

Here  $h_{eq}$  is the equivalent or effective heat transfer coefficient,  $T$  is the sample temperature,  $T_a$  is the ambient temperature,  $h_f$  and  $h_b$  are the actual front and back surface convective heat transfer coefficients,  $\epsilon_f$  and  $\epsilon_b$  are the front and back surface emissivities and  $\sigma$  is the Stefan-Boltzmann constant. Clearly the value of  $h_{eq}$  is dependent on the sample temperature; it is obtained empirically by measuring the steady-state temperature of a dummy sample for the incident heat flux of interest and then solving the above equation for  $h_{eq}$ ;  $h_f$  and  $h_b$  are calculated from standard correlations for the horizontal sample orientation used in these tests.

With the above linearized form of heat loss from the sample, its heating behavior can be described by the following equation.

$$(\delta\rho C)dT/dt = (1 - r)F_0 - h_{eq}(T - T_a) \quad (A2)$$

Here  $\delta$  is the sample thickness,  $\rho$  is the sample density,  $C$  is the sample heat capacity,  $t$  is time,  $r$  is the sample reflectivity (taken equal to 0.05 here because of the middle infrared nature of the radiation source in the LIFT apparatus) and  $F_0$  is the incident radiant flux on the sample. Assuming that an appropriate constant value of  $h_{eq}$  can be inserted into this equation, it can be integrated to yield

$$T(t) = T_a + [(1 - r)F_0/h_{eq}][1 - \exp(\alpha t)] \quad (A3)$$

where

$$\alpha = h_{eq}/(\delta\rho C) \quad (A4)$$

If one identifies the temperature on the left in Eq. A3 as the ignition temperature, the time is the ignition delay time. Solving for this one has the following.

$$t_{ign} = -(1/\alpha) \ln[1 - (h_{eq}(T_{ign} - T_a)/(1 - r)F_0)] \quad (A5)$$

This is our model equation for thermally thin ignition. Note that it contains within it an implicit minimum flux for ignition to occur. That is,  $t_{ign}$  goes to infinity when the argument of the logarithm goes to zero or

$$F_0 = h_{eq}(T_{ign} - T_a)/(1 - r) \quad (A6)$$

To fit the equation to the experimental ignition data there is only one adjustable parameter in Eq. A5, the value of  $\alpha$ ; in effect the adjustable parameter is the group  $(\delta\rho C)$  since  $h_{eq}$  must be chosen in accord with a value for  $T_{ign}$  so that Eq. A6 predicts the observed minimum flux for ignition. A value for  $\alpha$  can be obtained from the slope of a plot of  $t_{ign}$  versus

$$(h_{eq}(T_{ign} - T_a)/(1 - r)F_0)$$

To compute this one must first find  $h_{eq}$  and  $T_{ign}$  from Eq. A6 and the experimentally-obtained relation between  $T$  and  $h_{eq}$ . In this manner one obtains values for all of the parameters in Eq. A5. Since this equation is an approximation to the real behavior of a thermally thin material, there will inevitably be some ambiguity in the fitting process; one simply seeks the best fit in order to obtain a reasonable engineering description of the ignition process. The result should be usable in any other configuration where the heat losses from the sample are comparable. The value of  $\delta\rho C$  one obtains is typically appreciably larger than the room temperature value one would compute from the properties of the original sample material. This is compensating for the non-constancy of the real overall heat transfer coefficient and any chemical effects that may be altering the sample's thermal properties. Such changes may be substantial; recall, for example, that Lexan intumesces as it is heated.

Lateral flame spread. An appropriate model expression for lateral flame spread velocity can be readily derived using the above result and following the analogous derivation for a thermally thick material from Ref. A2. Consider a flame spreading laterally over a thermally thin material at a steady rate. The material has been pre-heated by an external flux to some temperature  $T_s$  well away from any influence of the flame, where  $T_s$  is obtained from Eq. A3 above by inserting the time of pre-heating.

As the flame moves over the material at a velocity  $V_F$ , it heats it from  $T_s$  to its ignition temperature. Assuming that the flame heat flux,  $q_F$ , is spatially constant over a length  $\delta_F$ , one finds from a simple steady-state energy balance on the material that

$$(\delta\rho C)V_F(T_{ign} - T_s) = q_F\delta_F \quad (A7)$$

Here it has been assumed that, as in the LIFT tests, the flame is spreading on one side of the material. The quantity  $T_s$  can be eliminated from Eqs. A3 and A7 to yield the total temperature change in the material

$$(T_{ign} - T_a) = \{(1 - r)F_0/h_{eq}\}(1 - \exp(-\alpha t)) + q_F\delta_F/(\delta\rho C)V_F \quad (A7)$$

Now let  $\Phi$  equal the unknown quantity  $q_F\delta_F$  and rearrange Eq. A7 in such a way as to suggest what type of plotting of variables will yield a means to calculate an empirical value for the parameter  $\Phi$ .

$$(1/V_F) = (\delta\rho C/\Phi)\{(T_{ign} - T_a) - [(1 - r)F_0/h_{eq}][1 - \exp(-\alpha t)]\} \quad (A8)$$

This implies that a plot of  $(1/V_F)$  versus  $F_0[1 - \exp(-\alpha t)]$  should yield a straight line and the value of  $\Phi$  can be obtained from the slope of that line. Obtaining the most appropriate slope can be aided by noting that the intercept of such a plot should pass through the minimum flux for ignition. With the value of  $\Phi$  thus determined, all of the parameters in Eq. A8 are known and it can be used to predict the lateral flame spread rate for the material in similar heat loss conditions. Note that this model does not predict the minimum pre-heat flux or temperature for spread; this is obtained from the LIFT experiments directly.

#### References for Appendix A

- A1) Quintiere, J. and Harkleroad, M., "New Concepts for Measuring Flame Spread Properties", Fire Safety: Science and Engineering, American Society of Testing Materials Special Technical Publication No. 882, Philadelphia, Pa, (1985), p.239
- A2) Quintiere, J., Harkleroad, M., and Walton, D., "Measurement of Material Flame Spread Properties", Combustion Science and Technology, 32, (1983), p: 67

NIST-114A  
(REV. 3-90)

U.S. DEPARTMENT OF COMMERCE  
NATIONAL INSTITUTE OF STANDARDS AND TECHNOLOGY

# BIBLIOGRAPHIC DATA SHEET

1. PUBLICATION OR REPORT NUMBER	NISTIR 4591
2. PERFORMING ORGANIZATION REPORT NUMBER	NASA CR-187115
3. PUBLICATION DATE	June 1991

4. TITLE AND SUBTITLE  
Material Flammability Test Assessment for Space Station Freedom

5. AUTHOR(S)  
T. Ohlemiller, K.M. Villa

6. PERFORMING ORGANIZATION (IF JOINT OR OTHER THAN NIST, SEE INSTRUCTIONS)  
U.S. DEPARTMENT OF COMMERCE  
NATIONAL INSTITUTE OF STANDARDS AND TECHNOLOGY  
GAITHERSBURG, MD 20899

7. CONTRACT/GRANT NUMBER	
8. TYPE OF REPORT AND PERIOD COVERED	

9. SPONSORING ORGANIZATION NAME AND COMPLETE ADDRESS (STREET, CITY, STATE, ZIP)  
NASA Lewis Research Center  
21000 Brookpark Road  
Cleveland, OHIO 44135

10. SUPPLEMENTARY NOTES

11. ABSTRACT (A 200-WORD OR LESS FACTUAL SUMMARY OF MOST SIGNIFICANT INFORMATION. IF DOCUMENT INCLUDES A SIGNIFICANT BIBLIOGRAPHY OR LITERATURE SURVEY, MENTION IT HERE.)

The NASA Upward Flame Propagation test, which measures response to a well-defined laminar flame at the bottom of a test sample, is currently used to screen for flammability all materials intended for use in the interior of manned spacecraft. The response of a series of materials was compared in this test and in the standard NIST flammability tests (Cone Calorimeter for rate of heat release and LIFT tests for ignitability and lateral flame spread). The goal was to see if these differing flammability assessment approaches provide comparable information on the potential hazards of a material. In the first phase of this study only one of the samples exhibited appreciable flame spread in the NASA test, yielding very limited data for comparisons with the NIST test results. The NIST tests, which employ a variable external radiant flux as an additional test parameter, revealed a widely varying response to this flux. In the second phase of the study, the NASA test was modified to include radiative pre-heating of the samples before they were exposed to the standard NASA igniter in the standard manner. The response of the materials, as measured by the minimum pre-heat flux (or temperature) to yield upward spread, varied widely; for example, Nomex required very little pre-heating to yield full-length spread whereas Lexan 9034 was resistant. Rate of heat release behavior or lateral flame spread behavior alone did not appear to be predictive of behavior in the modified NASA test. A simplified upward flame spread model, which utilizes inputs derived from the NIST test, was employed in an attempt to predict the behavior in the modified NASA tests. The model greatly under-predicted the necessary pre-heat flux for some materials while doing the opposite for other materials. Thus, at the present, a firm relation between the behavior in the NASA test and in the NIST tests has not been established.

12. KEY WORDS (6 TO 12 ENTRIES; ALPHABETICAL ORDER; CAPITALIZE ONLY PROPER NAMES; AND SEPARATE KEY WORDS BY SEMICOLONS)  
flame spread; flammability; ignition; microgravity; heat release rate; test methods; spacecraft; small scale fire tests

13. AVAILABILITY

<input checked="" type="checkbox"/>	UNLIMITED
<input type="checkbox"/>	FOR OFFICIAL DISTRIBUTION. DO NOT RELEASE TO NATIONAL TECHNICAL INFORMATION SERVICE (NTIS).
<input type="checkbox"/>	ORDER FROM SUPERINTENDENT OF DOCUMENTS, U.S. GOVERNMENT PRINTING OFFICE, WASHINGTON, DC 20402.
<input checked="" type="checkbox"/>	ORDER FROM NATIONAL TECHNICAL INFORMATION SERVICE (NTIS), SPRINGFIELD, VA 22161.

14. NUMBER OF PRINTED PAGES

78

15. PRICE

A05

ELECTRONIC FORM